11-1-2019 2:00 PM

The role of Xenopus laevis RECK in ECM remodeling and tissue patterning

Jessica Willson, *The University of Western Ontario*

© Jessica Willson 2019

Recommended Citation

Abstract

Proper cell-cell and cell-extracellular matrix (ECM) interactions are vital for cell migration and patterning of the vertebrate embryo. Matrix metalloproteinases (MMPs) and their inhibitors, reversion-inducing cysteine-rich proteins with Kazal motifs (RECK) and tissue inhibitors of metalloproteinases (TIMPs), are all differentially expressed during embryogenesis to regulate such ECM remodeling events and cell interactions. While TIMPs are a family of 4 secreted proteins that share overlapping substrate specificities of MMPs, RECK is unique in that it is a membrane-anchored MMP inhibitor that is embryonic lethal in mice. I used *Xenopus laevis* as a model organism to investigate the role of RECK as a regulator of ECM turnover during development. The *X. laevis* RECK sequence was compared to a breadth of vertebrate and a few invertebrate RECK amino acid sequences. The *X. laevis* RECK amino acid sequence was found to be highly conserved with other RECK proteins. *RECK* knockdown in *X. laevis* embryos resulted in neural tube closure failure and axial defects, in part due to altered mRNA levels of *MT1-MMP*, *MMP-2*, and *TIMP-2*. Upon examination of RECK, MT1-MMP, and TIMP-2 protein localization in different tissues throughout early *X. laevis* development, I found that all 3 proteins showed highly similar localization patterns, particularly in the dorsal-ventral differentiation of the neural tube. To further investigate RECK regulation of MMP activity *in vitro*, I used *X. laevis* A6 cells to knockdown, overexpress, and shed RECK from the cell surface. I demonstrated that changes in *RECK* levels (overexpression and cell surface shedding) that may reduce the ability of the cell to remodel the ECM are compensated for by increases in MT1-MMP and MMP-2 levels and changes in ERK signaling. Altogether, these results support a role for RECK in the regulation of ECM remodeling and tissue patterning during *X. laevis* development.

Summary for Lay Audience

All cells secrete or release materials around themselves, allowing tissues to form. In multicellular organisms such as ourselves, some of these materials form a network (the extracellular matrix or ECM) in which the cells anchor themselves to. In adults, the ECM provides stability and a safe environment in which our cells can carry out their functions - muscle cells contract, nerve cells communicate, and so on. But the situation is different in a developing embryo. As animals grow from a fertilized egg, cells need to move. In adults, when cells move, it is often associated with a disease state, such as cancer cells metastasizing. Thus, understanding how cell movement is regulated is essential to both embryogenesis and adults. For cells to move around, the ECM network that surrounds them often has to be broken down and then remade. The molecules involved in this breakdown are called matrix metalloproteinases (MMPs), and one of their roles is to cleave the ECM. Their activity has to be tightly regulated as excessive ECM degradation is detrimental. Therefore, there are 2 other molecules, tissue inhibitors of metalloproteinases (TIMPs) and reversion-inducing cysteine-rich protein with Kazal motifs (RECK), whose roles are to control MMPs. RECK is a protein found on the surface of cells and stops cells from moving by preventing MMPs from cleaving components of the ECM. RECK has been identified as a crucial player during embryogenesis, though exactly why RECK is essential to development remains unclear. My research examined the role of RECK during frog development. I found that reducing RECK levels in frog embryos caused abnormal development, particularly in the formation of the spinal cord. These defects were in part due to improper ECM degradation. Additionally, I found that RECK is associated with MMPs even after cells migrate, at a time when embryonic cells are beginning to specialize, particularly into nerve cells. Thus, in addition to regulating MMPs when cells are migrating, RECK also plays a role after ECM

breakdown to signal to and help cells function. Overall, my study supports the role for RECK

as an important regulator of cell movement during embryogenesis.

Keywords

RECK; matrix metalloproteinase; tissue inhibitor of metalloproteinase; extracellular matrix;

development; *Xenopus laevis*; neural tube

Dedication

To my husband, who has always supported me

Acknowledgements

First and foremost, I would like to thank my supervisor, Dr. Sashko Damjanovski. I would not be where I am today without all of your guidance, support, motivation, and patience. It has been a huge privilege to work in your lab. You have not only been an amazing mentor, but also a great friend. Thank you for always believing in me.

I would also like to thank my advisory committee, Dr. Susanne Kohalmi and Dr. Robert Cumming. You have both been a constant source of support and guidance for me throughout the years.

To all members of the Damjanovski lab, past and present, thank you for all of the encouragement you have shown me over the years. I would like to especially thank Carlie Muir and Brad Bork for their constant support and help. Thank you for creating such a fun and memorable experience in and outside of the lab. You two are both incredibly talented scientists and I wish you nothing but the very best in your future endeavours.

A huge thanks also goes out to Dr. Kelly's lab and Dr. Cumming's lab for their generosity in providing the use of lab equipment and reagents, all of which have made this thesis possible.

I would also like to thank all of the staff in the Biology Department - especially Carol Curtis, Arzie Chant, Diane Gualey, Sherri Fenton, and Hillary Bain - for all of your hard work behind the scenes to ensure everything went smoothly over the years.

Lastly, I would like to thank my family. To my sister, Cassandra Barber, thank you for being my confidant throughout all of these years. I'm lucky to call you my best friend. To my mom, Vicki Barber, thank you for always being there for me and helping me achieve my goals. I would not be where I am today without all of your love and support. To my husband, Adam Willson, thank you for all the unconditional support and encouragement you've shown

me along this long journey. I will forever be grateful for all of the sacrifices you have made

for our family in order for me to accomplish my goals.

Table of Contents

List of Tables

List of Figures

List of Appendices

List of Abbreviations

ADAM   A disintegrin and metalloproteinase

ANOVA   Analysis of variance

AP   Anterior/posterior

A.U.   Arbitrary units

BB94   Batimastat

BMP   Bone morphogenetic protein

Bp   Base pair

BSA   Bovine serum albumin

CD   Clusters of differentiation

cDNA   Complementary deoxyribonucleic acid

DAPI   4',6-diamidino-2-phenylindole

DIC   Differential interference contrast

Dll   Delta-like

DMSO   Dimethyl sulfoxide

Dpf   Days post fertilization

DQ   Dye-quenched

DRG   Dorsal root ganglia

D-V   Dorsal-ventral

ED   Embryonic day

ECM   Extracellular matrix

EF1α Elongation factor one alpha

EGF   Epidermal growth factor

ERK   Extracellular signal-regulated kinase

FBS	Fetal bovine serum
Fra	Fos-related antigen
GDE	Glycerophosphodiester phosphodiesterase
GFP	Green fluorescent protein
GPI	Glycosylphosphatidylinositol
HA	Hemagglutinin
HDAC	Histone deacetylase
HRP	Horseradish peroxidase
ICD	Intracellular domain
IHC	Immunohistochemistry
MAPK	Mitogen-activated protein kinase
MMP	Matrix metalloproteinase
MMR	Marc's modified ringers
MO	Morpholino
mRNA	Messenger ribonucleic acid
MT	Membrane type
PBS	Phosphate-buffered saline
pERK	Phosphorylated extracellular signal-regulated kinase
PI-PLC	Phosphatidylinositol-specific phospholipase C
PVDF	Polyvinylidene fluoride
qPCR	Quantitative polymerase chain reaction
Rap	Ras-related protein
RECK	Reversion-inducing cysteine-rich protein with Kazal motifs
RIPA	Radioimmunoprecipitation assay

RLM-RACE	RNA Ligase Mediated Rapid Amplification of cDNA Ends
SDS	Sodium dodecyl sulphate
SE	Standard error
SEM	Standard error of the mean
SF	Serum-free
Shh	Sonic hedgehog
shRNA	Short hairpin ribonucleic acid
SMART	Simple Modular Architecture Research Tool
Sp	Specificity protein
Src	Proto-oncogene tyrosine-protein kinase
STAT3	Signal transducer and activator of transcription factor 3
TBST	Tris-buffered saline with Tween 20
TIMP	Tissue inhibitor of metalloproteinase
TRE	12-*O*-tetradecanoylphorbol-13-acetate-responsive element
VEGF	Vascular endothelial growth factor

Note: SI units are not listed above.

Chapter 1

1 Global Introduction and Literature Review

Portions of this chapter have been published as a review article: "Willson, J.A. and Damjanovski, S. (2014). Vertebrate RECK in development and disease. Trends in Cell and Molecular Biology, **9**: 95-105". (Reprint permission in Appendix A). The text has been modified from the original manuscript to adhere to formatting guidelines for this thesis. J.A.W. wrote the manuscript and S.D. edited the manuscript.

1.1   The Extracellular Matrix

The extracellular matrix (ECM) is the non-cellular network of interacting macromolecules that surrounds cells in metazoans. It is primarily composed of proteoglycans, which are large hydrophilic molecules, and large fibrous proteins, such as collagens and fibronectin, that provide structural support to cells. These fibrous proteins may contain important signaling domains, such as the epidermal growth factor (EGF) domain of laminin and heparin-II domain of fibronectin, which influence cell behaviour (Daley et al., 2008). There are 2 main types of ECM in animal tissues: basement membrane and interstitial matrix. The basement membrane is a thin layer of defined ECM that underlies epithelial cells, providing a barrier between epithelia and mesenchyme, whereas the interstitial matrix is a vast network of ECM surrounding sparsely packed cells that make up connective tissue, such as cartilage and bone (McKee et al., 2019). The amount and composition of ECM is specific to each type of tissue and is crucial for the overall integrity and function of that tissue.

The ECM not only provides a scaffolding network for cells, but it also sequesters a variety of signaling molecules including cytokines and growth factors, that once released, regulate cell growth, survival, migration, and differentiation (Daley et al., 2008). Changes in cell-cell and cell-ECM contact and the release of these sequestered proteins occur through cleavage and remodeling of the ECM, and as such, these processes are crucial for proper development and maintenance of multicellular organisms (Daley et al., 2008). The integrity and breakdown of the ECM is regulated mainly through the combined action of a group of extracellular proteases called matrix metalloproteinases (MMPs).

1.2   Matrix Metalloproteinases

There are 24 vertebrate MMPs, each with their own, but overlapping, ECM substrate specificities. MMPs are present in all metazoans and their expression is crucial in guiding many embryonic cell signaling and migration events (Visse and Nagase, 2003). MMPs are classified into 2 categories based on their localization and structure: secreted MMPs, which are soluble in the ECM, and membrane type (MT)-MMPs, which are tethered to the cell membrane. The 3 common domains of MMPs are an N-terminal signal sequence that targets them for secretion, a pro-domain that inhibits catalytic activity, and a catalytic domain with endopeptidase activity (summarized in Fig. 1.1). All MMPs are synthesized as inactive zymogens and become activated with the removal of their pro-domain. MT-MMPs reach the cell surface in an active form, as they have their pro-domain cleaved intracellularly in the Golgi by furin-like proteases, whereas secreted MMPs are activated in the ECM by other active MMPs already present (Sternlicht and Werb, 2001). Once active, the common, but not only function of all MMPs, is to cleave and remodel the ECM through selective degradation of ECM proteins (Vu and Werb, 2000).

1.2.1   MT1-MMP

A well-characterized member of the MMP family is MT1-MMP. Unlike secreted MMPs, which can diffuse freely though the ECM, MT-MMPs are anchored to the cell surface and their function is therefore restricted to the pericellular space (Seiki, 2002). Of the many *MMP* null mice, only *MT1-MMP* null mice die shortly after birth due to severe skeletal defects (Holmbeck et al., 1999). MT1-MMP can cleave major components of the ECM, including collagen types I, II, and III, but it can also cleave non-ECM proteins,

Figure 1.1 MMP domain structure.

The various domains of human MMPs are shown. SP=signal peptide, Pro=pro-domain, Cat=catalytic domain, F=fibronectin II repeats, PEX=hemopexin domain, TM=transmembrane domain, C=cytoplasmic domain, GPI=Glycosylphosphatidylinositol anchor, Cys=cysteine array, Ig=immunoglobulin-like domain. The flexible hinge region is shown by the black zigzag line. (Modified from Radisky and Radisky, 2015).

MMP-7, -26 | SP | Pro | Cat |

MMP-1, -3, -8, -10, -11, -12, -13, -19, -20, -21, -27, -28 | SP | Pro | Cat | PEX |

MMP-2, -9 | SP | Pro | Cat | F | F | F | PEX |

MT1-MMP (MMP-14), MT2-MMP (MMP-15), MT3-MMP (MMP-16), MT5-MMP (MMP-24) | SP | Pro | Cat | PEX | TM | C |

MT4-MMP (MMP-17), MT6-MMP (MMP-25) | SP | Pro | Cat | PEX | GPI |

MMP-23 | SP | Pro | Cat | Cys | Ig |
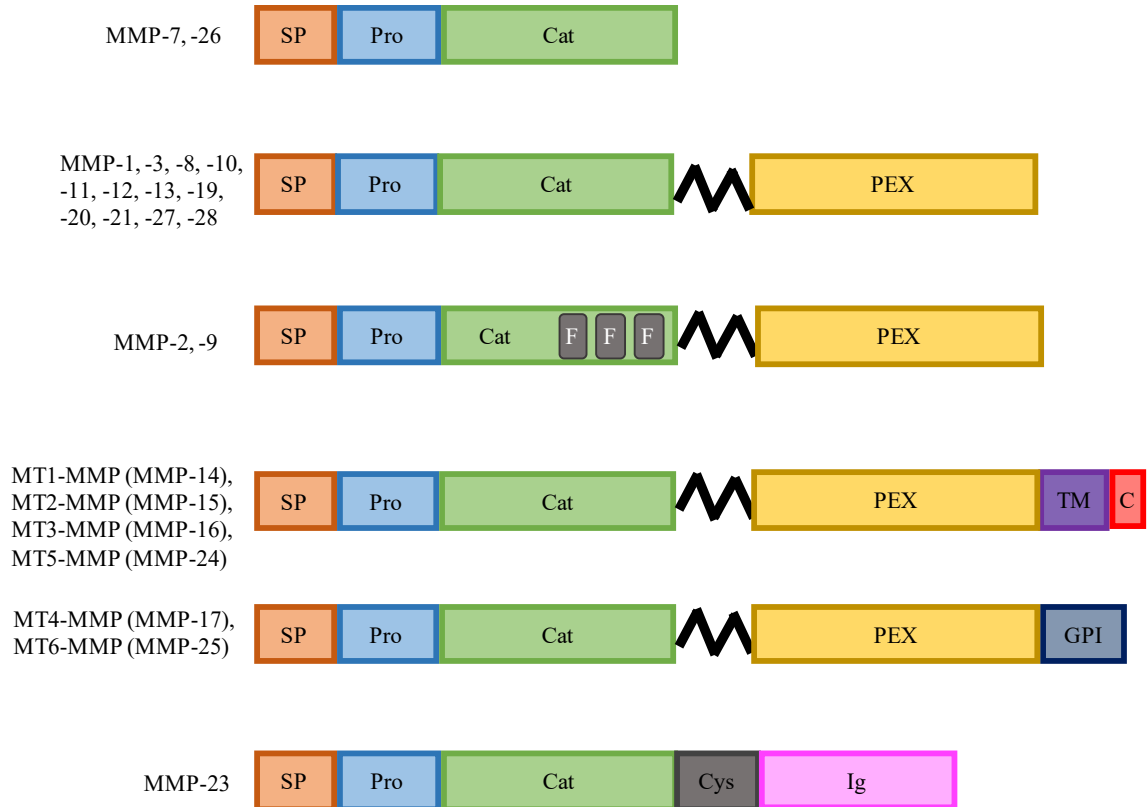
such as clusters of differentiation 44 (CD44) and activate pro-MMP-2 (Gifford and Itoh, 2019). These non-proteolytic functions may in fact help to explain its embryonic necessity.

One of the confounding properties of MT1-MMP is its ability to cause an increase in cell migration even when it is in a proteolytically inactive form (Bonnans et al., 2008; Hara et al., 2011). These studies suggest that MT1-MMP may influence cell migration beyond a role that relies solely on ECM degradation. In fact, recent studies have shed light on a new mechanism of MT1-MMP involving extracellular signal-regulated (ERK) activation (Cepeda et al., 2016; Cepeda et al., 2017; Takino et al., 2010; Willson et al., 2018). The mitogen-activated protein kinase (MAPK)/ERK pathway is a signaling cascade that is initiated by an extracellular mitogen, which subsequently leads to the activation of ERK and the transcription of various genes involved in growth, survival, differentiation, and development (Morrison, 2012). These multifunctional properties reveal the importance of MT1-MMP in both cell-ECM interactions as well as cellular behaviour.

1.2.2   The Gelatinases

The gelatinases, MMP-2 and MMP-9, have been identified as 2 potent secreted proteases due to their ability to cleave gelatin, but more importantly collagen type IV, a major component of basement membranes (Khasigov et al., 2003). Since cleavage of the basement membrane is an important step during cell migration, MMP-2 and MMP-9 have been implicated to play important roles during both development and cancer progression. Although the severity of defects that arise from knocking out only one *MMP* gene may be subdued due to functional redundancy between the different members of the MMP

family, defects have still been observed in single *MMP* knockout mice. For example, *MMP-2* null mice display craniofacial defects (Mosig et al., 2007), and *MMP-9* null mice exhibit defects in endochondral bone formation (Vu et al., 1998), both of which rely on extensive ECM degradation and cell migration.

In adults, ECM remodeling is limited, and any disturbances in *MMP* levels can contribute to the onset and progression of diseases (Visse and Nagase, 2003). While the dysregulation of MMPs is associated with a number of disease states that involve cell migration, including atherosclerosis (Lin et al., 2014), fibrosis (Giannandrea and Parks, 2014), and arthritis (Burrage et al., 2006), a major focus has been on their role in cancer, particularly the importance of MMP-2 and MMP-9, whose upregulation have been associated with tumour progression and metastasis (Bergers et al., 2000; Bernhard et al., 1994; Jodele et al., 2005; Mook et al., 2004). Therefore, as it is crucial that MMP activity be tightly regulated, there are a number of different endogenous inhibitors that control MMP activity, including tissue inhibitors of metalloproteinases (TIMPs) (Visse and Nagase, 2003).

1.3 Tissue Inhibitors of Metalloproteinases

TIMPs, endogenous inhibitors of MMPs, are a small family of secreted proteins. All 4 TIMPs have been identified in mammals, but not all 4 are found in all vertebrates. For example, only TIMP-1, TIMP-2, and TIMP-3 have been identified in frog. Depending on the type, TIMPs are either expressed constitutively or in a tissue-specific manner, and each are regulated at the transcriptional level through cytokine and growth factor signaling (Murphy, 2011). For example, *TIMP-2* is constitutively expressed, whereas *TIMP-3* is expressed predominantly in the central nervous system (Nuttall et al.,

2004). Overall, each TIMP has overlapping abilities to inhibit members of the MMP family. TIMPs contain structurally and functionally distinct N- and C-terminal domains. The N-terminal domain binds to MMPs with a 1:1 molar stoichiometry and inhibits MMP catalytic activity (Gomis-Ruth et al., 1997), whereas the C-terminal domain functions independently by binding to cell surface receptors and inducing cell signaling cascades (Visse and Nagase, 2003).

One of the best described non-MMP-inhibitory functions of TIMPs involves TIMP-2. As previously mentioned in Section 1.2.1, an important function of MT1-MMP is its ability to activate pro-MMP-2 (Itoh et al., 2001). The mechanism involves binding of the C-terminal domain of TIMP-2 to the hemopexin-like domain of pro-MMP-2, while the N-terminal domain of that same TIMP-2 molecule binds the catalytic site of MT1-MMP and inhibits its proteolytic activity. This complex then allows an adjacent active MT1-MMP molecule to cleave the pro-domain of MMP-2, which releases it from the complex in an intermediate form. The intermediate form of MMP-2 then autocatalyzes into its active form (Fig. 1.2) (Itoh et al., 2001). This ability of MT1-MMP to activate MMP-2 and thus increase ECM remodeling therefore further potentiates cell migration.

Due to their importance in mediating ECM turnover, the balance between MMPs and TIMPs is crucial for proper development to occur. For example, overexpression of *TIMP-1, TIMP-2* or *TIMP-3* during early *Xenopus laevis* development all resulted in severe developmental defects (Nieuwesteeg et al., 2012; 2014). Until recently, TIMPs were thought to be the main MMP inhibitors, however, another protein has been discovered to play a role in mediating MMP activity. Reversion-inducing cysteine-rich

Figure 1.2 Pro-MMP-2 activation.

The C-terminal domain of TIMP-2 binds to the hemopexin-like domain of pro-MMP-2, while the N-terminal domain of TIMP-2 binds the catalytic site of a MT1-MMP. An adjacent active MT1-MMP protein then cleaves the pro-domain of MMP-2, thus releasing MMP-2 in its intermediate form. The intermediate form of MMP-2 then undergoes autocatalytic cleavage to generate an active form of MMP-2. (Based on Itoh et al., 2001).
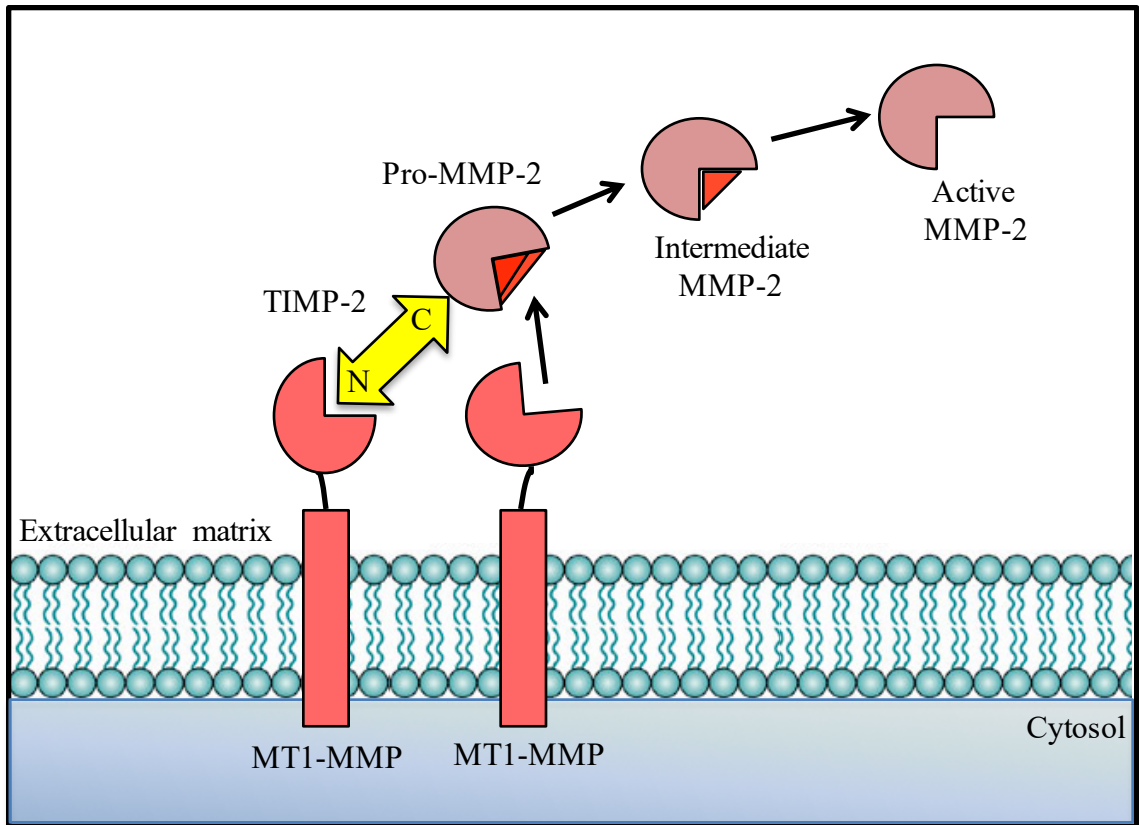
protein with <u>K</u>azal motifs (RECK) encodes a membrane-anchored protein and regulates ECM remodeling by inhibiting MMP activity (Takahashi et al., 1998).

1.4   RECK

1.4.1   Protein Structure

RECK was originally discovered by screening a human fibroblast cDNA library for genes that induced flat cell morphology (reversion-inducing clones) when expressed in transformed mouse fibroblasts (Takahashi et al., 1998). Mammalian RECK proteins are 971 amino acids in length and weigh approximately 110 kDa (Takahashi et al., 1998). Many vertebrate and invertebrate *RECK* sequences cloned to date are highly conserved at the amino acid level and share the domains characteristic of RECK (Willson and Damjanovski, 2014). RECK proteins contain hydrophobic regions flanking both ends of the protein. The N-terminal region encodes a signal peptide sequence and the C-terminal region encodes a glycosylphosphatidylinositol (GPI)-anchoring signal sequence (Fig. 1.3) (Takahashi et al., 1998). RECK was confirmed as a GPI-anchored protein by treatment with phospholipase C, an enzyme that selectively cleaves GPI-anchored proteins from the surface of cells (Takahashi et al., 1998). RECK proteins are also rich in cysteine residues (9%) and contain 5 repeats of a putative cysteine knot motif located near their N-terminus (Fig. 1.3) (Takahashi et al., 1998).

As the name suggests, RECK proteins contain Kazal motifs, which are serine-protease inhibitor-like domains (Fig. 1.3) (Rimphanitchayakit and Tassanakajon, 2010). There are 3 Kazal motif domains in RECK proteins. Evidence shows that these Kazal motifs play an important role in MMP inhibition (Chang et al., 2008). The middle portion of RECK proteins also contains 2 partial EGF-like repeats (Fig. 1.3) (Takahashi

Figure 1.3 Domain organization of a typical RECK protein based on the 971 amino acid human protein sequence.

Mammalian RECK proteins contain a signal sequence at the N-terminus and a GPI anchor signal sequence at the C-terminus (which are not present in the mature protein). The N-terminal region of RECK contains 5 putative cysteine knot motifs. The C-terminal region contains 3 Kazal motifs (MMP inhibitory domains) and 2 epidermal growth factor-like repeats. (Adapted from Takahashi et al., 1998).

🟥 Signal sequence	🟩 EGF-like repeat
🟦 Cysteine knot motif	🟨 Kazal motif
	🟪 GPI anchor sequence

et al., 1998). EGF domains are common to membrane-bound and secreted proteins and have the potential to bind to EGF receptors and stimulate mitosis (Wouters et al., 2005).

1.4.2   Tumour Suppression

Since its discovery in transformed fibroblasts, RECK quickly became recognized as a tumour suppressor protein, and studies were carried out to determine if there was a correlation between *RECK* expression and tumour cell invasiveness. In normal adult tissues, *RECK* mRNA is relatively highly expressed, however, *RECK* expression is low and sometimes undetectable in many tumour-derived cell lines (Takahashi et al., 1998). Takahashi et al. (1998) was the first to determine the *anti*-invasive properties of RECK by generating stable *RECK*-expressing fibrosarcoma cells and showing that invasiveness significantly decreased in *RECK*-expressing cells versus control. Soon after, various human tumours were analyzed to determine the relationship between *RECK* expression and prognosis, including breast (Span et al., 2003), lung (Takenaka et al., 2005), pancreatic (Masui et al., 2003), colorectal (Takeuchi et al., 2004), and prostate (Ohl et al., 2005) cancer. These studies concluded that high *RECK* expression in tumours correlated with better prognosis and survival rate.

Given that loss of RECK is associated with tumour progression, Walsh et al. (2015) examined if loss of RECK is sufficient to transform normal cells. They knocked down *RECK* in normal human mammary epithelial cells and examined cell transformation using xenograft assays. *RECK* knockdown was not sufficient to induce transformation (Walsh et al., 2015). Therefore, although reconstitution of *RECK* in transformed cells reduces invasiveness, loss of *RECK* does not lead to malignant transformation.

1.4.3   MMP Inhibition

RECK was originally identified as a tumour suppressor due to its ability to regulate MMP activity (Takahashi et al., 1998). Numerous *in vitro* studies have shown that RECK can negatively regulate MMP-2, MMP-9, and MT1-MMP activity (Fig. 1.4) (Chang et al., 2008; Matsuzaki et al., 2018; Oh et al., 2001; Simizu et al., 2005; Takahashi et al., 1998). The pioneering study was conducted by Takahashi et al. (1998) who saw a decrease in the amount of pro-MMP-9 in serum collected from fibrosarcoma cells transfected with *RECK*. This result only occurred when RECK was membrane-bound. When RECK was solubilized, pro-MMP-9 levels in the serum did not change (Takahashi et al., 1998). Oh et al. (2001) expanded on these results and reported that levels of active MMP-2 also decreased in *RECK*-expressing fibrosarcoma cells. They also showed that RECK can directly interact with MT1-MMP and inhibit its proteolytic activity.

Since RECK proteins contain Kazal motifs, which are protease-inhibitor domains, it is no surprise that evidence suggests these domains play a role in MMP inhibition. Chang et al. (2008) generated recombinant proteins containing all 3 Kazal motifs (K123) or only the last 2 Kazal motifs (K23). Using human lung cancer cells, they showed that K23 recombinant proteins reduced pro-MMP-9 and active MMP-2 and MMP-9 levels. Moreover, K23 recombinant proteins bound directly to MMP-9. Surprisingly, K123 did not show any MMP inhibition, however, they attributed this result to protein misfolding (Chang et al., 2008). Their results also showed that RECK does not need to be membrane-bound in order for inhibition of pro-MMP-9 to occur (Chang et al., 2008), which is contrary to earlier studies that claimed they did not see a reduction in

Figure 1.4 Role of RECK as an MMP inhibitor.

RECK is a membrane-anchored protein and has been shown to directly inhibit MT1-MMP, MMP-2, and MMP-9 activity. RECK can also inhibit the secretion of pro-MMP-9, although the mechanism is unknown. RECK has also been shown to inhibit *MMP-9* transcription by preventing Fra-1 and c-Jun from binding to the TRE-1 binding site on the *MMP-9* promoter region, leading to less secreted pro-MMP-9. (Based on Chang et al., 2008; Oh et al., 2001; Takagi et al., 2009; Takahashi et al., 1998).

Extracellular matrix

MMP-2

MMP-9

Pro-MMP-9

RECK

MT1-MMP

Cytosol

Nucleus

c-Jun Fra-1

TRE-1
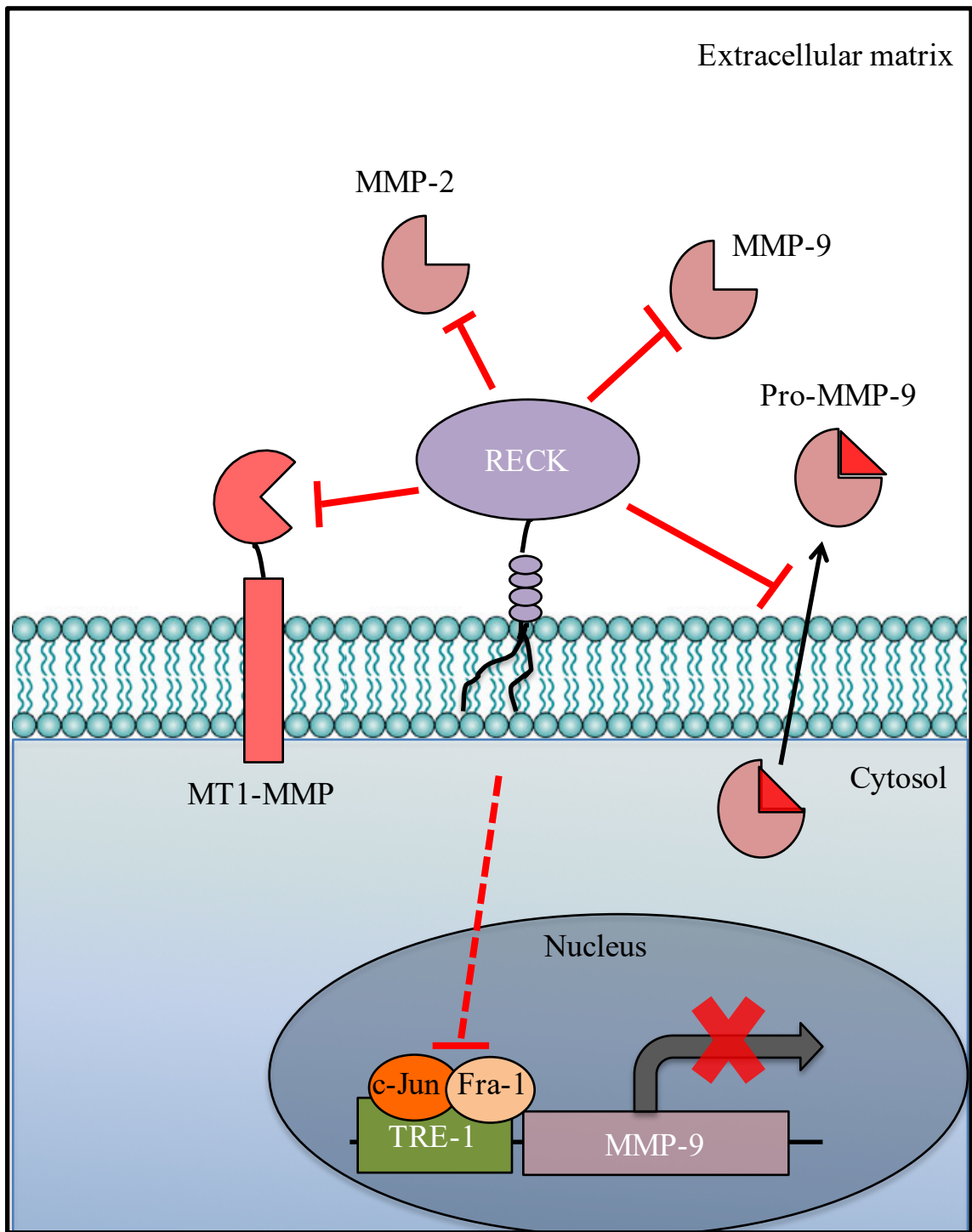
MMP-9

pro-MMP-9 levels using solubilized RECK proteins (Takahashi et al., 1998).

An important factor in the progression of tumour growth and metastasis is the branching of new vascular networks from pre-existing ones, termed angiogenesis (Hoeben et al., 2004). With respect to tumour progression, not only does RECK decrease invasiveness, but RECK has also been shown to suppress tumour angiogenesis. When *RECK*-expressing tumour cells were inoculated into mice, $RECK^+$-tumoured mice lived longer and displayed a reduction in angiogenic sprouting, as was seen by laminin staining versus the mice inoculated with control tumours (Oh et al., 2001).

As a GPI-anchored protein, RECK does not contain an intracellular domain, however, many GPI-anchored proteins are involved in transducing cell-signaling cascades by binding to neighboring receptors (Mayor and Riezman, 2004). Takagi et al. (2009) were the first to discover that RECK decreases *MMP-9* transcription. Overexpression of *RECK* in fibrosarcoma cells caused a decrease in *MMP-9* mRNA, but not *MMP-2* mRNA. Although they also saw a decrease in the amount of MMP-9 present in the serum from *RECK*-expressing fibrosarcoma cells, they attributed this result to the decrease in *MMP-9* mRNA, not inhibition of pro-MMP-9 secretion. They discovered that *RECK* overexpression suppressed the binding of Fos-related antigen 1 (Fra-1) and c-Jun transcription factors to the 12-*O*-tetradecanoylphorbol-13-acetate-responsive element-1 (TRE-1) binding site within the *MMP-9* promoter region in fibrosarcoma cells. However, the mechanisms underlying this process are currently unknown. For example, there is no evidence to suggest that RECK translocates to the nucleus. Instead, RECK may act on the surface of cells by interacting with other cell surface receptors (Takagi et al., 2009).

In fact, a study has suggested that RECK may not only bind to MT1-MMP to

inhibit its catalytic activity, but it may also modulate the endocytic pathway of MT1-MMP. A study performed by Miki et al. (2007) examined whether RECK influences the clearance of MT1-MMP and CD13, another membrane protease, from the cell surface. They found that when RECK was present, it complexed with MT1-MMP and CD13 and caused preferential endocytosis of these proteins using a novel endocytic pathway that was caveolae-independent. This study highlights the multifaceted properties of RECK as a cell surface protein.

1.5   Regulation of RECK

1.5.1   Oncogenic Signaling Represses *RECK* Expression

The MAPK/ERK pathway plays a crucial role in cell proliferation and differentiation, however, aberrant activity of this pathway can lead to malignant transformation (Kohno and Pouyssegur, 2006). For example, activated RAS causes a decrease in ECM proteins and receptors and an increase in MMPs, such as MT1-MMP (Howard et al., 1978; Plantefaber and Hynes, 1989; Thant et al., 1997). RECK was discovered as a downstream target of oncogenic signaling, as reconstitution of *RECK* in *ras*-transformed fibroblasts induced reversion (Takahashi et al., 1998). As such, studies have been carried out to determine how *RECK* is regulated at the transcriptional level by the MAPK/ERK pathway. There is a specificity protein 1 (Sp1)-binding site within the *RECK* promoter region that has been identified as a repressor of *RECK* transcription (Sasahara et al., 1999). Activation of ERK causes phosphorylation of Sp1, which is then recruited to the Sp1 binding site along with histone deacetylase 1 (HDAC) and results in repression of *RECK* transcription (Chang et al., 2004).

1.5.2 TIMP-2 Induces *RECK* Expression

TIMPs are multi-faceted proteins. Not only do TIMPs inhibit MMPs, but they can also bind to cell surface receptors and induce cell-signaling cascades (Li et al., 1999; Oh et al., 2004). Of importance is the upregulation of *RECK* expression by TIMP-2. TIMP-2 was shown to bind to α3β1 integrins on the surface of human endothelial cells, causing inactivation of proto-oncogene tyrosine-protein kinase (Src) through changes in paxillin phosphorylation (Oh et al., 2004). Alteration of paxillin phosphorylation regulates the activation of the small GTPase Ras-related protein 1 (Rap1), which ultimately results in increased expression of *RECK* through unknown mechanisms (Oh et al., 2004).

1.5.3 Glycosylation of RECK

RECK has also been shown to be regulated at the post-translational level. RECK contains 5 putative glycosylation sites at the N-terminal portion of the protein (Takahashi et al., 1998). Glycosylation of 3 of the 5 potential asparagines of RECK are required to suppress tumour cell invasion (Simizu et al., 2005). Simizu et al. (2005) generated *RECK* mutants where they replaced asparagines with glutamines. *RECK* mutant constructs were transfected into fibrosarcoma cells to measure the amount of MMP-2 and MMP-9 levels in the media. Glycosylation of Asn^{297} was required to inhibit MMP-9 secretion and Asn^{352} was required to inhibit the activation of pro-MMP-2. They also correlated glycosylation of RECK with tumour cell invasion and found that glycosylated Asn^{86}, Asn^{297}, and Asn^{352} residues were required to suppress fibrosarcoma cell invasion (Simizu et al., 2005).

1.6 RECK in Development

During embryonic development the ECM undergoes extensive remodeling. As

such, MMPs are expressed, and studies have found that aberrant upregulation of MMPs has been associated with developmental defects and death (Page-McCaw et al., 2007). Therefore, to maintain an appropriate level of MMP activity, MMP inhibitors are also crucial for proper development to occur. Although *TIMP-1* or *TIMP-2* deficiency in mouse embryos has little effect on development (Caterina et al., 2000; Nothnick et al., 1997), most likely due to functional redundancy between TIMPs, *RECK* is necessary for mouse development. Oh et al. (2001) were the first to report that *RECK* knockout in mice resulted in embryonic lethality.

1.6.1 Angiogenesis

When the *RECK* gene was knocked out in mice, about 2/3 of $RECK^{-/-}$ embryos died halfway through embryogenesis at embryonic day (ED) 10.5, and none survived past ED11.5 (Oh et al., 2001). $RECK^{-/-}$ embryos had overt phenotypes, which included abdominal hemorrhaging, disorganized vascularization, disrupted organogenesis, and smaller body sizes (Oh et al., 2001). Although vascular networks were present in $RECK^{-/-}$ embryos, histological examination of these tissues indicated abnormally large and deformed blood vessels, which indicated defects in angiogenesis rather than vasculogenesis (Oh et al., 2001).

Due to its characterized role in MMP inhibition, $RECK^{-/-}$ mice were analyzed to determine if there was aberrant upregulation of MMPs *in vivo*. Oh et al. (2001) plated ED10.5 cells and collected the serum. MMP-2 activity was elevated in $RECK^{-/-}$ embryos, however, since pro-MMP-9 is not expressed until ED11, MMP-9 activity was not detected (Oh et al., 2001). Collagen IV and laminin were also disrupted in areas surrounding blood vessels and the neural tube in $RECK^{-/-}$ embryos (Oh et al., 2001).

These results suggest that loss of *RECK* caused aberrant upregulation of MMPs and disruption of the basal lamina. This is supported by the fact that *RECK*, *MMP-2*, and *MT1-MMP* expression patterns overlap in the areas surrounding the neural tube. Furthermore, a similar phenotype was seen in *collagen 1*$^{-/-}$ mice, which also died due to ruptured blood vessels (Löhler et al., 1984). A partial rescue of the *RECK* mutant phenotype was obtained by generating *RECK*$^{-/-}$/*MMP-2*$^{-/-}$ double mutants. These embryos had larger body sizes and improved vascular integrity, however, they still died half a day later (ED11.5) (Oh et al., 2001). On the other hand, *RECK*$^{-/-}$/*MT1-MMP*$^{-/-}$ mutants did not rescue the *RECK* mutant phenotype (Oh et al., 2001).

Chandana et al. (2010) tried a conditional *RECK* knockout by silencing the *RECK* gene using tamoxifen-inducible treatment at ED11, however, mice still showed lethality. Conditional *RECK*$^{-/-}$ mutants had large and deformed blood vessels as well as large cavities in the brain vasculature at ED15.5 (Chandana et al., 2010). This phenotype was also apparent when Prendergast et al. (2012) knocked down *RECK* in zebrafish using Morpholinos (MO). *RECK* knockdown embryos had impaired vascular integrity and intracranial hemorrhaging 48 hours post-fertilization (Prendergast et al., 2012). This suggests that RECK function is conserved throughout development and essential particularly with respect to vascular development.

Since RECK was implicated to play a role in angiogenesis during development, Chandana et al. (2010) decided to examine the importance of RECK in maternal vascular remodeling in mice. The uterus of a pregnant mouse is one of the most active sites of angiogenesis in adult mice (Abrahamsohn and Zorn, 1993; Cross et al., 1994; Dey et al., 2004). *MMP-2* and *MMP-9* expression patterns are very dynamic during vascular

remodeling in the uterus and are required for proper ECM remodeling (Curry and Osteen, 2003; Wang and Dey, 2006). However, it is unclear how some blood vessels are protected while others undergo extensive vascular sprouting. RECK was implicated to play a role in vascular remodeling in maternal tissues. *RECK* is expressed in cells associated with remodeling blood vessels in the mouse implantation chamber (Chandana et al., 2010). When they knocked down *RECK* expression within the implantation chamber using short hairpin RNA (shRNA), cavities and tissue slits were present instead of organized and compact blood vessels (Chandana et al., 2010). They also saw decreased collagen IV surrounding the deformed blood vessels (Chandana et al., 2010). This phenotype is very similar to the vascular defects seen in *RECK*$^{-/-}$ embryos and supports the role of RECK as a key regulator during angiogenic sprouting (Chandana et al., 2010). Mechanisms of RECK action during angiogenesis have been proposed by Chandana et al. (2010). The most likely scenario suggests that RECK helps mark and protect the blood vessels that are preserved during angiogenic sprouting by inhibiting surrounding MMPs. However, *RECK*$^{-/-}$ embryos cannot be rescued by *MMP* null mutations, although this may be due to functional redundancy between MMPs. Instead, RECK may affect intracellular signaling pathways by protecting ECM proteins and other cell surface receptors (Chandana et al., 2010). Angiogenesis occurs when vascular endothelial growth factor (VEGF) and Notch signaling regulate endothelial tip cell formation (Adams and Alitalo, 2007; Carmeliet, 2005; Roca and Adams, 2007). Delta-like 4 (Dll4), a ligand of Notch signaling, has been reported to reduce tip cell formation and thus vascular sprouting (Phng and Gerhardt, 2009). Interestingly, the vascular defects seen in *RECK*$^{-/-}$ embryos are very similar to the phenotype that occurs in mouse embryos with attenuated Notch

signaling (Krebs et al., 2000; Xue et al., 1999). RECK has been shown to activate Notch signaling during cortical neurogenesis by protecting Dll4 from being shed from the membrane (Muraguchi et al., 2007). Therefore, *RECK* deficiency may suppress Notch signaling during embryonic and maternal angiogenesis and cause excessive sprouting (Fig. 1.5). However, this mechanism of action does not solely explain the large cavities formed in *RECK*-deficient tissues. The biggest unanswered question that remains is why RECK is necessary for embryonic angiogenesis but suppresses tumour angiogenesis. Although it was recently discovered that RECK suppresses angiogenesis by downregulating signal transducer and activator of transcription 3 (STAT3) (Walsh et al., 2015), no link has been made to whether or not this process occurs during developmental angiogenesis.

1.6.2 Neurogenesis

Notch signaling is a highly conserved pathway that is crucial during development to ensure cell fate specification, stem cell maintenance, and tissue patterning (Roca and Adams, 2007). In the mammalian central nervous system, Notch ligands, Dll and Jagged, are expressed on the surface of neural cells and bind to Notch present on the surface of neighboring neural precursor cells (Roca and Adams, 2007). Once activated, Notch signaling maintains neural precursor cells in an undifferentiated state (Roca and Adams, 2007). Notch signaling is regulated by a disintegrin and metalloproteinase-10 (ADAM-10) (Yang et al., 2006). ADAM-10 proteases are expressed throughout development in various neural cells in the mammalian central nervous system and inhibit Notch signaling by cleaving Notch ligands from the surface of neural cells to allow differentiation (Kärkkäinen et al., 2000; LaVoie and Selkoe, 2003; Mishra-Gorur et al.,

Figure 1.5 Role of RECK in vascular sprouting.

During vascular sprouting in tip cells, VEGF and Notch signaling modulate the selective formation of tip cells. VEGF signaling in tip cells leads to high levels of Dll4. Dll4 binds to Notch on neighboring stalk cells, which induces Notch signaling and attenuates VEGFR signaling. RECK has been proposed to regulate vascular sprouting by maintaining Notch signaling, however the mechanism is currently unknown. (Based on Muraguchi et al., 2007).

VEGF

VEGFR

Tip cell

RECK

Dll4

Notch

ICD

VEGFR signaling
(maintenance of stalk cells)

Stalk cell
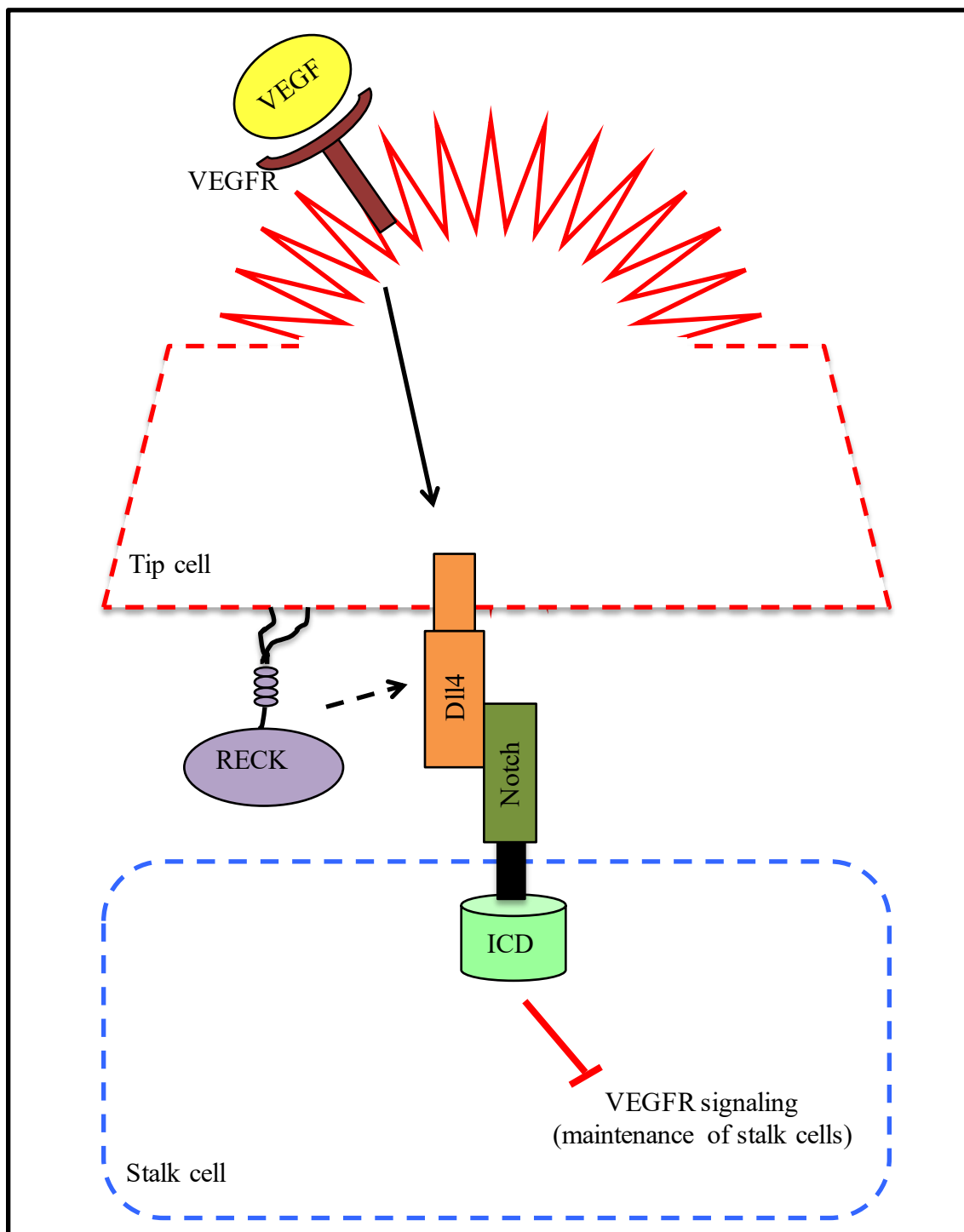
2002).

RECK$^{-/-}$ mice embryos not only had vascular defects, but they also had premature differentiation of neural precursor cells (Muraguchi et al., 2007). This phenotype was a result of impaired Notch signaling in the central nervous system (Muraguchi et al., 2007). They demonstrated that RECK regulated Notch signaling by directly inhibiting ADAM-10 in neural precursor cells. They confirmed this by showing a direct interaction between RECK and ADAM-10 by co-immunoprecipitation as well as by co-electroporating shRNA targeting *ADAM-10* and *RECK* in the central nervous system of ED12.5 wildtype embryos and rescuing the phenotype induced by *RECK* depletion (Muraguchi et al., 2007).

A more recent study expanded on these results and reported that RECK was regulated within this pathway by glycerophosphodiester phosphodiesterase 2 (GDE2) (Park et al., 2013). GDE2 is a 6-transmembrane protein that is crucial for the differentiation of spinal motor neurons by inhibiting Notch signaling (Rao and Sockanathan, 2005; Sabharwal et al., 2011; Yan et al., 2009). Interestingly, *GDE2* and *RECK* mRNA expression colocalize in differentiating motor neurons during neurogenesis in chicks (Park et al., 2013). Using chick spinal cord extracts, they determined that GDE2 cleaves RECK within the GPI-anchor. The release of RECK prevents inhibition of ADAM-10, which then sheds Dll from the surface and attenuates Notch signaling (Fig. 1.6) (Park et al., 2013).

1.6.3   Neural Crest Cell Migration

Neural crest cells are a transient population of migratory cells that differentiate into a variety of cell types within the vertebrate embryo, including melanocytes, smooth

Figure 1.6 Role of RECK in neurogenesis.

RECK maintains Notch signaling in neural progenitor cells by inhibiting the proteolytic activity of ADAM-10 on the surface of neural cells. ADAM-10 sheds Notch ligands from the surface, preventing the intracellular domain (ICD) of Notch to translocate to the nucleus and turn on target genes that maintain neural progenitor cells. The presence of RECK prevents shedding of Notch ligands and maintains Notch signaling. In addition, GDE2 regulates RECK by cleaving its GPI-anchor. This prevents inhibition of ADAM-10 and thus attenuates Notch signaling. (Based on Muraguchi et al., 2007; Park et al., 2013; Yang et al., 2006).

GDE2

Cytosol

ADAM-10

RECK

Dll4

Notch

Extracellular matrix

Neural progenitor cell

ICD

Maintenance of stem
cells

ICD
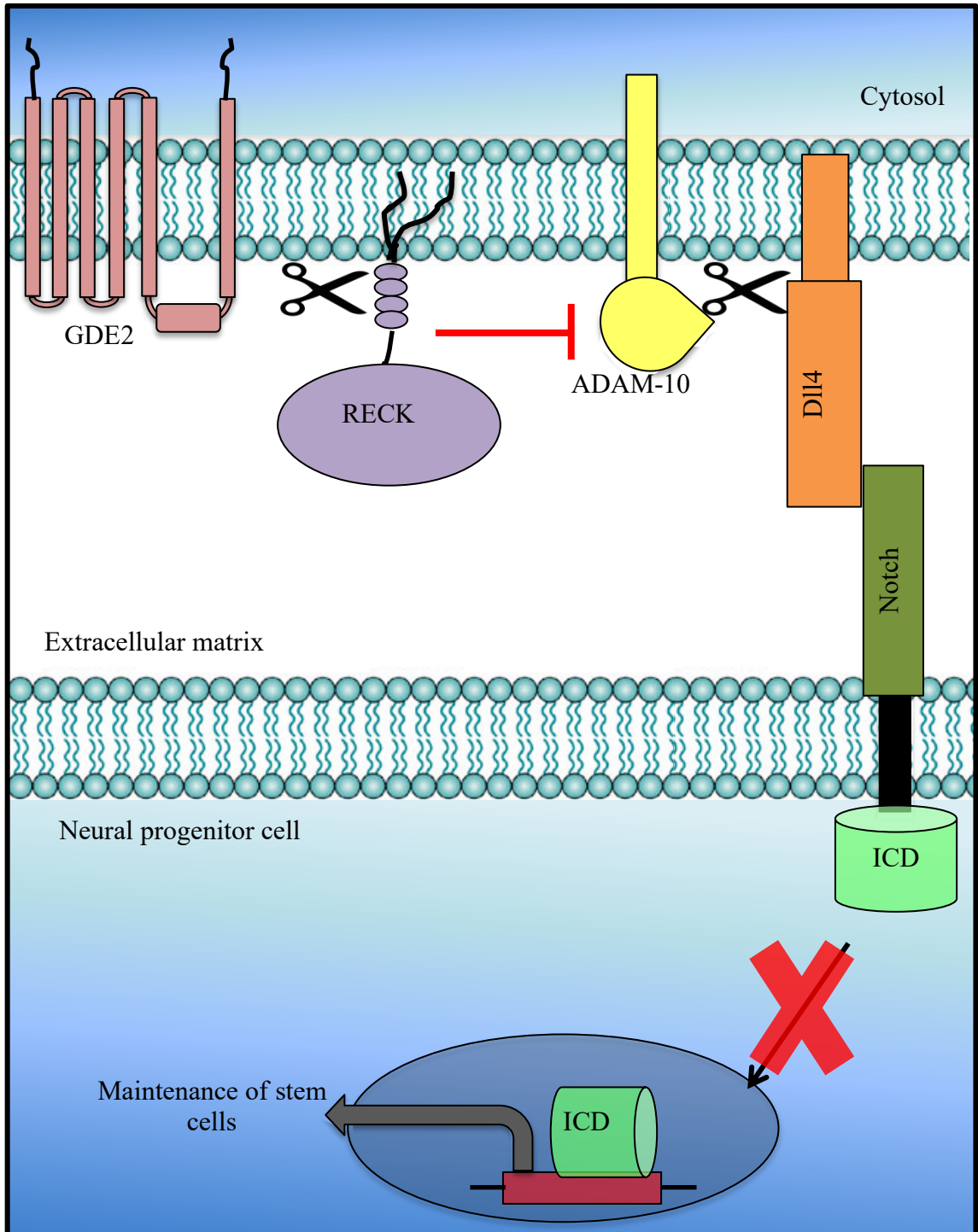
muscle, sensory ganglia, and craniofacial cartilage and bone (Le Douarin and Kalcheim, 1999). *RECK* knockdown in zebrafish embryos was also reported to have defects in neural crest migration (Prendergast et al., 2012). Prendergast et al. (2012) began their study by screening zebrafish mutants that were unable to form the dorsal root ganglia (DRG) by looking at *neurogenin* expression and found that this phenotype was a result of a mutation in the *RECK* gene. In the absence of *RECK*, neural crest cells exhibited aberrant migratory behaviour and were unable to migrate to the appropriate position for differentiation into DRG. They confirmed this phenotype by also knocking down *RECK* expression using MOs (Prendergast et al., 2012). *RECK* mutants displayed increased MMP activity, as shown by taking protein extracts from embryos and incubating them with dye-quenched (DQ) gelatin, a substrate that allows for quantification of MMP activity (Prendergast et al., 2012). However, this phenotype could not be rescued by the treatment of MMP inhibitors (Prendergast et al., 2012). This study was also the first to determine that RECK function is cell autonomous. Cells taken from wildtype embryos and transplanted into *RECK* knockdown embryos were able to form DRG, but they couldn't induce the host cells (*RECK* knockdown cells) to form DRG (Prendergast et al., 2012).

1.6.4   Limb Patterning

When the *RECK* gene was knocked out in mice, embryos did not survive past ED11 (Oh et al., 2001). Therefore, although studies have focused on the role of RECK early on during development, little is understood regarding developmental processes occurring later in embryogenesis. Therefore, Yamamoto et al. (2012) generated low-*RECK* mutants, which have reduced *RECK* expression, to examine later stages of

development. The most obvious phenotype displayed in these mutants was limb abnormalities. Further histological examination showed poor chondrocyte condensation in forelimb buds (Yamamoto et al., 2012). To determine potential morphogenetic signaling molecules affected by low *RECK* expression in mice such as Wnt7a signaling and sonic hedgehog (Shh) signaling, *in situ* hybridization was performed. These signaling pathways were all attenuated in low-*RECK* mutants (Yamamoto et al., 2012). Interestingly, *Wnt7a$^{-/-}$* embryos displayed very similar limb abnormality phenotypes, whereas deficiencies in the other signaling pathways (such as *Shh* or bone morphogenetic protein (*BMP*)) yielded distinctly different phenotypes (Adamska et al., 2004; Chiang et al., 1996; Selever et al., 2004). Indeed, *Wnt7a* expression was greatly reduced in low-*RECK* mutant forelimb buds. They came to the conclusion that RECK is required for Wnt7a signaling in the forelimb bud (Yamamoto et al., 2012).

1.7   The *X. laevis* System

The African clawed frog, *X. laevis,* has been widely used in the developmental biology field since the 1950s (Schmitt et al., 2014). The *X. laevis* system provides a number of advantages as a model organism, including the ease of *in vitro* fertilization and rearing as well as their resilience to experimental manipulation. Moreover, development occurs rapidly, and each stage has been well-characterized (Nieuwkoop and Faber, 1956). *X. laevis* embryos are large (approximately 1 mm in diameter) and therefore developmental stages are easily recognizable (Fig. 1.7). Development begins at fertilization (stage 1), followed by the blastula stage (stage 9), at which time zygotic transcription is turned on. Within the first 24 hours post fertilization, gastrulation occurs (stage 10-12), in which the 3 germ layers are formed (ectoderm, mesoderm, and

Figure 1.7 Schematic representation of *X. laevis* developmental stages.

(a) Development begins with a fertilized single cell egg. Stage 9 (blastula stage) marks the onset of zygotic transcription. Gastrulation occurs between stages 10 and 12 to form the 3 germ layers (ectoderm, mesoderm, and ectoderm) and the embryonic axes. Neurulation occurs between stages 14 and 20 to form the neural tube. Organogenesis and differentiation are predominant in the tailbud stages (stages 21-28) and beyond. By stage 37 the embryo has hatched, and by stage 41 embryos have developed into feeding tadpoles. (b) Schematic representation of an early tailbud embryo to denote the embryonic axes. Dorsal refers to back and ventral refers to front (belly). Anterior refers to head and posterior refers to tail. (Adapted from Nieuwkoop and Faber, 1956).

(a)

Fertilized (Stage 1)	Blastula (Stage 9)	Gastrula (Stage 12)	Neurula (Stage 14-20)	Tailbud (Stage 21-28)	Hatched (Stage 37)	Tadpole (Stage 41)
0 hrs	7 hrs	13 hrs	20 hrs	1 dpf	2 dpf	3 dpf

(b)

Anterior

Ventral — Dorsal

Posterior
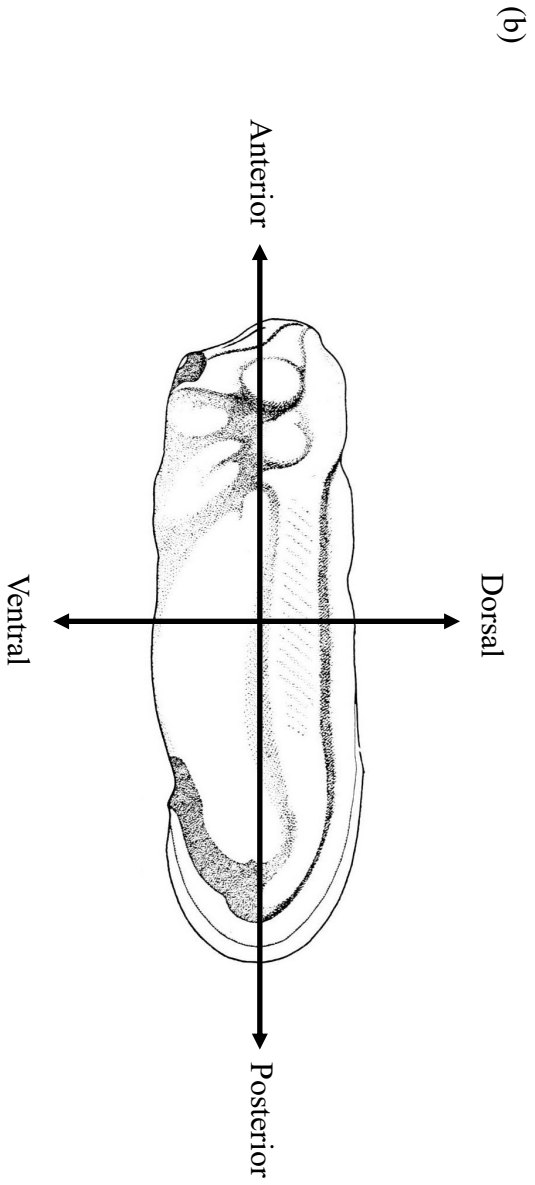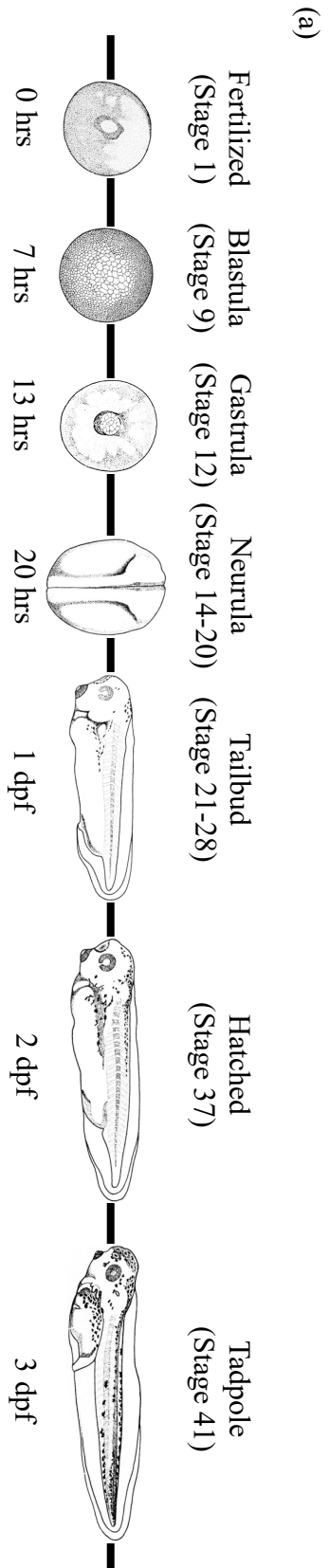
endoderm) as well as the embryonic axes, followed by neurulation, which occurs between stages 14 and 20 to form the neural tube (neural crest cell migration begins during these stages as well). Organogenesis and differentiation begin at the tailbud stages, and by 3 days post fertilization (dpf), a functional free-swimming tadpole has developed (Fig. 1.7). Thus, *X. laevis* has been a fundamental tool in studying cell cycle, cell metabolism, cell behaviour, and cell migration during development (Hardwick and Philpott, 2015).

For a long time, investigators have taken advantage of the parallels that exist between embryonic development and cancer metastasis. Many signaling pathways that are crucial for normal development, such as BMP, Shh, and Notch pathways, become unregulated during cancer metastasis (Bailey et al., 2007). ECM remodeling is yet another example of an event that is highly dynamic during both development and cancer metastasis. Therefore, using *X. laevis* as a model organism to study ECM remodeling during development can assist in understanding why this process becomes uncontrolled during tumour progression.

In vitro cell culture work can also be conducted using A6 cells, a well-established cell line derived from *X. laevis* kidney tissue. These cells behave like typical polarized epithelial cells and can be instrumental in studying cell signaling pathways and cell behaviour *in vitro* (Mimori-Kiyosue et al., 2007), pathways which can be difficult to discern in a multicellular embryo.

1.8   Research Project

1.8.1   Summary

ECM remodeling is a highly dynamic process that is important for the development and maintenance of multicellular organisms. ECM degradation occurs

primarily through MMPs, and their activity is modulated by their endogenous inhibitors, TIMPs and RECK. Numerous studies have shown that perturbing the delicate balance that exists between MMPs and their inhibitors can lead to devastating consequences to the integrity and function of tissues. For example, uncontrolled ECM remodeling can contribute to the onset and progression of cancer metastasis. For these reasons, it is essential to understand the functions and interplay of these proteins and how they control ECM remodeling to ensure proper development and tissue homeostasis.

The importance of RECK during development is becoming more evident, as studies have already identified a role for RECK during angiogenesis, neural crest cell migration, and limb patterning. Not only does RECK inhibit MMP function at many levels, there is also emerging evidence suggesting that RECK may play a more important role in regulating intracellular signaling. However, most research characterizing RECK function has been done *in vitro* in tumour-derived cell lines. My research focused on the functional characterization of RECK during *X. laevis* development, a well-established developmental model. By disrupting endogenous *RECK* levels, I attempted to elucidate the molecular mechanisms that are critical for balancing the proteolytic activity of MMPs with the role of RECK required for proper ECM remodeling and tissue patterning during development.

1.8.2   Hypotheses

1) Previous studies have revealed similar biological functions of RECK in vertebrates, therefore, I hypothesize that all domains of vertebrate RECK peptide sequences will share high evolutionary conservation.

2) Since *RECK* transcripts are localized to dorsal axial structures in *X. laevis* embryos, I hypothesize that alteration of *RECK* levels will cause axial and neural tube defects in *X. laevis* embryos resulting from excessive ECM remodeling.

3) Previous studies have demonstrated that RECK is an inhibitor of MT1-MMP, therefore, I hypothesize that *X. laevis* RECK will colocalize with MT1-MMP in dorsal axial structures, including the neural tube and head region.

4) Given that RECK has an established role as an MMP inhibitor, I hypothesize that knockdown/shedding of *RECK* in *X. laevis* A6 cells will result in increased MT1-MMP and MMP-2 levels, whereas overexpression of *RECK* will result in reduced MT1-MMP and MMP-2 levels.

1.8.3   Objectives

The overarching goal of this research was to characterize the role of *X. laevis* RECK during development. I previously cloned the mature *X. laevis RECK* sequence, which lacked the N-terminal signal sequence and C-terminal GPI-anchor signal sequence, as part of my Master's thesis, and performed a preliminary sequence comparison analysis of RECK. However, that study was limited by the number of available annotated sequences at the time. For this Doctoral study, I finished cloning the full-length *X. laevis RECK* gene and performed a detailed sequence comparison of RECK with more diverse species to determine evolutionary conservation. This research had the following objectives:

1) To perform a comparison of amino acid sequence identity of *X. laevis* RECK to other sequences to determine evolutionary conservation of domains (Chapter 2).

2) To knock down *RECK* in *X. laevis* embryos using a MO approach. Following *RECK* knockdown, to examine embryos for any subsequent morphological changes and developmental defects and correlate these defects with alterations in mRNA levels of developmental marker genes as well as ECM-remodeling genes (Chapter 2).

3) To perform immunohistochemistry (IHC) on transverse sections of embryos to determine the localization patterns of RECK, MT1-MMP, and TIMP-2 during *X. laevis* neurulation and organogenesis (Chapter 3).

4) To disrupt endogenous levels of RECK in *X. laevis* A6 cells using a combination of overexpression, knockdown, and phosphatidylinositol-specific phospholipase C (PI-PLC) treatment experiments and examine the effects on MT1-MMP, MMP-2 and phosphorylated ERK (pERK) levels (Chapter 4).

1.9 References

Abrahamsohn, P.A., Zorn, T.M. (1993). Implantation and decidualization in rodents. J Exp Zool. **266**: 603-628.

Adams, R.H., Alitalo, K. (2007). Molecular regulation of angiogenesis and lymphangiogenesis. Nat Rev Mol Cell Biol. **8**: 464-478.

Adamska, M., MacDonald, B.T., Sarmast, Z.H., Oliver, E.R. Meisler, M.H. (2004). En1 and Wnt7a interact with Dkk1 during limb development in the mouse. Dev Biol. **272**: 134-144.

Bailey, J.M., Singh, P.K., Hollingsworth, M.A. (2007). Cancer metastasis facilitated by developmental pathways: Sonic hedgehog, Notch, and bone morphogenic proteins. J Cell Biochem. **102**: 829-839.

Bergers, G., Brekken, R., McMahon, G., Vu, T.H., Itoh, T., Tamaki, K., Tanzawa, K., Thorpe, P., Itohara, S., Werb, Z., Hanahan, D. (2000). Matrix metalloproteinase-9 triggers the angiogenic switch during carcinogenesis. Nat Cell Biol. **2**: 737-744.

Bernhard, E.J., Gruber, S.B., Muschel, R.J. (1994). Direct evidence linking expressing of matrix metalloproteinase 9 (92-kDa gelatinase/collagenase) to the metastatic phenotype in transformed rat embryo cells. Proc Natl Acad Sci USA. **91**: 4293-4297.

Bonnans, C., Chou, J., Werb, Z. (2008). Remodelling the extracellular matrix in development and disease. Nat Rev Mol Cell Biol. **15**: 786-801.

Burrage, P. S., Mix, K.S., Brinckerhoff, C.E. (2006). Matrix metalloproteinases: role in arthritis. Front Biosci. **11**: 529-543.

Carmeliet, P. (2005). Angiogenesis in life, disease and medicine. Nature. **438**: 932-936.

Caterina, J.J., Yamada, S., Caterina, N.C., Longenecker, G., Holmback, K., Shi, J., Yermovsky, A.E., Engler, J.A., Birkedal-Hansen, H. (2000). Inactivating mutation of the mouse tissue inhibitor of metalloproteinases-2 (Timp-2) gene alters proMMP-2 activation. J Biol Chem. **275**: 26416-26422.

Cepeda, M.A., Evered, C.L., Pelling, J.H., Damjanovski, S. (2017). Inhibition of MT1-MMP proteolytic function and ERK1/2 signalling influences cell migration and invasion through changes in MMP-2 and MMP-9 levels. J Cell Commun Signal. **11**: 167-179.

Cepeda, M.A., Pelling, J.J., Evered, C.L., Williams, K.C., Freedman, Z., Stan, I., Willson, J.A., Leong H.S., Damjanovski, S. (2016). Less is more: low expression of MT1-MMP is optimal to promote migration and tumourigenesis of breast cancer cells. Mol Cancer. **15**: 65.

Chandana, E.P.S., Maeda, Y., Ueda, A., Kiyonari, H., Oshima, N., Yamamoto, M., Kondo, S., Oh, J., Takahashi, R., Yoshida, Y., Kawashima, S., Alexander, D.B., Kitayama, H., Takahashi, C., Tabata, Y., Matsuzaki, T., Noda, M. (2010). Involvement of the Reck tumor suppressor protein in maternal and embryonic vascular remodeling in mice. BMC Dev Biol. **10**: 84.

Chang, C.K., Hung, W.C., Chang, H.C. (2008). The Kazal motifs of RECK protein inhibit MMP-9 secretion and activity and reduce metastasis of lung cancer cells *in vitro* and *in vivo*. J Cell Mol Med. **12**: 2781-2789.

Chang, H.C., Liu, L.T., Hung, W.C. (2004). Involvement of histone deacetylation in *ras*-induced down-regulation of the metastasis suppressor RECK. Cell Signal. **16**: 675-679.

Chiang, C., Litingtung, Y., Lee, E., Young, K.E., Corden, J.L., Westphal, H., Beachy, P.A. (1996). Cyclopia and defective axial patterning in mice lacking Sonic hedgehog gene function. Nature. **383**: 407-413.

Cross, J.C., Werb, Z., Fisher, S.J. (1994). Implantation and the placenta: key pieces of the development puzzle. Science. **266**: 1508-1518.

Curry, T.E. Jr., Osteen, K.G. (2003). The matrix metalloproteinase system: changes, regulation, and impact throughout the ovarian and uterine reproductive cycle. Endocr Rev. **24**: 428-465.

Daley, W.P., Peters, S.B., Larsen, M. (2008). Extracellular matrix dynamics in development and regenerative medicine. J Cell Sci. **121**: 255-264.

Dey, S.K., Lim, H., Das, S.K., Reese, J., Paria, B.C., Daikoku, T., Wang, H. (2004). Molecular cues to implantation. Endocr Rev. **25**: 341-373.

Giannandrea, M., Parks, W.C. (2014). Diverse functions of matrix metalloproteinases during fibrosis. Dis Model Mech. **7**: 193-203.

Gifford, V., Itoh, Y. (2019). MT1-MMP-dependent cell migration: proteolytic and non-proteolytic mechanisms. Biochem Soc Trans. **47**: 811-826.

Gomis-Ruth, F.X., Maskos, K., Betz, M., Bergner, A., Huber, R., Suzuki, K., Yoshida, N., Brew, K., Bourenkov, G.P., Bartunik, H., Bode, W. (1997). Mechanism of inhibition of the human matrix metalloproteinase stromelysin-1 by TIMP-1. Nature. **221**: 77-81.

Hara, T., Mimura, K., Seiki, M., Sakamoto, T. (2011). Genetic dissection of proteolytic and non-proteolytic contributions of MT1-MMP to macrophage invasion. Biochem Biophys Res Commun. **413**: 277-281.

Hardwick, L.J.A., Philpott, A. (2015). An oncologist's friend: How Xenopus contributes to cancer research. Dev Biol. **408**: 180-187.

Hoeben, A., Landuyt, B., Highley, M.S., Wildiers, H., Van Oosterom, A.T., De Bruijn, E.A. (2004). Vascular endothelial growth factor and angiogenesis. Pharmacol Rev. **56**: 549-580.

Holmbeck, K., Bianco, P., Caterina, J., Yamada, S., Kromer, M., Kuznetsov, S.A., Mankani, M., Robey, P.G., Poole, A.R., Pidoux, I., Ward, J.M., Birkedal-Hansen, H. (1999). MT1-MMP deficient mice develop dwarfism, osteopenia, arthritis, and connective tissue disease due to inadequate collagen turnover. Cell. **99**: 81-92.

Howard, B.H., Adams, S.L., Sobel, M.E., Pastan, I., de Crombrugghe, B. (1978). Decreased levels of collagen mRNA in rous sarcoma virus-transformed chick embryo fibroblasts. J Biol Chem. **253**: 5869-5874.

Jodele, S., Chantrain, C.F., Blavier, L., Lutzko, C., Crooks, G.M., Shimada, H., Coussens, L.M., Declerck, Y.A. (2005). The contribution of bone marrow-derived cells to the tumor vasculature in neuroblastoma is matrix metalloproteinase-9 dependent. Cancer Res. **65**: 3200-3208.

Kärkkäinen, I., Rybnikova, E., Pelto-Huikko, M., Huovila, A.P. (2000). Metalloprotease-disintegrin (ADAM) genes are widely and differentially expressed in the adult CNS. Mol Cell Neurosci. **15**: 547-560.

Khasigov, P.Z., Podobed, O.V., Gracheva, T.S., Salbiev, K.D., Grachev, S.V., Berezov, T.T. (2003). Role of matrix metalloproteinases and their inhibitors in tumor invasion and metastasis. Biochemistry (Mosc). **68**: 711-717.

Krebs, L.T., Xue, Y., Norton, C.R., Shutter, J.R., Maguire, M., Sundberg, J.P., Gallahan, D., Closson, V., Kitajewski, J., Callahan, R., Smith, G.H., Stark, K.L., Gridley, T. (2000). Notch signaling is essential for vascular morphogenesis in mice. Genes Dev. **14**: 1343-1352.

Kohno, M., Pouyssegur, J. (2006). Targeting the ERK signaling pathway in cancer therapy. Ann Med. **38**: 200-211.

LaVoie, M.J., Selkoe, D.J. (2003). The Notch ligands, Jagged and Delta, are sequentially processed by alpha-secretase and presenilin/gamma-secretase and release signaling fragments. J Biol Chem. **278**: 34427-34437.

Le Douarin, N., Kalcheim, C. (1999). The Neural Crest. Cambridge University Press, Cambridge, UK.

Li, G., Fridman, R., Kim, H.R. (1999). Tissue inhibitor of metalloproteinase-1 inhibits apoptosis of human breast epithelial cells. Cancer Res. **59**: 6267-6275.

Lin, J., Kakkar, V., Lu, X. (2014). Impact of matrix metalloproteinases on atherosclerosis. Curr Drug Targets. **15**: 442-453.

Löhler, J., Timpl, R., Jaenisch, R. (1984). Embryonic lethal mutation in mouse collagen I gene causes rupture of blood vessels and is associated with erythropoietic and mesenchymal cell death. Cell. **38**: 597-607.

Masui, T., Doi, R., Koshiba, T., Fujimoto, K., Tsuji, S., Nakajima, S. (2003). RECK expression in pancreatic cancer: its correlation with lower invasiveness and better prognosis. Clin Cancer Res. **9**: 1779-1784.

Matsuzaki, T., Kitayama, H., Omura, A., Nishimoto, E., Alexander, D.B., Noda, M. (2018). The RECK tumor-suppressor protein binds and stabilizes ADAMTS10. Biol Open. **7**: bio033985.

Mayor, S., Riezman, H. (2004). Sorting GPI-anchored proteins. Nat Rev Mol Cell Biol. **5**: 110-120.

McKee, T.J., Perlman, G., Morris, M., Komarova, S.V. (2019). Extracellular matrix composition of connective tissues: a systematic review and meta-analysis. Sci Rep. **9**: 10542.

Miki, T., Takegami, Y., Okawa, K., Muraguchi, T., Noda, M., Takahashi, C. (2007). The reversion-inducing cysteine-rich protein with Kazal motifs (RECK) interacts with membrane type 1 matrix metalloproteinase and CD13/aminopeptidase N and modulates their endocytic pathways. J Biol Chem. **282**: 12341-12352.

Mimori-Kiyosue, Y., Matsui, C., Sasaki, H., Tsukita, S. (2007). Adenomatous polyposis coli (APC) protein regulates epithelial cell migration and morphogenesis via PDZ domain-based interactions with plasma membranes. Genes Cells: Devot Mol Cell Mech. **12**: 219-233.

Mishra-Gorur, K., Rand, M.D., Perez-Villamil, B., Artavanis-Tsakonas, S. (2002). Down-regulation of Delta by proteolytic processing. J Cell Biol. **159**: 313-324.

Mook, O.R., Frederiks, W.M., van Noorden, C.J. (2004). The role of gelatinases in colorectal cancer progression and metastasis. Biochim Biophys Acta. **1705**: 69-89.

Morrison, D.K. (2012). MAP Kinase Pathways. Cold Spring Harb Perspect Biol. **4**: a011254.

Mosig, R.A., Dowling, O., DiFeo, A., Ramirez, M.C.M., Parker, I.C., Etsuko, A. (2007). Loss of MMP-2 disrupts skeletal and craniofacial development, and results in decreased bone mineralization, joint erosion, and defects in osteoblast and osteoclast growth. Hum Mol Genet. **16**: 1113-1123.

Muraguchi, T., Takegami, Y., Ohtsuka, T., Kitajima, S., Chandana, E.P., Omura, A., Miki, T., Takahashi, R., Matsumoto, N., Ludwig, A., Noda, M., Takahashi, C. (2007). Reck modulates Notch signaling during cortical neurogenesis by regulating ADAM10 activity. Nat Neurosci. **10**: 838-845.

Murphy, G. (2011). Tissue inhibitors of metalloproteinases. Genome Biol. **12**: 233.

Nieuwesteeg, M.A., Walsh, L.A., Fox, M.A., Damjanovski, S. (2012). Domain specific overexpression of TIMP-2 and TIMP-3 reveals MMP-independent functions of TIMPs during *Xenopus laevis* development. Biochem Cell Biol. **90***: 585-595.

Nieuwesteeg, M.A., Willson, J.A., Cepeda, M., Fox, M.A., Damjanovski, S. (2014). Functional characterization of tissue inhibitor of metalloproteinase-1 (TIMP-1) N- and C-terminal domains during *Xenopus laevis* development. ScientificWorldJournal. **30**: 467907.

Nieuwkoop, P.D., Faber, J. (1956). Normal Table of *Xenopus laevis* (Daudin): A systematical and chronological survey of the development from the fertilized egg till the end of metamorphosis. North-Holland Publishing Company, Amsterdam.

Nothnick, W.B., Soloway, P., Curry, T.E. Jr. (1997). Assessment of the role of tissue inhibitor of metalloproteinase-1 (TIMP-1) during the periovulatory period in female mice lacking a functional TIMP-1 gene. Biol Reprod. **56**: 1181-1188.

Oh, J., Seo, D.W., Diaz, T., Wei, B., Ward, Y., Ray, J.M. (2004). Tissue inhibitors of metalloproteinase 2 inhibits endothelial cell migration through increased expression of RECK. Cancer Res. **64**: 9062-9069.

Oh, J., Takahashi, R., Kondo, S., Mizoguchi, A., Nishimura, S., Imamura, Y., Kitayama, H., Alexander, D.B., Horan, T.P., Arakawa, T., Yoshida, H., Nishikawa, S., Itoh, Y., Seiki, M., Itohara, S., Takahashi, C., Noda, M. (2001). The membrane-anchored MMP inhibitor RECK is a key regulator of extracellular matrix integrity and angiogenesis. Cell. **107**: 789-800.

Ohl, F., Jung, M., Xu, C., Stephan, C., Rabien, A., Burkhardt, M. (2005). Gene expression studies in prostate cancer tissue: which reference gene should be selected for normalization? J Mol Med (Berl). **83**: 1014-1024.

Page-McCaw, A., Ewald, A.J., Werb, Z. (2007). Matrix metalloproteinases and the regulation of tissue remodelling. Nat Rev Mol Cell Biol. **8**: 221-233.

Park, S., Lee, C., Sabharwal, P., Zhang, M., Meyers, C.L., Sockanathan, S. (2013). GDE2 promotes neurogenesis by glycosylphosphatidylinositol-anchor cleavage of RECK. Science. **339**: 324-328.

Phng, L.K., Gerhardt, H. (2009). Angiogenesis: a team effort coordinated by Notch. Dev Cell. **16**: 196-208.

Plantefaber, L.C., Hynes, R.O. (1989). Changes in integrin receptors on oncogenically transformed cells. Cell. **56**: 281-290.

Prendergast, A., Linbo, T.H., Swarts, T., Ungos, J.M., McGraw, H.F., Krispin, S., Weinstein, B.M., Raible, D.W. (2012). The metalloproteinase inhibitor RECK is essential for zebrafish DRG development. Development. **139**: 1141-1152.

Radisky, E.S., Radisky, D.C. (2015). Matrix metalloproteinases as breast cancer drivers and therapeutic targets. Front Biosci (Landmark Ed). **20**: 1144-1163.

Rao, M., Sockanathan, S. (2005). Transmembrane protein GDE2 induces motor neuron differentiation *in vivo*. Science. **309**: 2212-2215.

Rimphanitchayakit, V., Tassanakajon, A. (2010). Structure and function of invertebrate Kazal-type serine proteinase inhibitors. Dev Comp Immunol. **34**: 377-386.

Roca, C., Adams, R.H. (2007). Regulation of vascular morphogenesis by Notch signaling. Genes Dev. **21**: 2511-2524.

Sabharwal, P., Lee, C., Park, S., Rao, M., Sockanathan, S. (2011). GDE2 regulates subtype-specific motor neuron generation through inhibition of Notch signaling. Neuron. **71**: 1058-1070.

Sasahara, R.M., Takahashi, C., Noda, M. (1999). Involvement of the Sp1 site in ras-mediated downregulation of the RECK metastasis suppressor gene. Biochem Biophys Res Commun. **264**: 668-675.

Schmitt, S.M., Gull, M., Brandli, A.W. (2014). Engineering *Xenopus* embryos for phenotypic drug discovery screening. Adv Drug Deliv Rev. **69-70**: 225-246.

Selever, J., Liu, W., Lu, M.F., Behringer, R.R., Martin, J. F. (2004). Bmp4 in limb bud mesoderm regulates digit pattern by controlling AER development. Dev Biol. **276**: 268-279.

Simizu, S., Takagi, S., Tamura, Y., Osada, H. (2005). RECK-mediated suppression of tumor cell invasion is regulated by glycosylation in human tumor cell lines. Cancer Res. **65**: 7455-7461.

Span, P.N., Sweep, C.G., Manders, P., Beex, L.V., Leppert, D., Lindberg, R.L. (2003). Matrix metalloproteinase inhibitor reversion-inducing cysteine-rich protein with Kazal motifs: a prognostic marker for good clinical outcome in human breast carcinoma. Cancer. **97**: 2710-2715.

Sternlicht, M.D., Werb, Z. (2001). How matrix metalloproteinases regulate cell behavior. Annu Rev Cell Dev Biol. **17**: 463-516.

Takagi, S., Simizu, S., Osada, H. (2009). RECK negatively regulates matrix metalloproteinase-9 transcription. Cancer Res. **69**: 1502-1508.

Takahashi, C., Sheng, Z., Horan, T.P., Kitayama, H., Maki, M., Hitomi, K., Kitaura, Y., Takai, S., Sasahara, R.M., Horimoto, A., Ikawa, Y., Ratzkin, B.J., Arakawa, T., Noda, M. (1998). Regulation of matrix metalloproteinase-9 and inhibition of tumor invasion by the membrane-anchored glycoprotein RECK. Proc Natl Acad Sci USA. **95**: 13221-13226.

Takenaka, K., Ishikawa, S., Yanagihara, K., Miyahara, R., Hasegawa, S., Otake, Y., Morioka, Y., Takahashi, C., Noda, M., Ito, H., Wada, H., Tanaka, F. (2005). Prognostic significance of reversion-inducing cysteine-rich protein with Kazal motifs expression in resected pathologic stage IIIA N2 non-small-cell lung cancer. Ann Surg Oncol. **12**: 817-824.

Takeuchi, T., Hisanaga, M., Nagao, M., Ikeda, N., Fujii, H., Koyama, F., Mukogawa, H., Kondo, S., Takahashi, C., Noda, M., Nakajima, Y. (2004). The membrane-anchored matrix metalloproteinase (MMP) regulator RECK in combination with MMP-9 serves as an informative prognostic indicator for colorectal cancer. Clin Cancer Res. **10**: 5572-5579.

Takino, T., Tsuge, H., Ozawa, T., Sato, H. (2010). MT1-MMP promotes cell growth and ERK activation through c-Src and paxillin in three-dimensional collagen matrix. Biochem Biophys Res Commun. **396**: 1042-1047.

Thant, A.A., Serbulea, M., Kikkawa, F., Liu, E., Tomoda, Y., Hamaguchi, M. (1997). c-Ras is required for the activation of the matrix metalloproteinases by concanavalin A in 3Y1 cells. FEBS Lett. **406**: 28-30.

Visse, R., Nagase, H. (2003). Matrix metalloproteinases and tissue inhibitors of metalloproteinases: structure, function, and biochemistry. Circ Res. **92**: 827-839.

Vu, T.H., Shipley, J.M., Bergers, G., Berger J.E., Helms, J.A., Hanahan, D., Shapiro, S.D., Senior, R.M., Werb, Z. (1998). MMP-9/gelatinase B is a key regulator of growth plate angiogenesis and apoptosis of hypertrophic chondrocytes. Cell. **93**: 411-422.

Vu, T.H., Werb, Z. (2000). Matrix metalloproteinases: effectors of development and normal physiology. Genes Dev. **14**: 2123-2133.

Walsh, L.A., Roy, D.M., Reyngold, M., Giri, D., Snyder, A., Turcan, S., Badwe, C.R., Lyman, J., Bromberg, J., King, T.A., Chan, T.A. (2015). RECK controls breast cancer metastasis by modulating a convergent, STAT3-dependent neoangiogenic switch. Oncogene. **34**: 2189-2203.

Wang, H., Dey, S.K. (2006). Roadmap to embryo implantation: clues from mouse models. Nat Rev Genet. **7**: 185-199.

Willson, J.A., Damjanovski, S. (2014). Vertebrate RECK in development and disease. Trends Cell Mol Biol. **9**: 95-105.

Willson, J.A., Muir, C.A., Evered, C.L., Cepeda, M.A., Damjanovski, S. (2018). Stable expression of α1-Antitrypsin Portland in MDA-MB-231 cells increased MT1-MMP and MMP-9 levels, but reduced tumour progression. J Cell Commun Signal. **12**: 479-488.

Wouters, M.A., Rigoutsos, I., Chu, C.K., Feng, L.L., Sparrow, D.B., Dunwoodie, S.L. (2005). Evolution of distinct EGF domains with specific functions. Protein Sci. **14**: 1091-1103.

Xue, Y., Gao, X., Lindsell, C.E., Norton, C.R., Chang, B., Hicks, C., Genfron-Maguire, M., Rand, E.B., Weinmaster, G., Gridley, T. (1999). Embryonic lethality and vascular defects in mice lacking the Notch ligand Jagged1. Hum Mol Genet. **8**: 723-730.

Yamamoto, M., Matsuzaki, T., Takahashi, R., Adachi, E., Maeda, Y., Yamaguchi, S., Kitayama, H., Echizenya, M., Morioka, Y., Alexander, D.B., Yagi, T., Itohara, S., Nakamura, T., Akiyama, H., Noda, M. (2012). The transformation suppressor gene Reck is required for postaxial patterning in mouse forelimbs. Biol Open. **1**: 458-466.

Yan, Y., Sabharwal, P., Rao, M., Sockanathan, S. (2009). The antioxidant enzyme Prdx1 controls neuronal differentiation by thiol-redox-dependent activation of GDE2. Cell. **138**: 1209-1221.

Yang, P., Baker, K.A., Hagg, T. (2006). The ADAMs family: coordinators of nervous system development, plasticity and repair. Prog Neurobiol. **79**: 73-94.

Chapter 2

2   Analysis of *Xenopus laevis* RECK and Its Relationship to Other Vertebrate RECK Sequences

2.1   Introduction

During development the ECM undergoes extensive remodeling to allow needed large-scale cell movements to occur. Degradation of the ECM occurs through a large family of extracellular proteases called MMPs. Aberrant regulation of MMPs is associated with developmental defects, and therefore, a delicate balance between the levels of MMPs and their endogenous inhibitors is crucial for proper development. RECK has recently been discovered to play a role in regulating MMP activity (Takahashi et al., 1998).

The *RECK* gene encodes a GPI-anchored protein with 3 serine-protease inhibitor-like domains (Kazal motifs) and 5 repeats of a putative cysteine knot motif. The N-terminus contains a signal peptide sequence and the C-terminus contains a GPI-anchoring signal sequence (Fig. 1.3) (Takahashi et al., 1998). All mammalian *RECK* genes that have been sequenced to date are highly conserved at the amino acid level and share the domains mentioned above. Mammalian RECK proteins are 971 amino acids in length and mass of approximately 110 kDa (Takahashi et al., 1998). *RECK* has also been sequenced from a variety of non-mammalian vertebrate and invertebrate species and has been found to be evolutionarily conserved, however, *X. laevis RECK* has yet to be characterized. Indeed, while numerous putative *RECK* genes can be predicted as many organism genomes are being sequenced, proportionally reptile and amphibian (herptile) *RECK* sequences are incomplete, of poor quality, or lacking in various phylogenic databases.

RECK was first described as a tumour suppressor protein due to its *anti*-invasive properties. Numerous *in vitro* studies showed that RECK can inhibit the proteolytic

activity of 3 types of MMPs: MMP-2, MMP-9, and MT1-MMP (Oh et al., 2001; Takagi et al., 2009; Takahashi et al., 1998). Since RECK functions by inhibiting MMPs, its presence during development would suggest that it plays important embryonic roles as well. Vertebrate RECK importance was demonstrated in knockout and knockdown studies in mice and zebrafish, respectively. Oh et al. (2001) revealed that *RECK*-deficient mice died halfway through embryogenesis with halted vascular development. In addition, *RECK* knockdown in zebrafish resulted in impaired vascular integrity and lack of DRG formation (Prendergast et al., 2012). RECK has also been shown to be important during mouse secondary palate development (de Oliveira Demarchi et al., 2010) and mouse forelimb development (Yamamoto et al., 2012). More recently RECK has also been shown to modulate cell-migratory signaling pathways, independent of its MMP inhibitory role (Chang et al., 2008; Walsh et al., 2015). As the developmental processes of neural development and vascular branching both involve RECK and tightly controlled cell migration and ECM remodeling events in mice and zebrafish, this implicates the importance of RECK as a key embryonic regulator in other vertebrates.

While much *in vitro* analysis of RECK function is currently being carried out, there is limited *in vivo* information regarding this protein, particularly in non-mammalian vertebrates. In this chapter, I cloned and analyzed the sequence of *X. laevis RECK* and examined its expression pattern during development. Expression analysis revealed that *X. laevis RECK* expression is consistent with its vascular and nervous system roles seen in mouse and zebrafish. I then used a MO approach to disrupt endogenous *RECK* levels in *X. laevis* embryos. *RECK* knockdown led to severe neural tube closure defects, axial defects, and reduced head structures. Additionally, polymerase chain reaction (PCR)

analysis showed that *RECK* knockdown resulted in differential changes in *MMP* and *TIMP* genes, suggesting that RECK is an important modulator of ECM remodeling during *X. laevis* embryogenesis.

2.2 Materials and Methods

2.2.1 Animal Care and Rearing

Adult *X. laevis* were purchased from Xenopus 1, Inc (Dexter, MI). Animal rearing and fertilizations were carried out as previously described (Sive et al., 2000). Developing embryos were staged according to Nieuwkoop and Faber (1956) (Fig. 1.6). Animals were housed and treated in accordance with UWO and CCAC guidelines.

2.2.2 Cloning *X. laevis RECK*

Since the *X. laevis RECK* sequence was not available online at the beginning of this project, the *Xenopus tropicalis* database was used instead as the sequence of this closely related species is better annotated. Based on the putative *X. tropicalis RECK* sequence [XM_002938937.2], forward (5'-ATGTGTCGTGATGTATGTGA-3') and reverse (5'-TGGCGACAAAGAATACACCA-3') primers were designed flanking the predicted full-length coding region of the *RECK* gene. Total RNA was isolated from adult *X. laevis* lung tissue using a RNeasy Kit (Qiagen) according to manufacturer's instructions. First-strand cDNA synthesis and PCR were performed on total RNA using qScript Reverse Transcriptase (Quanta Biosciences) and Kapa Hi-Fi Taq PCR Kit (Kapa Biosystems) according to manufacturer's instructions.

The putative *X. tropicalis RECK* sequence [XM_002938937.2] was only partial and lacked the signal peptide sequence at the 5' end and the GPI-anchoring signal

sequence at the 3' end of the gene. Therefore, the nested gene specific primers for the 5' end (outer: 5'-ATGTGTCGTGATGTATGTGAACAG-3' and inner: 5'-CCTCCCTTAG TTCAGTGTGT-3') and 3' end (outer: 5'-CCTGCAATTCCTGTCACAG-3' and inner: 5'-CAACATGTCTCTGTACCTCAG-3') were also generated to isolate the missing domains of *X. laevis RECK* using the FirstChoice RNA Ligase Mediated Rapid Amplification of cDNA Ends (RLM-RACE) Kit (Life Technologies) according to manufacturer's instructions. The amplicons were cloned into the pCR 4-TOPO vector (Life Technologies) and sequenced at the DNA Sequencing Facility (Robarts Research, London, ON, Canada). The final amplification of the full-length coding region of *X. laevis RECK* was done using SuperTaq Plus (Life Technologies).

2.2.3   Sequence Analysis

The *X. laevis RECK* sequence obtained from PCR was translated using the ExPASy Bioinformatics Resource Portal online Translate tool (http://web.expasy.org/translate/). This *X. laevis RECK* sequence was submitted to genbank as [AIZ00509.1]. Other well-annotated, full-length RECK protein sequences at the time of publication along with the accession numbers used for comparison were from the following species: human *Homo sapiens* [NP_066934.1], chimp *Pan troglodytes* [XP_520575.2], rhesus monkey *Macaca mulatta* [XP_001083599.1], dog *Canis lupus familiaris* [NP_001002985.1], cow *Bos taurus* [NP_001179394.1], mouse *Mus musculus* [NP_057887.2], tiger *Panthera tigris altaica* [XP_007076663.1], alpaca *Vicugna pacos* [XP_006204234.1], little brown bat *Myotis lucifugus* [XP_006102759.1], 13 lined squirrel *Ictidomys tridecemlineatus* [XP_005326326.1], common shrew *Sorex araneus* [XP_004600290.1], fresh water dolphin *Lipotes vexillifer* [XP_007456041.1], platypus

Ornithorhynchus anatinus [XP_007661391.1], tasmanian devil *Sarcophilus harrisii* [XP_003761399.1], chicken *Gallus gallus* [XP_418897.4], penguin *Pygoscelis adeliae* [XP_009322770.1], bald eagle *Haliaeetus leucocephalus* [XP_010575445.1], ibis *Nipponia nippon* [XP_009473764.1], hummingbird *Calypte anna* [XP_008500730.1], pike *Esox lucius* [XP_010884005.1], croaker *Larimichthys crocea* [XP_010749852.1], zebra fish *Danio rerio* [XP_009295477.1], sole *Cynoglossus semilaevis* [XP_008305649.1], alligator *Alligator sinensis* [XP_006019052.1], soft shell turtle *Pelodiscus sinensis* [XP_006113101.1], frog *X. tropicalis* [XP_002938983.2], ghost shark *Callorhinchus milii* [XP_007896317.1], coelacanth *Latimeria chalumnae* [XP_006005911.1], fruit fly *Drosophila melanogaster* [NP_001261853.1], mosquito *Anopheles gambiae* [XP_311364.4].

Full-length RECK amino acid sequences were aligned using Clustal Omega Multiple Sequence Alignment web software at the European Bioinformatics Institute (EBI) site (http://www.ebi.ac.uk/Tools/msa/clustalo/) and given a score based on similarity. The signal sequence, structural domains of RECK (cysteine knots and Kazal motifs), and GPI anchor were determined using the Simple Modular Architecture Research Tool (SMART) web software (at http://smart.embl.de/). All analyses were performed using default program settings.

2.2.4   Immunohistochemistry and Fluorescence Microscopy

Embryos were fixed in 3.7% paraformaldehyde in 1X phosphate-buffered saline (PBS) for 2 hours at room temperature. Fixed embryos were sent to the Molecular Pathology Core Facility at Robarts Research Institute (London, ON) for paraffin embedding and sectioning. 10 µm de-waxed sections were probed with primary antibody

(mouse anti-RECK, Santa Cruz, #sc-373929) followed by fluorescently-labeled secondary antibody (Alexa Fluor goat anti-mouse IgG, Life Technologies). Slides were mounted using ProLong Gold Antifade Mountant with 4',6-diamidino-2-phenylindole (DAPI) (Life Technologies). Slides were visualized using a Leica automated inverted microscope.

2.2.5   Morpholino Design

The design and synthesis of MO were performed by Gene Tools (Philomath, OR). A translation-blocking MO (3'-CATCACATCCCCACTCCTTCTCTTC-5') and splice-blocking MO (3'-CTTTTAGTTTGACTTACCAGGTGGT-5') were engineered to target *X. laevis RECK* (GenBank, AIZ00509.1). A carboxyfluoresceinated-labelled translation-blocking MO targeted to the *X. laevis β-catenin* gene (3'-TTTCAACCGTTTC CAAAGAACCAGG-5') was also purchased from Gene Tools as a control.

2.2.6   Morpholino Microinjection

Just fertilized *X. laevis* embryos were transferred from 0.1X Marc's modified ringers (MMR) into 1X MMR containing 4% Ficoll. 2.3 nL (6 ng/nL) of splice-blocking *RECK* MO or translation-blocking *RECK* MO were microinjected at the 1-cell stage using 10 μm diameter glass needles. *β-catenin* MO (9 ng/nL) was used as a positive control, and water-injected and un-injected embryos were used as negative controls. Embryos were maintained in 1X MMR with Ficoll for 6 hours following injection, then transferred to 0.1X MMR solution for rearing. Any dead or abnormal embryos 2 hours post-injection were removed, and the remaining embryos were examined for phenotypic abnormalities. Embryos were analyzed for 3 days following injection. Images of embryos were taken using an Olympus SXZ9 microscope with a Nikon camera attachment.

2.2.7   Immunoblot Analysis

RECK-MO injected and un-injected embryos from 1 dpf were collected, 1 embryo each, and homogenized in 50 µL of radioimmunoprecipitation assay (RIPA) buffer supplemented with phosphatase/protease inhibitors (Thermo Scientific). Protein extracts were centrifuged at 12,000 g at 4°C for 30 minutes and the supernatant was collected. Protein extracts were run on a 10% sodium dodecyl sulfate (SDS) polyacrylamide gel and transferred to a polyvinylidene fluoride (PVDF) membrane. Membranes were blocked with 0.5% bovine serum albumin (BSA) (Fisher Scientific) in tris-buffered saline with Tween-20 (TBST) (pH 7.5) for 30 minutes at room temperature and incubated overnight at 4°C with primary antibody (RECK, 1:200, Cell Signaling Technology, #3433; β-actin, 1:1000, Santa Cruz, #sc-47778) followed by 1 hour incubation at room temperature with either horseradish peroxidase (HRP)-labeled goat anti-rabbit or anti-mouse secondary antibodies (Thermo Fisher Scientific) diluted 1:10,000 in blocking solution. Signal was detected using a SuperSignal Chemiluminescent kit (Thermo Scientific) as per the manufacturer's instructions. Blots were visualized using the Bio-Rad ChemiDoc Imaging system.

2.2.8   Quantitative Real-Time PCR

To investigate changes in developmental marker genes and ECM remodeling genes, quantitative real-time PCR was performed. 10 embryos at 1 dpf were collected from *RECK* MO-injected and un-injected embryos. Total RNA was isolated using an RNeasy Mini kit (Qiagen) according to manufacturer's instructions. cDNA was synthesized from 1 µg of RNA using qScript™ CDNA SuperMix (Quanta) according to manufacturer's instructions. qPCR was carried out using SYBR Green PCR Master Mix

(Applied Biosystems). For quantification, the *X. laevis* target genes (*RECK* 5'-ATGGCG GCGGTCCCGGCCTC-3' and 5'-ATGTGTCGTGATGTATGTGAACAG-3', *chordin* 5'-AACTGCCAGGACTGGATGGT-3' and 5'-GAAGCAACTCTAAATCCTGCC-3', *XCG* 5'-CTGTACTGGTTCACCAATAATCCC-3' and 5'-GTGAGACGACTGCAATG TAGC-3', *FoxD3* 5'-TCTCTGGGGCAATCACACTC-3' and 5'-CCCTTTATCAACAA ATGTAC-3', *Xnot1* 5'-GCAGGCAGAGTTCAGTTGTG-3' and 5'-CCACAGGCAAAG CAACTCAC-3', *ß-catenin* 5'-CCCGATGAATCTGCATTGTGA-3' and 5'-GCAAGCT GGAACTTATCAG-3', *MMP-2* 5'-CAGGGAATGAGTACTGGGTCTATT-3' and 5'-G TAGATGCTGCCTTTAACTGGAGT-3', *MMP-9* 5'-AATCTCTTCTAGAGACTGGGA AGGAG-3' and 5'-TCCAGCTACTTTAGTCAATCAGCT-3', *MT1-MMP* 5'-CATGGG CAGCGATGAAGTCT-3' and 5'-TACTTCTACAAGGGGAACAAATACTGG-3', and *TIMP-2* 5'-GCCCCCGCCCGCCCAGCC-3' and 5'-TCGGCAGTGTGTGGGGTCTCG GGA-3') were normalized to the internal standard of elongation factor one alpha (*EF1α* 5'-CAGATTGGTGCTGGATATGC-3' and 5'-CTAGGAGTCATCAAGGCAGT-3') (Krieg et al., 1998). The amplification was calculated according to the ΔΔCT method (Livak and Schmittgen, 2001).

2.2.9 Statistical Analysis

Statistical analysis and graphing were performed using Microsoft Excel. Data is presented as ± standard error of the mean (SEM). One-way analysis of variance (ANOVA) followed by unpaired student's T-tests were used. The different levels of significance are denoted as follows: ns, $p>0.05$; *, $p \le 0.05$; **, $p \le 0.01$; ***, $p \le 0.001$.

2.3 Results and Discussion

2.3.1 Sequence Analysis

Since no record existed to date, I began by cloning and sequencing *X. laevis RECK*. The full-length coding region of *X. laevis RECK* was amplified from adult lung tissue RNA by PCR using primers designed against the *X. tropicalis RECK* sequence [XM_002938937.2] and 5' and 3' RACE. The putative *X. laevis RECK* full-length mRNA sequence was submitted to GenBank with accession # [AIZ00509.1] (Appendix B). The derived *X. laevis RECK* had a full-length coding region of 2,904 bp and a predicted protein length of 967 amino acids (Fig. 2.1a). SMART domain analysis of *X. laevis* RECK was used to identify the hallmark protein domains characteristic of other RECK proteins (Fig. 2.1a). This included an N-terminal signal sequence and a C-terminal GPI anchor signal - both of which are removed in the mature protein. Also present were 5 characteristic cysteine knot motifs and 3 Kazal inhibitory domains. I then analyzed the predicted *X. laevis* RECK protein sequence along with RECK sequences from both vertebrate and insect species. Clustal Omega was used to align various RECK protein sequences, and conserved amino acids that were identical for all animals were counted (Table 2.1). Conserved RECK amino acid sequences were examined in all 31 animals selected at the time of publication. RECK proteins had a 33% and higher amino acid identity when compared across all vertebrates and insects. Vertebrate RECK amino acids were 58% and higher identical, with fish, herptile and mammalian RECK being 68%, 75% and 85% and higher identical within each group. The selected bird RECK amino acids showed the most identity with a conservation of 93% and higher.

Hallmark domains of RECK were further analyzed to determine conservation within RECK proteins that may reveal important domain functions. One of the hallmark domains of all RECK proteins is 3 protease inhibitor-like domains (Kazal motifs).

Figure 2.1 *X. laevis* **RECK amino acid sequence**

(a) *X. laevis* RECK is 967 amino acids in length and contains an N-terminus signal sequence and a C-terminus GPI-anchoring sequence (bold and italic). The N-terminal region of RECK contains 5 repeats of a putative cysteine knot motif (underlined). The middle portion of RECK contains a highly conserved 32 amino acid stretch I termed a LAD-RSC domain (dashed underline). 3 Kazal motifs serine-protease inhibitor-like domains (wavy underline) are found towards the C-terminus. (b) Amino acid sequence of the described *X. laevis* RECK LAD-RSC domain and its Clustal Omega alignment with other select animals. Star (*): identical amino acids are found in all sequences, colon (:): strong similarity, period (.): weak similarity.

(a) Predicted *X. laevis* RECK amino acid sequence

MKRRSGDVMHAAVRVMSASASCLGLLGIWFFLLIFLLLEAADASCCNQAKDNLMCRDVC
EQILSSKSESRIKHLLLRAPDYCPTSMIDVWTCINSSLPGVSKKSEGWVGLGCCELAIA
VECRRACKQASSQNDISKSCRKQYETALISCINRNEMGSVCCSYAGRHTNCREYCQAIF
RTDSSPGPSQIKAVENFCASISPPLVQCVNNYTQSYPMRNPVDSLYCCDRAEDPQCQSA
CKRILMSKKTEPEIVDSLSEGCTKPLPQDPLWQCFLESSRTVHSGVNIVPPPSAGLDGA
ELHCCSKANSSNCRDLCTKLYSTSWGNTQVWQEFEFACEYNPLEAPMLTCLADVREPCQ
LGCRNLTFCTNFNNRPTELFRSCNVQSDQGAMNDMKLWEKGSIKMPFMNIPVLDIKKCH
PEMWKAIACSLQIKPCHSKSRGSIICKTDCVEILTKCGDHSRFPESHTAESICELLSPS
DENEDCIPLDTYLRSSPLDNAIEEVTHPCNPNPCPANHLCEVNRKGCLPGEPCLPYFCS
QGCKLGETSDFLVRHGVLIQMPSGSVGCYKICTCGQSGTLENCLDMQCVDLHKSCLVGG
QRKNHGESFKVDCNICSCVAGTLRCSNHQCPHSEEDRRMFTGLPCNCEDQFVPVCGQNG
RTYPSACIARCVGLLDHQFEFGLCSSVCNPNPCSRNGIPKRKVCLTSYEKFGCAQYECI
PRHLKCEHSRDPMCDTENVEHINLCTLYQRGRLLSYKGSCQPFCKSAEPVCGHNGETYP
NVCSAYSDRVAVDYYGHCQDVGIFSDQGLHNECLSIQCPAIPVTVCKPIIPPGACCPLC
AGVLRILFDKEKLDTFATATKNTPITVMDILQKIRQHVSVPQCDVFGYLSMESDIIILI
VPVDSPPKSIQIDACNKEAEKINSLINSDSPTLVSQVPLSALITSEVQVS***TTLNSDCNR
ICLSIHYIYLYLGIALLYVTLNA***

(b) LAD-RSC domain conservation

```
zebra fish    LADVREPCQLGCKELSYCTNFNNRPTELFRSC
coelacanth    LADVREPCQLGCKDLTFCTNFNNRPTELFRSC
x laevis      LADVREPCQLGCRNLTFCTNFNNRPTELFRSC
chicken       LADVREPCQLGCRNLSYCTNFNNRPTELFRSC
hummingbird  LADVREPCQLGCRNLTYCTNFNNRPTELFRSC
platypus      LADVREPCQLGCRNLTFCTNFNNRPTELFRSC
human         LADVREPCQLGCRNLTYCTNFNNRPTELFRSC
fruit fly     IESVDAPCELGCQGLSFCSNFNNRPTELFRSC
mosquito      IDEVDEPCELGCDGLSFCSNFNNRPTELFRSC
              : .*   **:***   * :*:************
```

Table 2.1 Percent amino acid identity of select RECK domains

	Full-length	Kn1 (48aa)	Kn2 (38aa)	Kn3 (47aa)	Kn4 (48aa)	Kn5 (47aa)	LAD-RSC (32aa)	KZ1 (46aa)	KZ2 (43aa)	KZ3 (35aa)
All	33%	(8) 17%	(7) 18%	(8) 17%	(11) 23%	(11) 23%	(21) 67%	(19) 41%	(5) 12%	(7) 20%
Vertebrates	58%	(15) (31%)	(17) 45%	(28) 60%	(20) 42%	(19) 40%	(28) 88%	(27) 59%	(11) 26%	(14) 40%
Mammals	85%	(35) 73%	(35) 92%	(42) 89%	(41) 85%	(41) 87%	(29) 91%	(40) 87%	(28) 65%	(21) 60%
Birds	93%	(48) 100%	(35) 92%	(46) 98%	(46) 96%	(45) 96%	(30) 94%	(46) 100%	(36) 84%	(31) 89%
Fish	68%	(29) 60%	(30) 79%	(38) 81%	(34) 71%	(31) 66%	(31) 97%	(31) 67%	(28) 57%	(20) 57%
Herptile	75%	(37) 77%	(30) 79%	(40) 85%	(38) 79%	(30) 64%	(31) 97%	(38) 83%	(26) 60%	(27) 77%

Note: Select full-length RECK amino acid sequences were aligned with Clustal Omega. Cysteine knot (Kn) and Kazal (KZ) motif domains were identified at http://smart.embl.de/. Clustal outputs were used to identify identical amino acids amongst all species within a given group of animals. For the full-length sequence, the percent identity (%) listed is the minimum amongst the group. For the various domains (whose amino acid size is indicated in brackets), the number of identical amino acids in each aligned group (also in brackets) is represented as a percentage of amino acid identity within that domain.

According to Takahashi et al. (1998) only the first domain in human RECK completely matches a Kazal motif sequence, whereas the 2nd and 3rd domains contain partial Kazal motif sequences. A recently published *in silico* search of nucleotide databases revealed the presence of members of the Kazal-family in the 4 major subphyla of the Arthropoda (van Hoef et al., 2013). While most insect Kazal motifs contain the 6 cysteines that are characteristic to this domain and are responsible for the formation of 1-5, 2-4, and 3-6 disulfide bridges between the 6 cysteines, only Kazal motif 1 has these 6 cysteines in vertebrates. This conserved presence of Kazal domains in animals that have very diverse developmental histories also suggests that such proteins may also play important roles in general tissue maintenance, as well as in developmental processes. While SMART domain analysis of *X. laevis* RECK identified only 2 Kazal motif domains (this is the same for *X. tropicalis* and Drosophila RECK proteins), my analysis showed that all 3 Kazal motif domains are highly conserved and contain conserved cysteines. In agreement with Takahashi et al. (1998), who suggested that the 1st domain best matches a classic Kazal motif sequence, the 1st Kazal motif is best conserved in all animals and within animal groups. Moreover, all vertebrate Kazal motifs contain the same number of amino acids between conserved cysteines among all species examined (Appendix C). The conservation of all cysteines in all motifs suggests that the 2 partial Kazal motifs also contribute an important function to the protein in vertebrates. As the Kazal motifs are protease inhibitor-like domains and play an important role in inhibiting MMPs (Chang et al., 2008), the consistent high conservation of Kazal motif 1, and the presence of 3 such domains in all vertebrates, suggests a conservation of RECK function as an MMP inhibitor in these species.

The N-terminal region of RECK contains 5 large repeats of a cysteine knot motif. Collectively, these 5 putative cysteine knot motifs share relatively moderate similarity among all animals (17-23%) with higher conservation of identity being seen in vertebrates and the subgroups examined, with the most striking conservation of these domains being in birds (Table 2.1). While in general it was cysteine knot 3 and 4 that were the most conserved, all knot motifs in all animals had 6 conserved cysteines. This included 2 cysteines at the beginning of each knot, a gap of 7 or 8 amino acids, followed by the 3rd cysteine with 3 or 4 amino acids before cysteine 4. The conservation of 6 cysteines in 5 knots in all animals, with the spacing of the first 4 cysteines being almost identical in animals ranging from insects to amphibians to mammals is quite remarkable. The conservation in the number of cysteines and their spacing, but the dissimilarity in amino acids between the cysteines, suggests that these motifs play structural roles that are important to the overall functions of folded RECK proteins. While the overall RECK protein displays high levels of sequence conservation, analysis revealed a 32 amino acid sequence following the 5th cysteine knot that was the most conserved of any other region of the protein. I have termed this region a LAD-RSC domain based on the first 3 (LAD) and last 3 (RSC) amino acids. This stretch of amino acids shares no sequence similarity with any characterized functional domain to date. This stretch of amino acids is, however, 68% identical between all of the animals I investigated, 88% identical in vertebrates, and over 90% identical within the various vertebrate sub-groups. While domains such as the cysteine knot and Kazal motifs are hallmarks of RECK, these hallmark domains make up only a portion of its almost 1,000 amino acid sequence. The high conservation of other regions, such as the LAD-RSC domain, suggest novel and as yet to be characterized roles

for RECK, such as its roles in cell signaling (Walsh et al., 2015) - functions that are MMP-independent and thus may not involve the Kazal motifs.

2.3.2   RECK Protein Localization

As previous research has demonstrated both a neural and vascular role for RECK during development of fish and mouse (Oh et al., 2001; Prendergast et al., 2012), I sought to investigate if a similar embryonic expression pattern existed for *X. laevis* RECK. My previous *in situ* analysis revealed that *RECK* transcripts are present in dorsal neural structures and the head region, such as the branchial arches, in early tailbud (stage 24) embryos (Willson et al., 2015). To confirm neural and branchial arch *RECK* localization, IHC was performed to localize RECK proteins on histological sections of late tailbud (stage 28) embryos (Fig. 2.2). Punctate staining of RECK proteins was present in the dorsal side of the neural tube (Fib. 2.2b). In the head region of late tailbud embryos, RECK proteins were localized in the area of the branchial arches (Fig. 2.2d). RECK presence in neural structures and branchial arch regions of the developing *X. laevis* embryo is similar to that observed in zebrafish embryos, and consistent with the finding that RECK plays an important role in the differentiation of neural crest cells into the DRG (Prendergast et al., 2012). Additionally, the expression of *RECK* in anterior structures coincides with the expression of ECM proteinases (*stromelysin-3* and *ADAM-19*) (Damjanovski et al., 2001; Neuner et al., 2009), and *TIMPs* (Pickard and Damjanovski, 2004), reflecting the complex regulation of the ECM remodeling events occurring in these anterior tissues. Further, RECK presence in the area of the branchial arches, which will contribute to the formation of the gills, is consistent with a role for RECK in vascular development as its localization is consistent with *Xfli1*, whose similar

Figure 2.2 Localization of RECK proteins in late tailbud embryos.

IHC was performed on sections of late tailbud embryos to detect RECK protein (red). (a), (c) Brightfield differential interference contrast (DIC) images are shown. (b) RECK proteins are localized on the dorsal side of the neural tube and dorsal fin. (d) RECK proteins are localized in regions consistent with branchial arches.

(a) dorsal fin
neural tube
notochord
somite

Stage 28: Tail Region

(b) Anti-RECK

(c) Branchial arches
Cement gland

Stage 28: Head Region

(d) Anti-RECK

a, b

c, d

Tailbud
(stage 28)
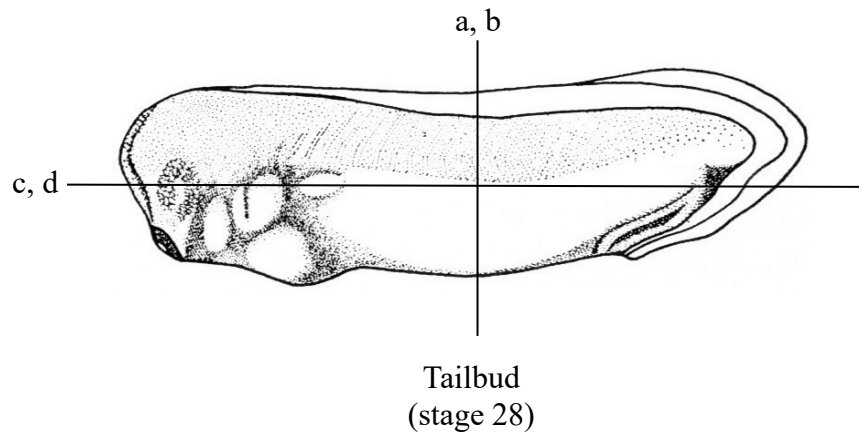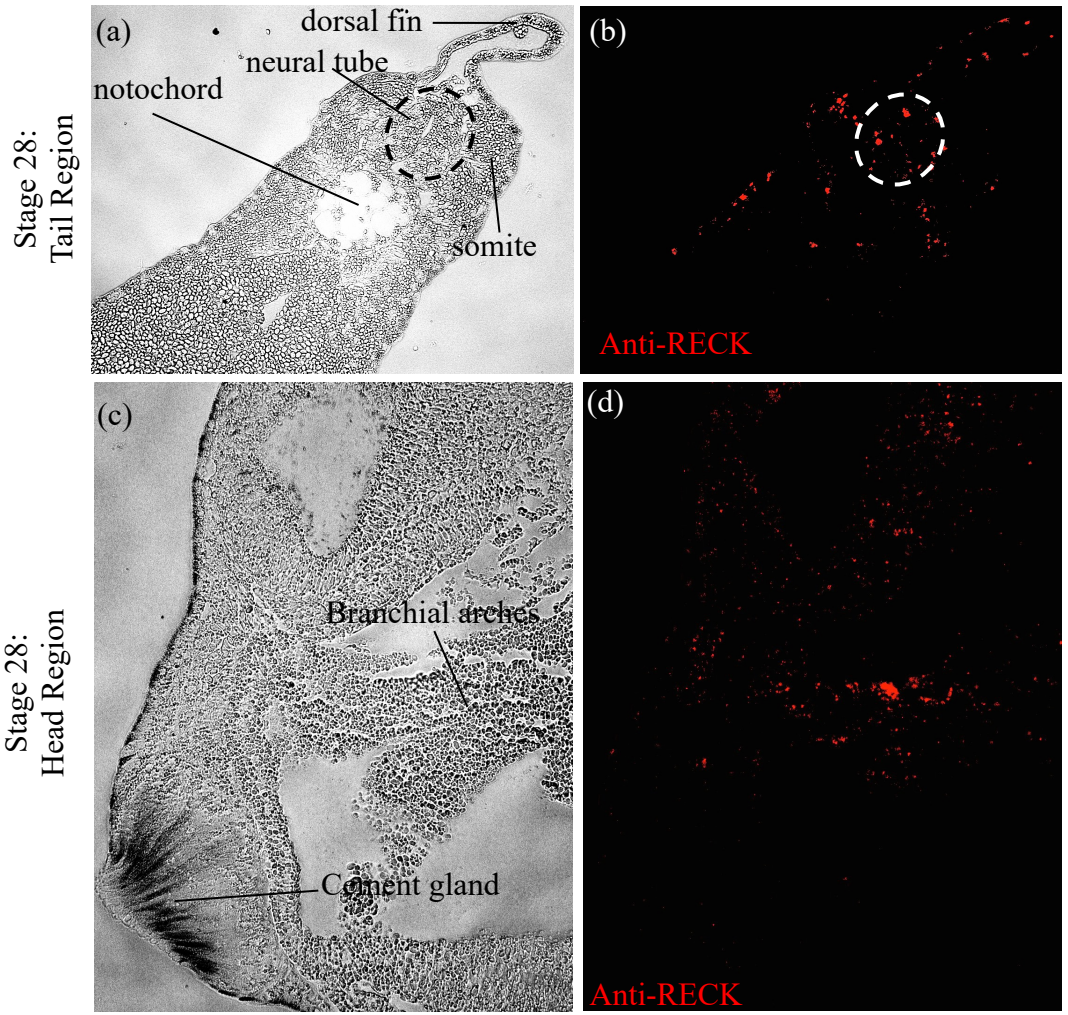
expression demarks endothelial cell differentiation (Ciau-Uitz et al., 2000).

2.3.3   Functional Analysis

2.3.3.1   *RECK* Knockdown in *X. laevis* Embryos Causes Developmental Defects

To investigate the effects of disrupting *RECK* expression during *X. laevis* embryogenesis, *RECK* MO were microinjected into 1-cell stage embryos. *β-catenin* MO-injected, water-injected, and un-injected embryos were used as controls. Both a translation-blocking *RECK* MO and splice-blocking *RECK* MO were used to verify *RECK* knockdown phenotypes. Confirmation of *RECK* knockdown using each MO was confirmed by either Western blotting or qPCR (Fig. 2.3). Embryos were analyzed for morphological changes in development for 3 days following *RECK* MO injection. The percent survival was determined and quantified 1 dpf (st 24) and 2 dpf (st 30) (Fig. 2.4). Over 90% of control embryos (un-injected and water-injected) developed normally, whereas approximately 60% of *RECK* MO-injected embryos survived to 2 dpf (Fig. 2.4). The surviving *RECK* MO-injected embryos successfully underwent gastrulation, however, they showed severe developmental defects, including neural tube closure failure at 1 dpf (Fig. 2.5b) axial defects and curvature at 2 dpf (Fig. 2.5d), and reduced head structures and yolk reduction at 3 dpf (Fig. 2.5f).

My IHC analysis had revealed that RECK proteins are localized to the neural tube and head region (Fig. 2.2). The phenotypic defects of the dorsal axis seen in *RECK* MO-injected embryos coincide with the expression pattern of *RECK* during normal development (Fig. 2.2). Neurulation requires tightly coordinated cell movements and timed interactions of germ layer tissues, that of which also rely on proper ECM

Figure 2.3 Microinjection of *RECK* translation-blocking or splice-blocking MO decreased *RECK* levels in *X. laevis* embryos.

(a) Following injection of *RECK* translation-blocking MO (6 ng/nL) at the 1 cell stage, protein was isolated from both *RECK*-MO injected and un-injected embryos 1 dpf. Knockdown of RECK (110 kDa) protein occurred in *RECK* MO-injected embryos. β-actin (42 kDa) was used as a loading control. (b) Following injection of *RECK* splice-blocking MO (6 ng/nL) at the 1-cell stage, RNA was isolated from embryos 1 dpf. *RECK* RNA levels were reduced in *RECK* MO-injected embryos compared to control. Results are based on 3 biological replicates (mean ± SEM; technical replicates, N=9). Data is analyzed via t-test; ***, $p \leq 0.001$.

(a)

| Un-injected | *RECK* Translation-Blocking MO |

RECK

β-actin
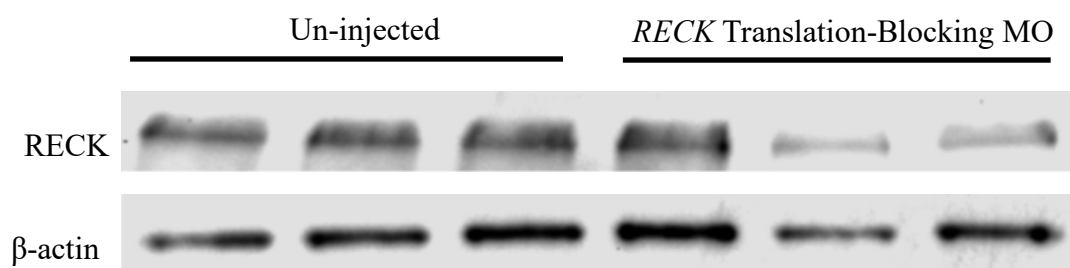
(b)
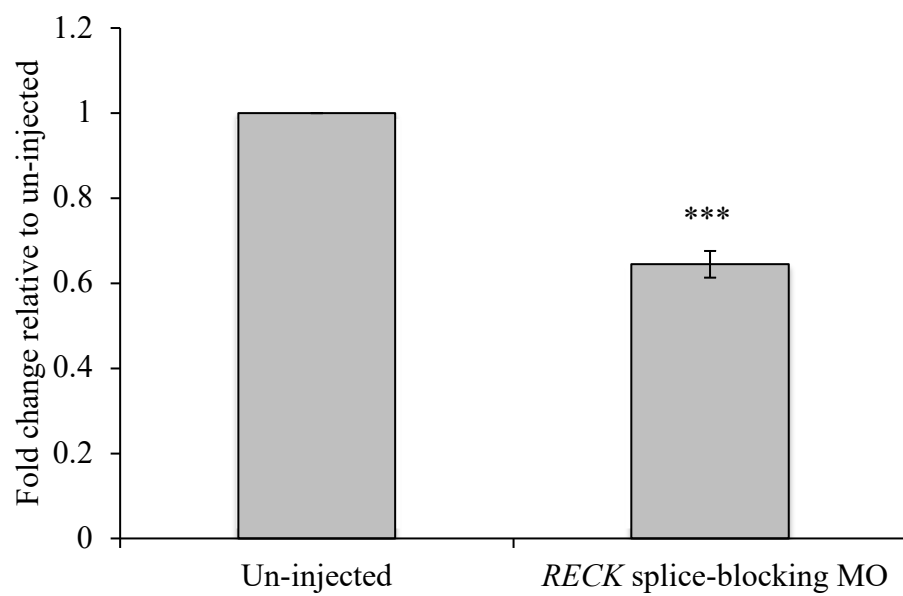
Figure 2.4 *RECK* knockdown embryos displayed reduced survival.

2.3 nl (6 ng/nL) of *RECK* MO was injected into *X. laevis* embryos at the 1-cell stage. Following injection, embryos were scored for a normal phenotype 1 and 2 dpf. The percent of embryos that survived following injection is graphed. Results are based on the average of 3 biological replicates, where a minimum of 100 embryos were injected and counted for each replicate. Bars indicate standard error (SE).

69
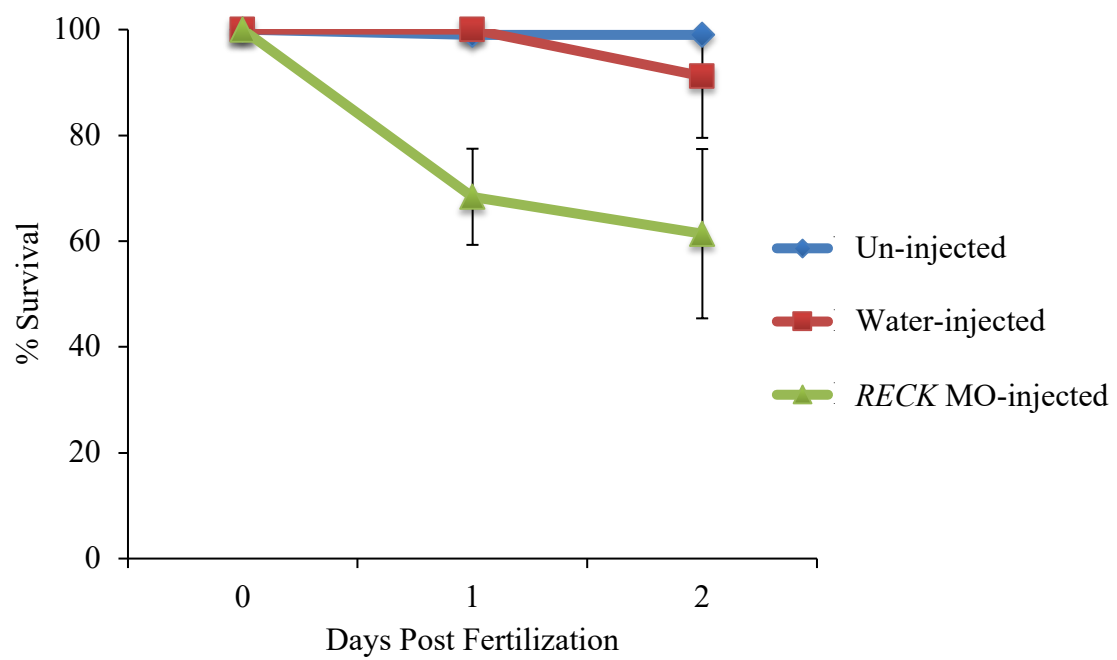
Figure 2.5 *RECK* knockdown resulted in developmental defects.

RECK MO (6 ng/nL) were injected into *X. laevis* embryos at the 1-cell stage. Following injection, embryos were scored for a normal phenotype 1, 2, and 3 dpf. Following injection, photographs were taken of representative embryos. Un-injected embryos were phenotypically normal (a,c,e). Knockdown of RECK caused neural tube closure failure at 1 dpf (b), axial defects and curvature at 2 dpf (d), and head defects at 3 dpf (f). Abbreviations: A=anterior, CG=cement gland, H=head, NF=neural tube closure failure, P=posterior.

	Un-injected	*RECK* MO
1 dpf	(a)	(b) kink, NF →, NF →, kink
2 dpf	(c)	(d) CG
3 dpf	(e)	(f) P→, A →
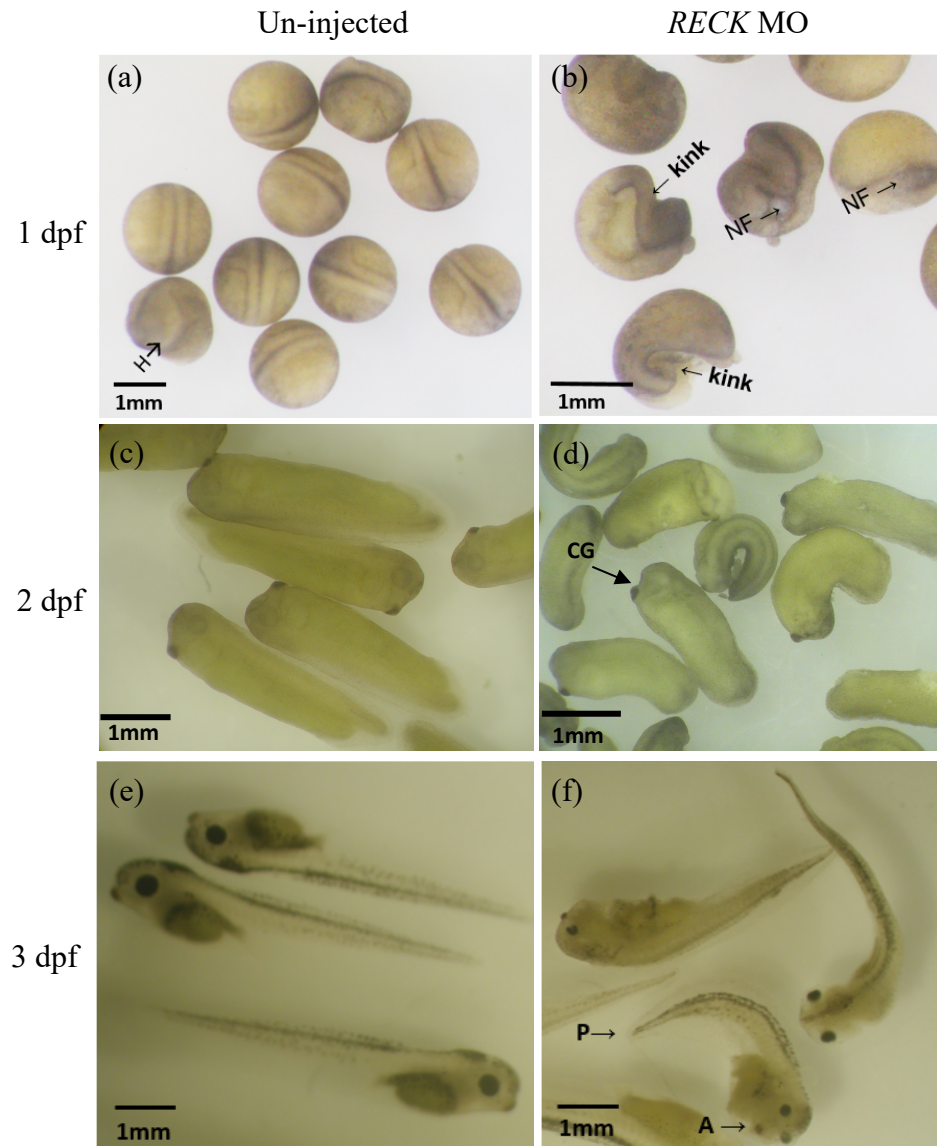
remodeling (Nikolopoulou et al., 2017). Failure of the neural tube to close can arise from defects in cell movement as well as cell fate determination (Nikolopoulou et al., 2017). *RECK* MO-injected embryos observed at stage 20 (neurula stage) exhibited a truncated and twisted axis, with delayed neural tube fusion (Fig. 2.5b) (Appendix D). Predictably, the failure of the neural tube to close will lead to abnormal head development in subsequent stages, as was seen in *RECK* MO-injected embryos at 3 dpf (Fig. 2.5f).

The embryos that survived to 2 dpf (about 61%) exhibited axial defects and delayed development (Fig. 2.5d). By 3 dpf (stage 40), the full effects of *RECK* knockdown were evident. *RECK* MO-injected embryos exhibited a curved dorsal axis and reduced yolk endoderm (Fig. 2.5f). *RECK* MO-injected embryos also exhibited reduced head structures, such as the eye, however, the development of the cement gland was unaffected (Fig. 2.5f). The cement gland is the first fully developed and most anterior organ in the embryo and is a visual indicator that embryos have successfully completed gastrulation (Sive and Bradley, 1996). At 3 dpf, *RECK* MO-injected embryos also exhibited abnormal swelling on the ventral-lateral sides of their bodies (Fig. 2.5f). This could be an indication of poor development of the vasculature due to *RECK* knockdown, as RECK proteins were localized in the branchial arches in normally developed embryos (Fig. 2.2), and RECK has previously been shown to play a role in vascular development (Oh et al., 2001; Prendergast et al., 2012). Moreover, reduced head structures observed in *RECK* MO-injected embryos at 3 dpf could also be attributed to defects in neural crest cell migration. Neural crest cells contribute to a variety of structures in the body, including craniofacial bones and cartilage, smooth muscle, and many peripheral neurons (Mayor and Theveneau, 2013). Indeed, Prendergast et al. (2012)

have previously shown RECK as an important modulator during neural crest cell migration in zebrafish.

2.3.3.2   Real-Time PCR Analysis of Developmental Marker Genes in

RECK MO-Injected Embryos

To understand the morphological phenotypes observed in *RECK* MO-injected embryos, real-time qPCR was performed on key developmental marker genes (*chordin*, *Xnot1*, *FoxD3*, *β-catenin*, and *XCG*) at 1 dpf (stage 20). *RECK* MO-injected embryos at stage 20 (1 dpf) had a significant increase in *chordin* mRNA levels compared to un-injected embryos (Fig. 2.6). The *chordin* gene encodes a dorsal organizing protein, important for patterning the dorsoventral axis and inducing neural structures (Sasai et al., 1994). *Xnot1* is a dorsal marker that acts upstream of chordin and plays a fundamental role in notochord formation (Fujimi et al., 2012). *FoxD3* encodes a transcription factor important in the determination, migration, and differentiation of neural crest cells (Cheung et al., 2005; Dottori et al., 2001; Sasai et al., 2001). The significant change seen in *chordin* transcript levels coincide with the neural tube defects that occurred in *RECK* MO-injected embryos. The increase in *chordin* mRNA levels would subsequently cause an increase in the delineated border of cells that could give rise to the neural crest, which would subsequently require more *Xnot1* and *FoxD3* transcription to give rise to neural crest cells. Therefore, *RECK* MO-injected embryos may have increased the number of neural crest cells that could potentially, but do not actually, migrate due to *RECK* knockdown. This may offer an explanation to the effects of neural tube closure failure, subsequent twisting and curving of the dorsal axis, and reduced head structures. In fact, my results are consistent with past studies that have implicated RECK to be important

Figure 2.6 Effect of *RECK* knockdown on transcript levels.

Effect of *RECK* knockdown on transcript levels. Real-time qPCR was used to measure the changes in transcript levels following injection of 6 ng/nL of *RECK* MO into *X. laevis* embryos at the 1-cell stage. Changes in transcript levels were measured relative to *EF1α* and normalized to control (un-injected) embryos (set to 1). Results are based on the average of 3 biological replicates (mean ± SE; technical replicates, N=9). Data is analyzed via t-test: *, p≤0.05.
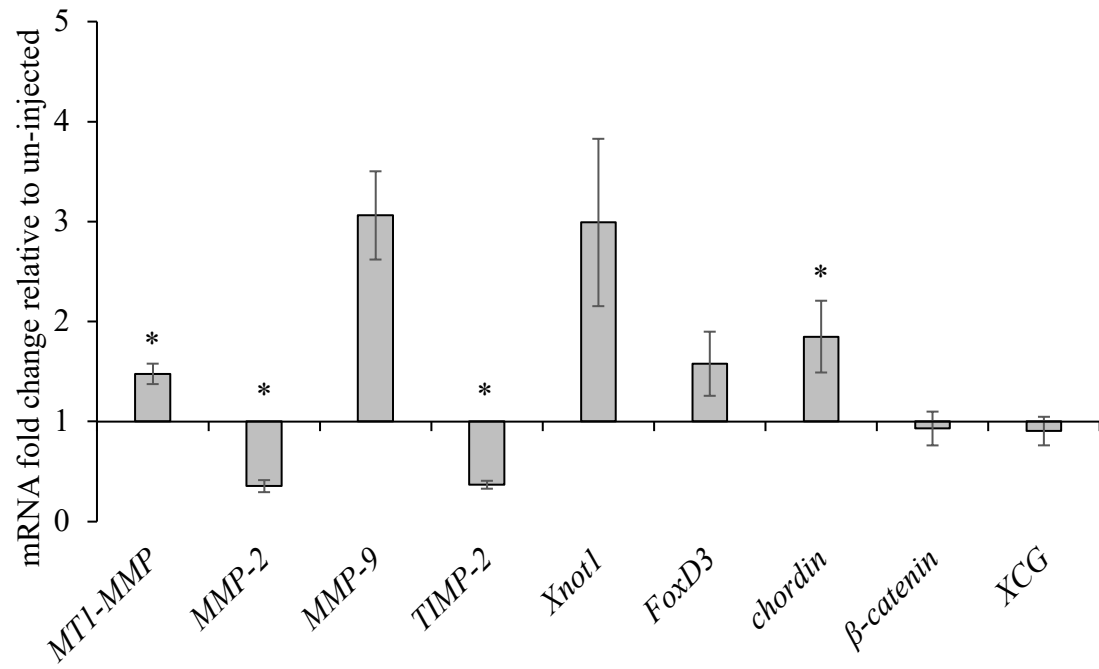
during neural crest cell migration (Prendergast et al., 2012) and neurogenesis (Muraguchi et al., 2007). *β-catenin* (a marker for gastrulation initiation) and *XCG* (cement gland marker) levels did not change in *RECK* MO-injected embryos compared to control (Fig. 2.6), as expected, as *RECK* MO-injected embryos successfully underwent gastrulation.

2.3.3.3   Real-Time qPCR Analysis of ECM Remodeling Genes in *RECK* MO-Injected Embryos

To further understand the morphological phenotypes observed in *RECK* MO-injected embryos, real-time qPCR was performed on ECM remodeling genes that have previously been associated with RECK function (*MT1-MMP*, *MMP-2*, *MMP-9*, and *TIMP-2*) 1 dpf. *RECK* MO-injected embryos at stage 20 (1 dpf) had a significant increase in *MT1-MMP* mRNA levels and a significant decrease in *MMP-2* and *TIMP-2* mRNA levels compared to control (un-injected) embryos (Fig. 2.6). *MMP-9* mRNA levels also changed; however, the increase was not significant compared to control embryos (Fig. 2.6).

MT1-MMP expression is activated early during *X. laevis* development at the gastrula stage, and multiple studies have noted severe developmental defects following disruption of endogenous *MT1-MMP* levels during development (Hasebe et al., 2007; Holmbeck et al., 1999; Zhou et al., 2000). Interestingly, overexpression of *MT1-MMP* in *X. laevis* embryos led to a similar curved dorsal axis phenotype (Hasebe et al., 2007) as I saw in *RECK* MO-injected embryos (Fig. 2.5). My real-time qPCR results indicated a significant increase in *MT1-MMP* transcript levels following *RECK* knockdown (Fig. 2.6), therefore, the morphological defects observed in *RECK* MO-injected embryos could be attributed to aberrant up-regulation of *MT1-MMP* expression. Indeed, RECK is a

known inhibitor of MT1-MMP activity *in vitro* (Oh et al., 2001), and therefore may also play an important MMP-inhibitory role during *X. laevis* development as well.

TIMP-2 is expressed from the neural stage onwards during *X. laevis* development. TIMP-2 also plays an important role during development. Overexpression of *TIMP-2* in *X. laevis* embryos results in severe developmental defects, including neural tube closure failure and axial defects (Nieuwesteeg et al., 2012), similar to what I saw in *RECK* MO-injected embryos (Fig. 2.5). I saw a significant decrease in *TIMP-2* mRNA in *RECK* MO-injected embryos compared to control (Fig. 2.6), which further implies a disruption occurred in the balance between MMPs and their inhibitors in *RECK* MO-injected embryos that led to developmental defects.

It is difficult to determine the exact molecular mechanisms impacted by *RECK* knockdown that led to these specific developmental defects. However, the changes that occurred in the levels of ECM remodeling genes (*MT1-MMP* and *TIMP-2*), suggest that *RECK* expression is a critical factor in regulating cell-ECM interactions during *X. laevis* development.

2.4   Conclusions

This study has revealed the important developmental roles of RECK by demonstrating its high level of evolutionary sequence conservation, developmental localization, and functional importance. All examined animal RECK amino acid sequences contain all hallmark domains. IHC analysis of *RECK* during early *X. laevis* development revealed that *RECK* is present in dorsal and anterior structures such as the neural tube and head region. Disrupting endogenous levels of *RECK* using a MO approach in *X. laevis* embryos resulted in specific developmental phenotypes, including

neural tube closure failure, axial defects, and reduced head formation. Neural tube closure defects were further analyzed by real-time qPCR. Significant increases in *chordin* mRNA levels suggest *RECK* knockdown impacts neural tube closure and subsequent neural crest cell migration. Changes in important ECM remodeling genes (*MT1-MMP*, *MMP-2*, and *TIMP-2*), also propose a possible explanation for the observed phenotypic defects seen in *RECK* MO-injected embryos that may relate to improper ECM degradation and remodeling. My results suggest that during *X. laevis* development, RECK is an important player in neural tube closure and dorsal axis patterning.

2.5   References

Chang, C.K., Hung, W.C., Chang, H.C. (2008). The Kazal motifs of RECK protein inhibit MMP- 9 secretion and activity and reduce metastasis of lung cancer cells *In vitro* and *In vivo*. J Cell Mol Med. **12**: 2781- 2789.

Cheung, M., Chapboissier, M.C., Mynett, A., Hirst, E., Schedi, A., Briscoe, J. (2005). The transcriptional control of trunk neural crest induction, survival, and delamination. Dev Cell. **8**: 179-192.

Ciau-Uitz, A., Walmsley, M., Patient, R. (2000). Distinct origins of adult and embryonic blood in Xenopus. Cell. **102**: 787-796.

Damjanovski, S., Amano, T., Li, Q., Pei, D., Shi, Y. (2001). Overexpression of matrix metalloproteinases leads to lethality in transgenic *Xenopus laevis*: Implications for tissue-dependent functions of matrix metalloproteinases during late embryonic development. Dev Dynam. **221**: 37-47.

de Oliveira Damarchi, A.C., Zambuzzi, W.F., Paiva, K.B., da Silva-Valenzuela, M.D., Nunes, F.D., de Cássia Sávio Figueira, R., Sasahara, R.M., Demasi, M.A., Winnischofer, S.M., Sogayar, M.C., Granjeiro, J.M. (2010). Development of secondary palate requires strict regulation of ECM remodeling: sequential distribution of RECK, MMP-2, MMP-3, and MMP-9. Cell Tissue Res. **340**: 61-69.

Dottori, M., Gross, M.K., Labosky, P., Goulding, M. (2001). The winged-helix transcription factor Foxd3 suppresses interneuron differentiation and promotes neural crest cell fate. Development. **128**: 4127-4138.

Fujimi, T.J., Hatayama, M., Aruga, J. (2012). Xenopus Zic3 controls notochord and organizer development through suppression of the Wnt/ß-catenin signaling pathway. Dev Biol. **361**: 220-231.

Krieg, P.A., Varnum, S.M., Wormington, W.M., Melton, D.A. (1989). The mRNA encoding elongation factor 1-alpha (EF-1 alpha) is a major transcript at the midblastula transition in Xenopus. Dev Biol. **133**: 93-100.

Livak, K., Schmittgen, T. (2001) Analysis of relative gene expression data using real-time quantitative PCR and the $2^{-\Delta\Delta CT}$ method. Method. **25**: 402.

Jung, J.C., Leco, K.J., Edwards, D.R., Fini, M.E. (2002). Matrix metalloproteinases mediate the dismantling of mesenchymal structures in the tadpole tail during thyroid hormone-induced tail resorption. Dev Dyn. **223**: 402-413.

Mayor, R., Theveneau, E. (2013). The neural crest. Development. **140**: 2247-2251.

Muraguchi, T., Takegami, Y., Ohtsuka, T., Kitajima, S., Chandana, E.P., Omura, A., Miki, T., Takahashi, R., Matsumoto, N., Ludwig, A., Noda, M., Takahashi, C. (2007). Reck modulates Notch signaling during cortical neurogenesis by regulating ADAM10 activity. Nat Neurosci. **10**: 838-845.

Neuner, R., Cousin, H., McCusker, C., Coyne, M., Alfandari, D. (2009). Xenopus ADAM19 is involved in neural, neural crest and muscle development. Mech Dev. **126**: 240-255.

Nieuwesteeg, M.A., Walsh, L.A., Fox, M.A., Damjanovski, S. (2012). Domain specific overexpression of TIMP-2 and TIMP-3 reveals MMP-independent functions of TIMPs during *Xenopus laevis* development. Biochem Cell Biol. **90**: 585-95.

Nieuwkoop, P.D., Faber, J. (1956). Normal table of *Xenopus laevis* (Daudin): A systematical and chronological survey of the development from the fertilized egg till the end of metamorphosis. North-Holland Publishing company, Amsterdam.

Nikolopoulou, E., Galea, G.L., Rolo, A., Greene, N.D., Copp, A.J. (2017). Neural tube closure: cellular, molecular and biomechanical mechanisms. Development. **144**: 552-566.

Oh, J., Takahashi, R., Kondo, S., Mizoguchi, A., Nishimura, S., Imamura, Y., Kitayama, H., Alexander, D.B., Horan, T.P., Arakawa, T., Yoshida, H., Nishikawa, S., Itoh, Y., Seiki, M., Itohara, S., Takahashi, C., Noda, M. (2001). The membrane-anchored MMP inhibitor RECK is a key regulator of extracellular matrix integrity and angiogenesis. Cell. **107**: 789-800.

Pickard, B., Damjanovski, S. (2004). Overexpression of the tissue inhibitor of metalloproteinase-3 during Xenopus embryogenesis affects head and axial tissue formation. Cell Res. **14**: 389-399.

Prendergast, A., Linbo, T.H., Swarts, T., Ungos, J.M., McGraw, H.F., Krispin, S., Weinstein, B.M., Raible, D.W. (2012). The metalloproteinase inhibitor RECK is essential for zebrafish DRG development. Development. **139**: 1141-1152.

Sasai, N., Mizuseki, K., Sasai, Y. (2001). Requirement of FoxD3-class signaling for neural crest determination in Xenopus. Development. **128**: 2525-2536.

Sasai, Y., Lu, B., Steinbeisser, H., Geissert, D., Gont, L.K., De Robertis, E.M. (1994). Xenopus chordin: a novel dorsalizing factor activated by organizer-specific homeobox genes. Cell. **79**: 779:790.

Sive, H., Bradley, L. (1996). A sticky problem: the Xenopus cement gland as a paradigm for anteroposterior patterning. Dev Dyn. **205**: 265-280.

Sive, H.L., Grainger, R.M., Harland, R.M. (2000). Early Development of *Xenopus laevis*: A Laboratory Manual. Cold Spring Harbor Laboratory Press, New York.

Takagi, S., Simizu, S., Osada, H. (2009). RECK negatively regulates matrix metalloproteinase-9 transcription. Cancer Res. **69**: 1502-1508.

Takahashi, C., Sheng, Z., Horan, T.P., Kitayama, H., Maki, M., Hitomi, K., Kitaura, Y., Takai, S., Sasahara, R.M., Horimoto, A., Ikawa, Y., Ratzkin, B.J., Arakawa, T., Noda, M. (1998). Regulation of matrix metalloproteinase-9 and inhibition of tumor invasion by the membrane-anchored glycoprotein RECK. Proc Natl Acad Sci USA. **95**: 13221-13226.

van Hoef, V., Breugelmans, B., Spit, J., Simonet, G., Zels, S., Vanden Broeck, J. (2013). Phylogenetic distribution of protease inhibitors of the Kazal-family within the Arthropoda. Peptides. **41**: 59-65.

Visse, R., Nagase, H. (2003). Matrix metalloproteinases and tissue inhibitors of metalloproteinases: structure, function, and biochemistry. Circ Res. **92**: 827-839.

Walsh, L.A., Roy, D.M., Reyngold, M., Giri, D., Snyder, A., Turcan, S., Badwe, C.R., Lyman, J., Bromberg, J., King, T.A., Chan, T.A. (2015). RECK controls breast cancer metastasis by modulating a convergent, STAT3-dependent neoangiogenic switch. Oncogene. **34**: 2189-2203.

Willson, J.A., Nieuwesteeg, M.A., Cepeda, M., Damjanovski, S. (2015). Analysis of *Xenopus laevis* RECK and its relationship to other vertebrate RECK sequences. JSRR. **6**: 504-513.

Yamamoto, M., Matsuzaki, T., Takahashi, R., Adachi, E., Maeda, Y., Yamaguchi, S., Kitayama, H., Echizenya, M., Morioka, Y., Alexander, D.B., Yagi, T., Itohara, S., Nakamura, T., Akiyama, H., Noda, M. (2012). The transformation suppressor gene Reck is required for postaxial patterning in mouse forelimbs. Biol Open. **1**: 458-466.

Chapter 3

3   Spatial Analysis of RECK, MT1-MMP, and TIMP-2 Proteins During Early *Xenopus laevis* Development

3.1   Introduction

MMPs have long been classified as crucial players during vertebrate development due to their ability to cleave components of the ECM (Visse and Nagase, 2003). 24 vertebrate MMPs have been characterized and divided into 2 distinct categories: secreted or MT-MMPs. Each MMP has a specific substrate specificity, carrying out distinct functions during ECM remodeling (Visse and Nagase, 2003). During development MMPs facilitate extensive and necessary ECM remodeling events that allow large-scale cell rearrangements and alter cell signaling. This ECM remodeling is required, as aberrant up-regulation of MMPs has been associated with developmental defects and death. Indeed, previous work with transgenic *X. laevis* embryos demonstrated that overexpression of the MMPs - *collagenase 4 (MMP-18)* or *stromelysin 3 (MMP-11)* - resulted in embryonic lethality (Damjanovski et al., 2001). Therefore, a delicate balance exists between the levels of MMPs and their endogenous inhibitors, TIMPs and RECK. Severe developmental defects have been observed when this balance is shifted towards MMP inhibition via *TIMP-2* overexpression during early *X. laevis* development (Nieuwesteeg et al., 2012). While much research has examined MMP and inhibitor activity levels with respect to large-scale cell movements, less is known about interactions modulating cell signaling events, particularly interactions involving pericellular molecules such as RECK, MT1-MMP, and TIMP-2.

MT1-MMP is unique in that of all *MMPs* only *MT1-MMP* null mice resulted in death, with neonatal mice dying by 12 weeks of age due to severe skeletal and vascularization defects (Holmbeck et al., 1999; Zhou et al., 2000). As a transmembrane protein, MT1-MMP not only remodels the surrounding milieu, but can also interact with

nearby cell surface receptors and facilitate intracellular signaling cascades (Deryugina et al., 2002; Kajita et al., 2001; Seiki, 2002). A well-characterized function of MT1-MMP is its ability to activate pro-MMP-2, a potent protease, in coordination with TIMP-2 (Fig. 1.2). TIMP-2 is unique as it remains more proximal to the cell surface in comparison to the other 3 secreted TIMPs (Itoh et al., 2001).

RECK is another inhibitor of MMPs and is present on the cell surface as a GPI-anchored protein (Oh et al., 2001; Takagi et al., 2009; Takahashi et al., 1998). Expression of *RECK* during development is crucial, as *RECK* null mice were embryonic lethal due to severe vascular defects, in part due to altered MMP activity (Chandana et al., 2010; Oh et al., 2001). *In vitro* studies have shown that RECK not only attenuates the proteolytic activity of MT1-MMP, but it can also modulate its endocytosis from the cell surface (Miki et al., 2007), again demonstrating the functional importance of the pericellular colocalization of these proteins.

MMPs, TIMPs, and RECK all play a crucial role during events that require extensive ECM remodeling, such as during development and tissue repair (Lemaitre and D'Armiento, 2006; McCawley and Matrisian, 2001; Visse and Nagase, 2003; Willson and Damjanovski, 2014). Past studies have examined the roles of MMPs and their inhibitors during early embryonic processes (Alexander et al., 1996; Balbín et al., 2001; Pagenstecher et al., 1997; Prendergast et al., 2012; Wilson et al., 1995). Nuttall et al. (2004) were the first to characterize the expression pattern of every mouse *MMP*, *TIMP*, and *RECK* gene in different tissues throughout mouse development using qPCR analysis. They reported high RNA levels of *MT-MMPs* and *TIMPs*, and low levels of secreted *MMPs*, in most differentiated tissues, though they did not examine protein localization.

In vitro studies have been carried out to show that MT1-MMP interacts individually with RECK and TIMP-2 on the cell surface (Itoh et al., 2001; Miki et al., 2007). Toward furthering our understanding of their roles *in vivo*, in this chapter I investigated the localization of these 3 proteins throughout early development using IHC. At different developmental time points (neurulation, axis elongation, and organogenesis - stages 17-38), RECK, MT1-MMP, and TIMP-2 proteins show strikingly similar localization patterns, particularly in their shifting localization from the dorsal to ventral sides of the neural tube, and in the differentiating somite, suggesting they may function together during specific patterning processes throughout early *X. laevis* development.

3.2   Materials and Methods

3.2.1   Animal Care and Rearing

Adult *X. laevis* were purchased from Xenopus 1, Inc (Dexter, MI). Animal rearing and fertilizations were carried out as described in Section 2.2.1.

3.2.2   Immunohistochemistry and Fluorescence Microscopy

Embryos at stages 17, 20, 28, 34, and 38 (Fig. 1.6) were fixed as described in Section 2.2.4. Fixed embryos were sent to the Molecular Pathology Core Facility at Robarts Research Institute (London, ON) for paraffin embedding and sectioning. Transverse sections (10 μm apart) were made either along the mid anterior-posterior axis or in the anterior head region (as illustrated in Supplementary Fig. S3.1). De-waxed sections were probed with primary antibody (mouse anti-RECK, Santa Cruz, #sc-373929; rabbit anti-RECK, Santa Cruz, #sc-28918; rabbit anti-MT1-MMP, Santa Cruz, #sc-30074; mouse anti-TIMP2, Santa Cruz, #sc21735) diluted 1:100 followed by fluorescently labeled secondary antibody (Alexa Fluor goat anti-mouse and anti-rabbit

IgG, Thermo Fisher Scientific) diluted 1:200. Slides were mounted as described in Section 2.2.4. Antibody validation for rabbit anti-RECK, rabbit anti-MT1-MMP, and mouse anti-TIMP-2 was performed using Western blotting with either *X. laevis* whole embryo lysate or *X. laevis* A6 cell lysate (Supplementary Fig. S3.2). Of note, the epitope region of mouse anti-TIMP-2 shares 82% sequence identity with the *X. laevis* TIMP-2 amino acid sequence. Serial sections were probed with pairs of antibodies: RECK with MT1-MMP, RECK with TIMP-2, and TIMP-2 with MT1-MMP. Thus, the fidelity of an antibody's localization could be confirmed across 2 colocalization studies. Negative controls, following the above protocol, but without primary antibody, were performed to analyze nonspecific binding of the secondary antibody (Supplementary Fig. S3.3). Slides were visualized using a Leica DM16000 B microscope with Hamamatsu camera controller (C10600) using Leica automated inverted microscope and analyzed using Image J 2.0.0 software (NIH, Bethesda). 4 sections per embryo, from 3 embryos per stage were analyzed for each pair of antibodies. Images are representative of 1 section from 1 embryo; however, consistent staining patterns were seen between the sections from each embryo.

3.3   Results and Discussion

To determine the spatial expression patterns of *X. laevis* RECK, MT1-MMP, and TIMP-2 proteins during development, IHC was performed on mid-anterior/posterior (AP) axis transverse sections of embryos (the position as illustrated in Supplementary Fig. S3.1a,b). Transverse sections through the head region on stage 38 embryos were also examined (the position as illustrated in Supplementary Fig. S3.1c). Stages examined included 17-20, representing neural tube closure; 28-34, tailbud stages during which axial

elongation is accompanied by neural and mesodermal patterning; and stage 38, when nerve and muscle cells are differentiating, and organ formation is occurring, most notably the eye and heart (Fig. 1.6). Because *RECK*, *MT1-MMP*, and *TIMP-2* mRNA transcript levels are low prior to and during gastrulation in *X. laevis* (Hasebe et al., 2007; Willson et al., 2015), I decided to begin my analysis following gastrulation. Of note, 2 primary RECK antibodies (mouse anti-RECK (red) and rabbit anti-RECK (green)) were used to verify the validity of RECK localization by probing sections with both antibodies (Supplementary Fig. S3.3). A negative control omitting primary antibodies was also performed to demonstrate specificity (Supplementary Fig. S3.3).

3.3.1 RECK Localization During Early *X. laevis* Development

I have previously shown through whole mount *in situ* hybridization that *X. laevis RECK* mRNA is present in tailbud embryos in dorsal axial structures, including the neural tube and the eye (Willson et al., 2015). My previous analysis of RECK protein localization using IHC on stage 28 embryos demonstrated neural and branchial arch localization (Fig. 2.2). To expand on these results, here I examined RECK protein localization, together with MT1-MMP and TIMP-2, throughout early *X. laevis* development from stages 17 to 38.

During neural plate bending (stage 17), there was broad but weak punctate RECK staining unassociated with specific regions (Fig. 3.1A$_2$, 3.2A$_2$), suggesting RECK does not have a distinct localization in any tissue at this stage. However, at stage 20, when the neural tube has just closed and is beginning to elongate, RECK localization was distinct with robust staining appearing along epidermal tissues as well as along the dorsal side of the neural tube (Fig. 3.1B$_2$, 3.2B$_2$). Since the neural crest resides on the dorsal side of the

Figure 3.1. Localization of RECK and MT1-MMP proteins during early *X. laevis* development.

IHC was performed using Alexa Fluor 555-labeled anti-RECK (red) and Alexa Fluor 488-labeled anti MT1-MMP (green) antibodies on stage 17-38 embryos. Brightfield DIC images are shown in the left panel. Mono-colour images for RECK and MT1-MMP are presented individually. Colocalization of RECK and MT1-MMP (yellow) is shown on the right panel. Dotted line in stage 28 merged image indicates overlapping signal within the middle of somites. Dashed line in stages 34 and 38 merged images indicates overlapping signal along the ventral neural tube. Scale bar= 100 µm. Abbreviations: E=endoderm, Ep=epidermis, D=dorsal NT, DF=dorsal fin, N=notochord, NC=neural crest, NP=neural plate, NT=neural tube, S=somitic mesoderm, V=ventral NT.

	DIC	RECK	MT1-MMP	Merged
St 17	A₁	A₂	A₃	A₄
St 20	B₁	B₂	B₃	B₄
St 28	C₁	C₂	C₃	C₄
St 34	D₁	D₂	D₃	D₄
St 38	E₁	E₂	E₃	E₄

Figure 3.2. Localization of RECK and TIMP-2 proteins during early *X. laevis* development.

IHC was performed using Alexa Fluor 488-labeled anti RECK (green) and Alexa Fluor 555-labeled anti-TIMP-2 (red) antibodies on stage 17-38 embryos. Brightfield DIC images are shown in the left panel. Mono-colour images for RECK and TIMP-2 are presented individually. Colocalization of RECK and TIMP-2 (yellow) is shown on the right panel. Dotted line in stage 28 merged image indicates overlapping signal within the middle of somites. Dashed line in stages 34 and 38 merged images indicates overlapping signal along the ventral neural tube. Scale bar= 100 µm. Abbreviations: E=endoderm, Ep=epidermis, D=dorsal NT, DF=dorsal fin, N=notochord, NC=neural crest, NP=neural plate, NT=neural tube, S=somitic mesoderm, V=ventral NT.

DIC RECK TIMP-2 Merged
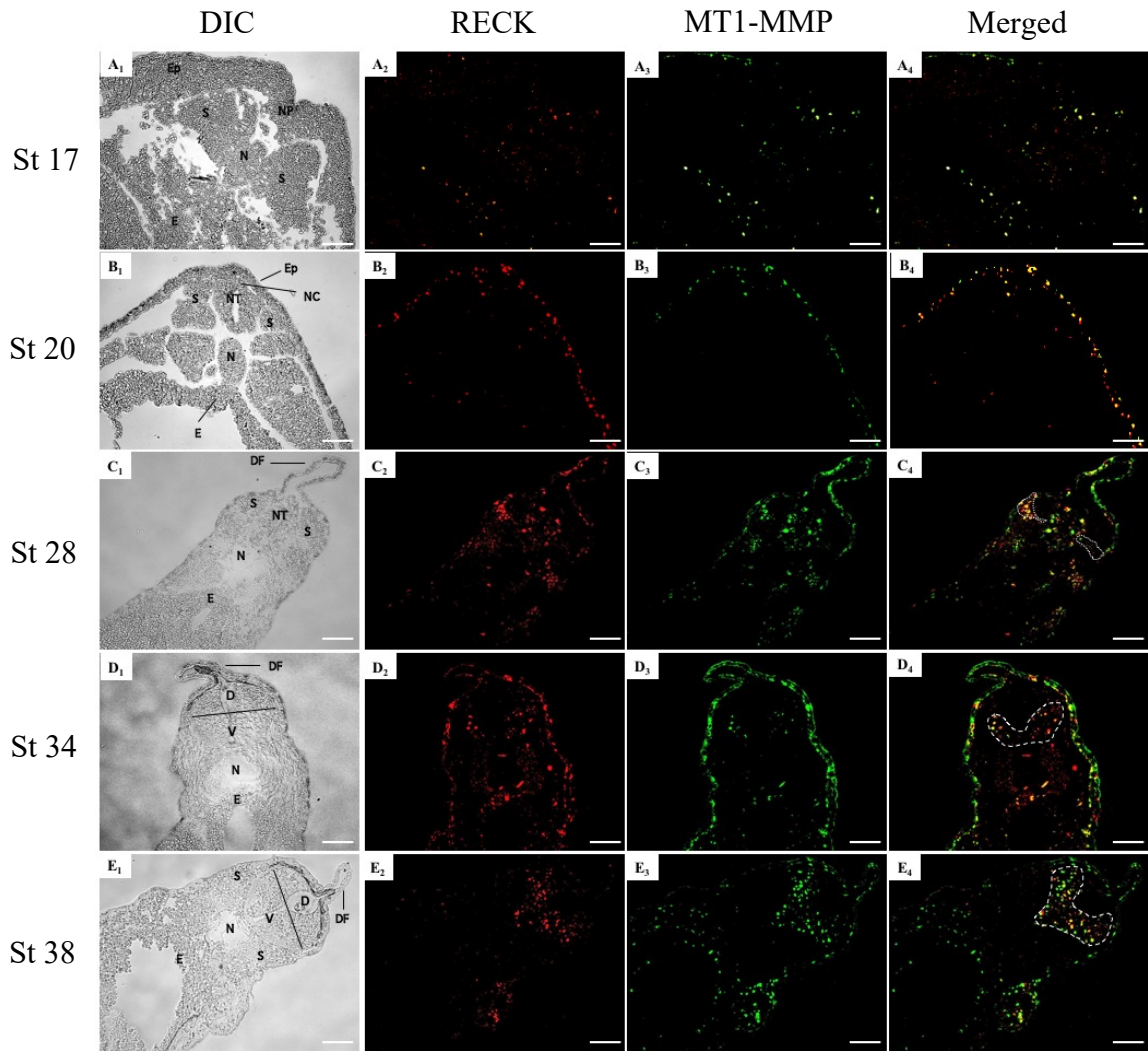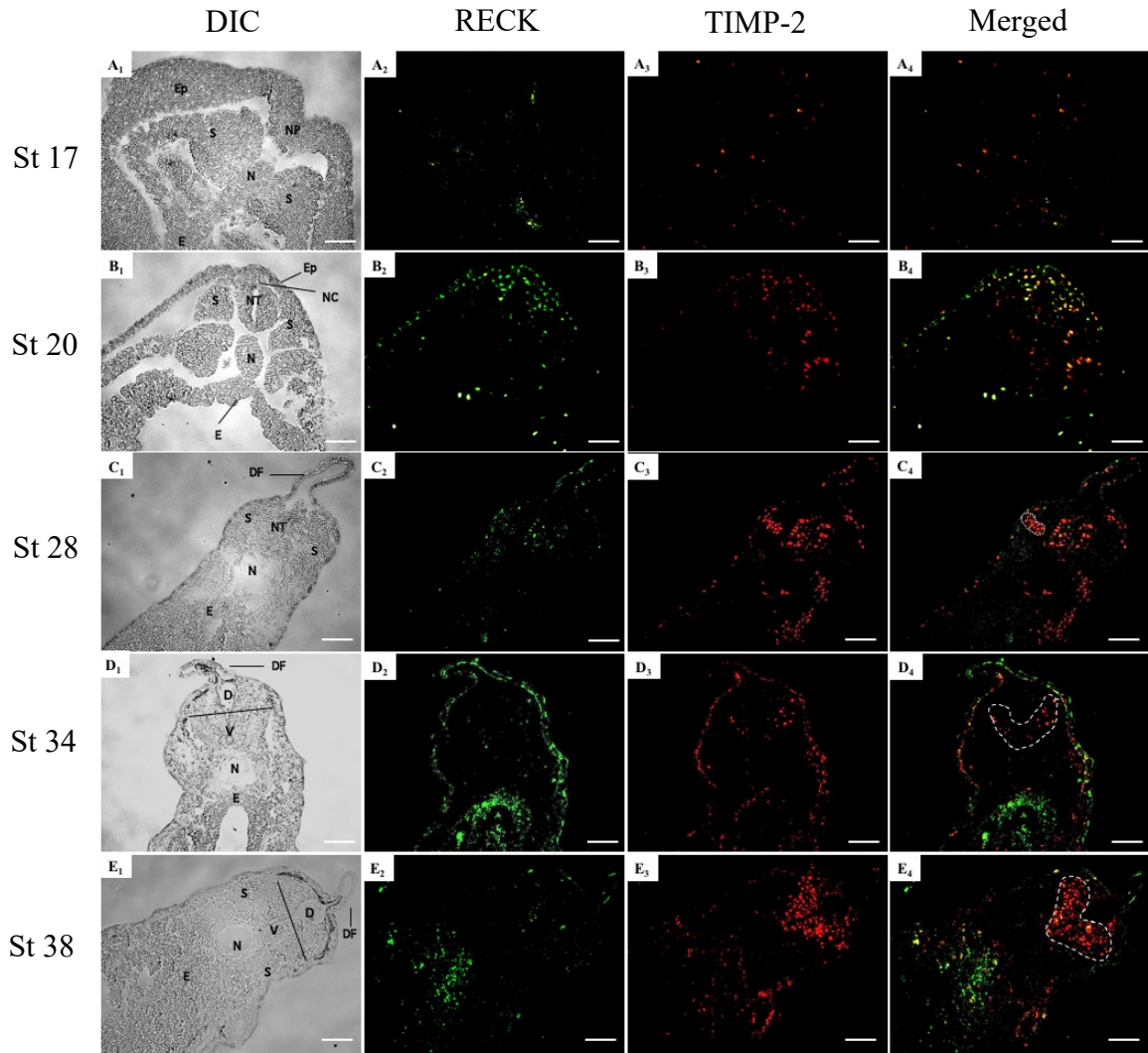
St 17

A$_1$ Ep S NP N S E

A$_2$

A$_3$

A$_4$

St 20

B$_1$ Ep S NT NC S N E

B$_2$

B$_3$

B$_4$

St 28

C$_1$ DF S NT S N E

C$_2$

C$_3$

C$_4$

St 34

D$_1$ DF D V N E

D$_2$

D$_3$

D$_4$

St 38

E$_1$ S D V N DF E S

E$_2$

E$_3$

E$_4$

neural tube upon closure (Le Douarin and Kalcheim, 1999), it appears that RECK proteins are present within neural crest cells at this stage (Fig. $3.1B_2$ and Fig. $3.2B_2$). This is evident in Fig. $3.2B_2$ (arrow) where RECK staining appears to localize in cells that are located along the periphery of the neural tube, not within the neural tube itself, in agreement with the known migratory path of neural crest cells (Le Douarin and Kalcheim, 1999). Indeed, RECK is essential during neural crest cell migration in zebrafish (Prendergast et al., 2012), and I have previously shown *RECK* mRNA and protein staining within the head and branchial arches, structures in the embryo where neural crest cells are known to migrate (Lumsden et al., 1991; Tosney, 1982).

There was also faint RECK staining in endodermal cells at stage 20 embryos (Fig. $3.1B_2$, $3.2B_2$). At stage 28, when axis elongation is prevalent and mesodermal/neural tissues are being patterned, RECK proteins were localized in the dorsal epidermis and within most areas of the neural tube (Fig. $3.1C_2$, $3.2C_2$), which is consistent with my past *in situ* data of *RECK* (Willson et al., 2015). RECK also localized to the middle portion of the somitic mesoderm. (Fig. $3.1C_2$, $3.2C_2$). This horizontal RECK expression domain in the middle of the somite lies across the differentiating dermatomes, myotomes, and sclerotomes, which are differentiating vertically. This suggests RECK is present briefly in the mid-region of the dermatomes, myotomes, and sclerotomes as they are being differentiated; in agreement with past studies that have shown RECK as a regulator of myogenesis *in vitro* (Echizenya et al., 2005).

By late tailbud stages (stage 34), RECK staining was absent in the somites, but appeared in the cells surrounding the notochord (Fig. $3.1D_2$, $3.2D_2$). Also at stages 34 and 38, RECK localization shifted from being present within the entire neural tube (stage 28),

to becoming more pronounced along the ventral side of the neural tube (stages 34) (Fig. 3.1C$_2$-E$_2$, 3.2C$_2$-E$_2$). RECK staining was also present in the anterior (head) region of stage 38 embryos in the epidermis and eye region, consistent with my past *in situ* data (Willson et al., 2015), and as with the mid AP-axis sections, along the ventral side of the neural tube (Fig. 3.4A$_2$, B$_2$).

Given that RECK has been implicated to play a role in neurogenesis in mice (Muraguchi et al., 2007), it is consistent with my results that show RECK proteins localize to the epidermis and neural tube during *X. laevis* development. Neurulation involves ectodermal migration, patterning, and differentiation of neural tissue. This patterning, particularly the dorsoventral (D-V) patterning of the neural tube after closure, is well characterized and involves dorsal BMP signals and ventral Shh signals (De Robertis and Kuroda, 2008). Ventral Shh signals are responsible for motor neuron differentiation and dorsal BMP signals are responsible for sensory neurons, with interneurons present in between. The distinct shift in RECK localization from the dorsal (stage 20), to entire (stage 28), to ventral side (stage 34) of the neural tube implicates its role in D-V differentiation, though not of any specific neuron type. Here, I found that RECK proteins appear to be present when patterning and differentiation events are occurring.

3.3.2   MT1-MMP Localization During Early *X. laevis* Development

Following RECK protein localization, I next examined MT1-MMP localization. While MT1-MMP has been associated with events that encompasses extensive ECM degradation and remodeling, including important roles during frog metamorphosis

(Hasebe et al., 2007; Jung et al., 2002; Patterton et al., 1995), MT1-MMP protein localization within *X. laevis* neurulation has not been examined.

During neurulation (stages 17 and 20), MT1-MMP protein staining displayed a strikingly similar localization pattern as RECK. At stage 17, prior to neural tube formation, there was punctate MT1-MMP staining that was not associated with distinct tissues (Fig. 3.1A$_3$, 3.3A$_3$). However, at stage 20 following neural tube closure, MT1-MMP proteins localized to the dorsal side of the neural tube and along the epidermal tissue (Fig. 3.1B$_3$, 3.3B$_3$). This staining pattern on the dorsal side of the neural tube appears to be localized where neural crest cells reside, similar to what I saw with RECK. This is not surprising, since recently MT1-MMP has been shown to be required for proper neural crest cell migration during *X. laevis* development (Garmon et al., 2018).

At stage 28, MT1-MMP staining was distinct, localizing to the entire neural tube, somitic mesoderm, and epidermis (Fig. 3.1C$_3$, 3.3C$_3$). During the late tailbud stages (stages 34 and 38), MT1-MMP staining disappeared from the somites, became more robust along the epidermis, and shifted to the ventral side of the neural tube (Fig. 3.1D$_3$-E$_3$, 3.3D$_3$-E$_3$). MT1-MMP also exhibited staining in the anterior (head) region of stage 38 embryos in the epidermis, eye region, and, as with the mid AP-axis sections, along the ventral side of the neural tube (Fig. 3.4A$_3$, C$_3$). Like RECK, MT1-MMP was present transiently in the middle of somites at stage 28, with a distinct shift in MT1-MMP localization from the dorsal (stage 20), to entire (stage 28), to ventral side (stage 34) of the neural tube during the tailbud stages. These observations implicate a role for MT1-MMP in patterning and differentiation.

Figure 3.3. Localization of TIMP-2 and MT1-MMP proteins during early *X. laevis* development.

IHC was performed using Alexa Fluor 555-labeled anti-TIMP-2 (red) and Alexa Fluor 488-labeled anti MT1-MMP (green) antibodies on stage 17-34 embryos. Brightfield DIC images are shown in the left panel. Mono-colour images for TIMP-2 and MT1-MMP are presented individually. Colocalization of TIMP-2 and MT1-MMP (yellow) is shown on the right panel. Dotted line in stage 28 merged image indicates overlapping signal within the middle of somites. Dashed line in stage 34 merged image indicates overlapping signal along the ventral neural tube. Scale bar= 100 μm. Abbreviations: E=endoderm, Ep=epidermis, D=dorsal NT, DF=dorsal fin, N=notochord, NC=neural crest, NP=neural plate, NT=neural tube, S=somitic mesoderm, V=ventral NT.

DIC	TIMP-2	MT1-MMP	Merged

St17

St 20

St 28

St 34

St 38
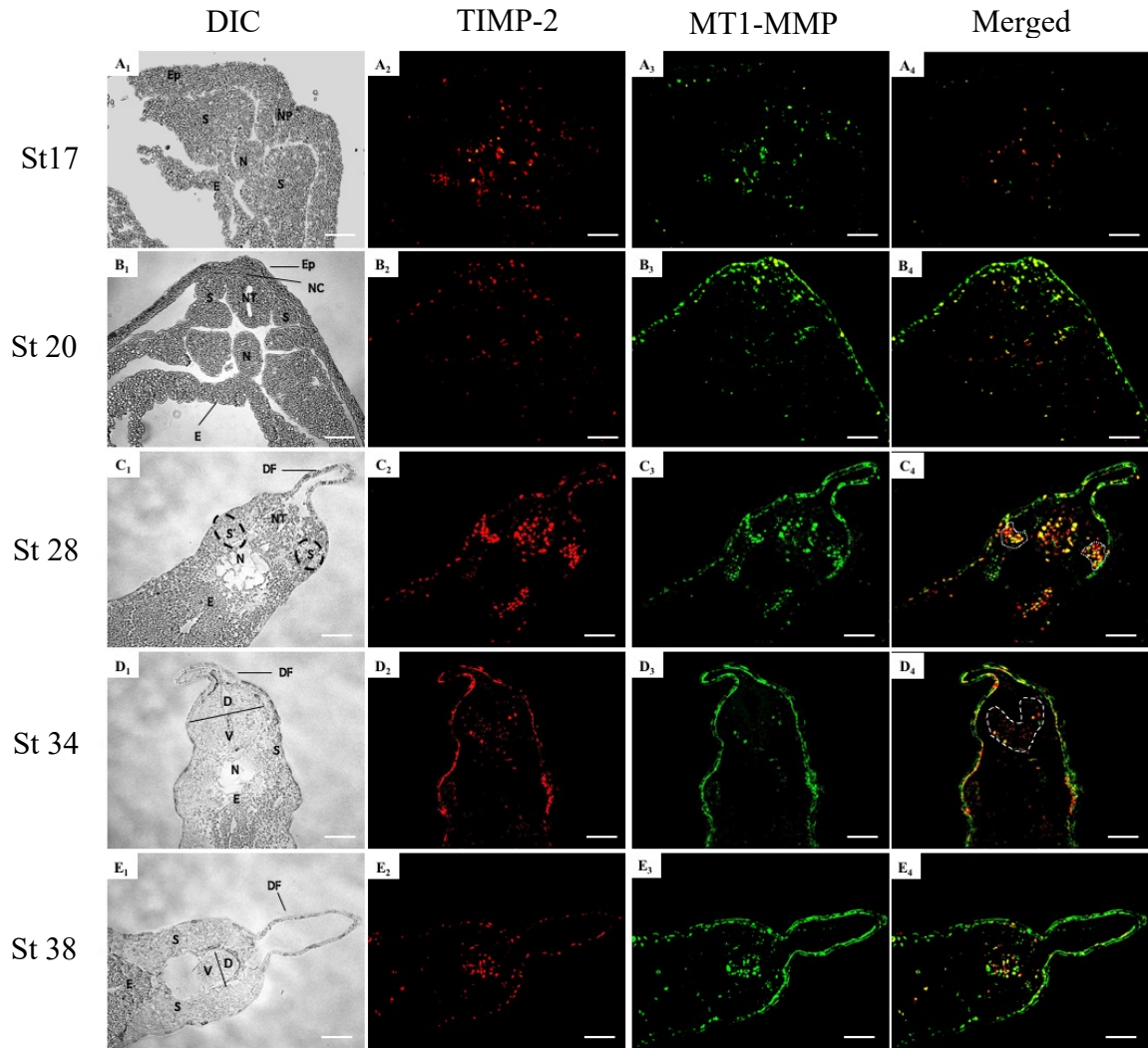
Figure 3.4. Localization of RECK, MT1-MMP, and TIMP-2 proteins in the anterior region of stage 38 *X. laevis* **embryos.**

IHC was performed using Alexa Fluor 555-labeled anti-RECK and anti TIMP-2 (red) and Alexa Fluor 488-labeled anti-MT1-MMP and anti-RECK (green) antibodies on stage 38 embryos. Brightfield DIC images are shown in the left panel. Mono-colour images for RECK, MT1-MMP, and TIMP-2 are presented individually. Colocalization of RECK and MT1-MMP, RECK and TIMP-2, or TIMP-2 and MT1-MMP (yellow) is shown on the right panel. Scale bar= 100 μm. Abbreviations: E=endoderm, NT=Neural tube.
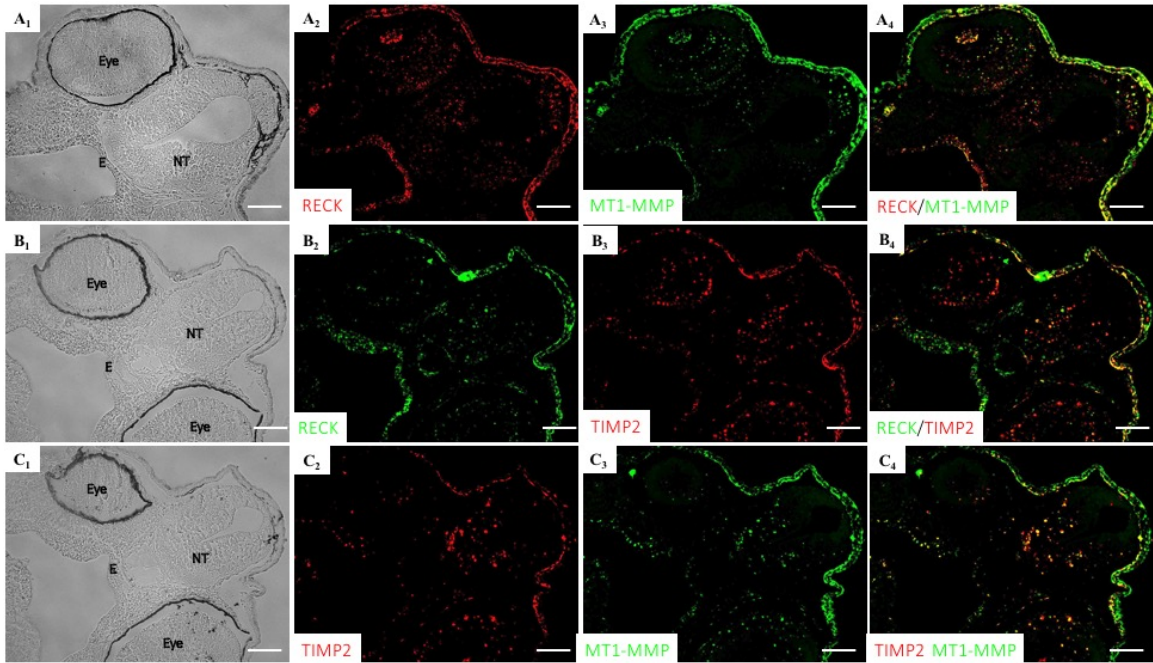
3.3.3   TIMP-2 Localization During Early *X. laevis* Development

TIMP-2 not only inhibits MMPs but has also been associated with a number of cell signaling pathways due to its pericellular localization (Stetler-Stevenson 2008). I have previously shown that *TIMP-2* overexpression in *X. laevis* embryos resulted in severe developmental defects and death (Nieuwesteeg et al., 2012). To further elucidate the role of TIMP-2 during development, I analyzed the spatial localization of TIMP-2 proteins in *X. laevis* embryos.

During neurulation (stages 17 and 20), while present in the ectoderm and dorsal side of the neural tube, TIMP-2 proteins were localized to a number of tissues including somitic mesoderm and endoderm (Fig. 3.2A_3, B_3 and 3.3A_2, B_2). As I saw with RECK and MT1-MMP, TIMP-2 staining also occurred along the dorsal side of the neural tube where the neural crest resides (Fig. 3.2A_3, B_3 and 3.3A_2, B_2), which coincides with past studies implicating a role for TIMP-2 in the migration of neural crest cells in chick (Cantemir et al., 2004).

In the tailbud (stage 28), there was robust TIMP-2 staining in the entire neural tube, the middle of the somites, and epidermis (Fig. 3.2C_3, 3.3C_2), similar to RECK and MT1-MMP. By stage 34, TIMP-2 staining within the neural tube decreased and shifted ventrally, was greatly reduced in the somites, but persisted in the epidermis. Punctate TIMP-2 staining also appeared in some endodermal cells during these stages (Fig. 3.2D_3, 3.3D_2). By stage 38, TIMP-2 again exhibited punctate staining within the entire neural tube, as well as the eye (Fig. 3.4B_3, C_2). Like RECK and MT1-MMP, TIMP-2 was present transiently in the middle of somites at stage 28, with a distinct shift in TIMP-2 localization from the dorsal (stage 20), to entire (stage 28), to ventral (stage 34) side of

the neural tube during the tailbud stages, which also implicates a role for TIMP-2 in patterning and differentiation.

3.3.4   RECK, MT1-MMP, and TIMP-2 Exhibit Similar Localization Patterns

The relationship between MT1-MMP, RECK, and TIMP-2 has been examined *in vitro*, however, due to the complex nature of amniote vertebrate embryos and the redundant functions of MMPs and TIMPs, it has been difficult to elucidate any cooperative roles they may play *in vivo*. Here, the examination of anamniote frog embryos allows us to examine their localization in very early developmental processes.

RECK, MT1-MMP, and TIMP-2 exhibited distinct overlapping expression patterns throughout all stages examined (summarized in Table 3.1). Shortly after neural tube closure (stage 20) and in early tailbud stages, RECK, MT1-MMP, and TIMP-2 proteins were localized to the dorsal side of the neural tube and along the epidermal tissue (Fig. 3.1B$_4$, 3.2B$_4$, 3.3B$_4$). The localized staining of all 3 proteins at the most dorsal spot of the neural tube and alongside the left and right periphery of the neural tube suggest they are present within the neural crest cell migration domains (Fig. 3.1B$_4$, 3.2B$_4$, 3.3B$_4$). Without the use of a neural crest cell marker, however, the migration of this transient population of cells could not be observed in later stages (stages 28-38). Since all 3 proteins have been implicated individually to play an important role in the migration of neural crest cells (Cantemir et al., 2004; Garmon et al., 2018; Prendergast et al., 2012), future work examining if MT1-MMP, TIMP-2, and RECK interact with each other to properly regulate neural crest cell migration would be of great interest.

At stage 28, when somitogenesis (segmentation and differentiation) is ongoing,

Table 3.1: Summary of the spatial expression pattern of RECK, MT1-MMP, and TIMP-2 proteins in various tissue types throughout early *X. laevis* developmental stages.

Tissue Type	Neurula (Stages 18-20)	Early Tailbud (Stage 28)	Late Tailbud (Stages 34-38)
Epidermis	RECK MT1-MMP TIMP-2	RECK MT1-MMP TIMP-2	RECK MT1-MMP TIMP-2
Neural Tube	RECK MT1-MMP TIMP-2	RECK MT1-MMP TIMP-2	RECK MT1-MMP TIMP-2
Somites	TIMP-2	RECK MT1-MMP TIMP-2	RECK MT1-MMP TIMP-2
Notochord	-----	-----	-----
Endoderm	RECK MT1-MMP TIMP-2	-----	RECK MT1-MMP TIMP-2
Eye Region	N/A	RECK MT1-MMP TIMP-2	RECK MT1-MMP TIMP-2

all 3 proteins localized to the middle of the somitic mesoderm (Fig. $3.1C_4$, $3.2C_4$, $3.3C_4$). By stages 34 and 38, when signals for myotome, dermatome, and sclerotome specification are largely complete, RECK, MT1-MMP, and TIMP-2 localization within the somites is reduced while at the same time their localization within the neural tube shifts to the ventral side (Fig. 3.1-$3.3D_4$-E_4). All 3 proteins also localize in endodermal tissues in the late tailbud stages (Fig. 3.1-$3.3D_4$-E_4).

3.4   Conclusions

Due to their highly similar localization patterns throughout *X. laevis* development, my results suggest that RECK, MT1-MMP, and TIMP-2 function together during different developmental events to influence cell behaviour and ECM remodeling. Despite the original description of MMPs as enzymes that remodel the ECM, and TIMPs and RECK as inhibitors of this process, the pericellular localization of MT1-MMP, RECK, and TIMP-2 suggests that they have regulatory activities independent of their ECM remodeling role. Indeed, similar to the expression analysis of Nuttall et al. (2004), where they suggest that MT-MMPs are expressed in cells that are in an active state and high expression of TIMPs are associated with the maintenance of tissue integrity, here, I see colocalization of MT1-MMP, TIMP-2, and RECK in later developmental stages in which tissues undergo patterning and differentiation (Table 3.1). While my findings do not preclude the modulation of ECM remodeling, my data do support an additional important role for these proteins in the patterning and differentiation of the neural tube and somites. Early embryogenesis requires the control of cell proliferation, cell migration, differentiation and ultimately distinct cell functions - processes that need to be

coordinated by molecules that govern such events - molecules such as RECK, MT1-MMP, and TIMP-2.

3.5   Supplementary Data

Figure S3.1 Schematic diagram representing the location of the transverse sections on *X. laevis* embryos.

Transverse sections (10 μm apart) were made in the mid anterior-posterior axis (as delineated by the boxes) of (a) neurulating embryos (stages 17 and 20) and (b) early/late tailbud embryos (stages 28, 34, and 38). (c) Transverse sections (10 μm apart) were made in the anterior head region (as delineated by the box) in late tailbud embryos (stage 38).
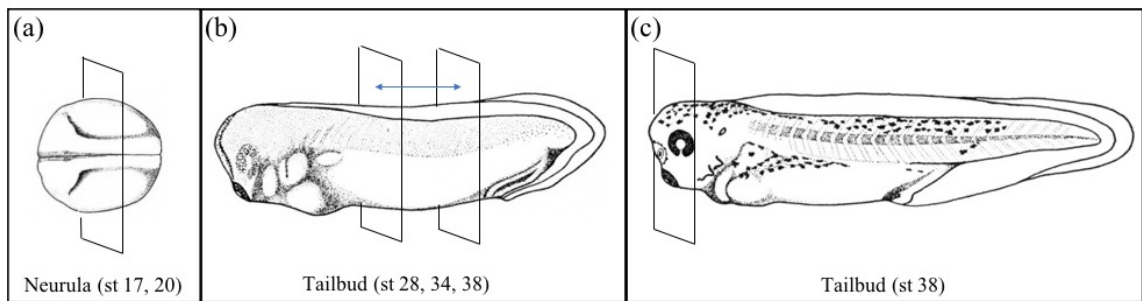
(a) Neurula (st 17, 20)

(b) Tailbud (st 28, 34, 38)

(c) Tailbud (st 38)

Figure S3.2 Validation of antibodies using Western blotting.

(a) A blot probed with human rabbit anti-RECK shows a specific band at the expected molecular weight (110 kDa) in *X. laevis* A6 cell lysate. (b) A blot probed with human mouse anti-TIMP-2 shows a specific band at the expected molecular weight (21 kDa) in *X. laevis* A6 cell lysate. (c) A blot probed with human rabbit anti-MT1-MMP shows a specific band at the expected molecular weight (63 kDa) in *X. laevis* whole embryo lysate.
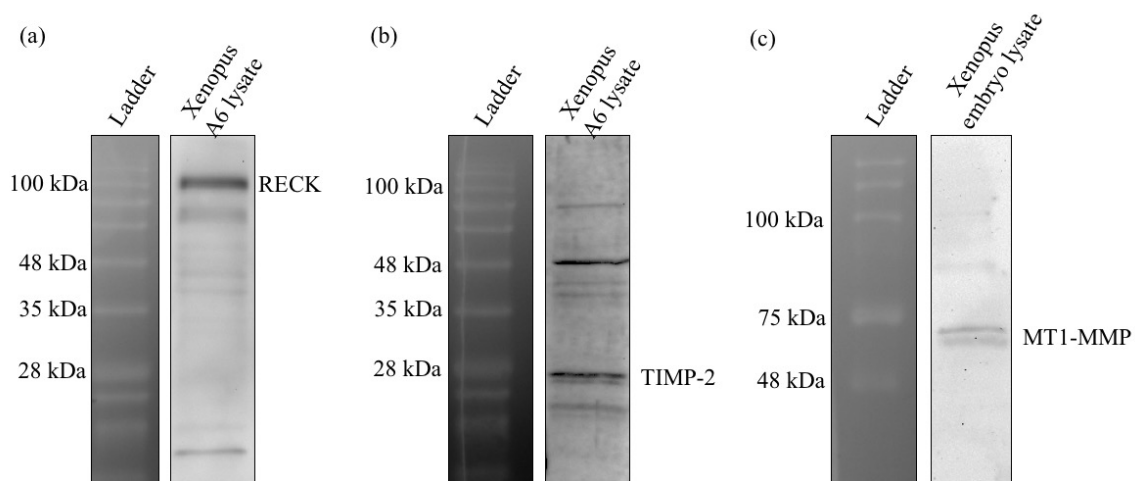
(a)

Ladder

Xenopus
A6 lysate

100 kDa — — RECK

48 kDa —

35 kDa —

28 kDa —

(b)

Ladder

Xenopus
A6 lysate

100 kDa —

48 kDa —

35 kDa —

28 kDa —

TIMP-2

(c)

Ladder

Xenopus
embryo lysate

100 kDa —

75 kDa —

48 kDa —

MT1-MMP

Figure S3.3 Validity of antibodies.

IHC was performed using only secondary antibodies (Alexa Fluor 555-labeled anti-mouse (red) and Alexa Fluor 488 anti-rabbit (red)) and costained with DAPI (blue) on stage 34 embryos to establish specificity in the experiment (right panels). Sections were also probed with both primary RECK antibodies used in these experiments (Alexa Fluor 555-labeled mouse anti-RECK (red) and Alexa Fluor 488 labeled rabbit anti-RECK (green)) and costained with DAPI (blue) to validate their specificity. Colocalization is indicated on the bottom right panel (yellow). Brightfield DIC images are shown on the left panels.
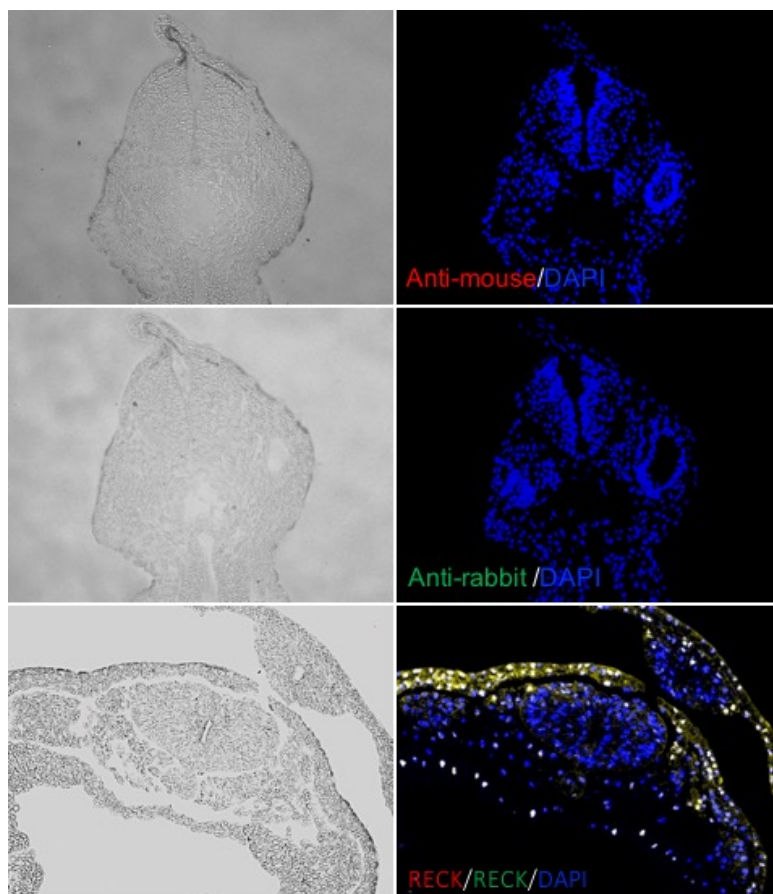
3.6   References

Alexander, C.M., Hansell, E.J., Behrendtsen, O., Flannery, M.L., Kishnani, N.S., Hawkes, S.P., Werb, Z. (1996). Expression and function of matrix metalloproteinases and their inhibitors at the maternal-embryonic boundary during mouse embryo implantation. Development. **122**: 1723-1736.

Balbín, M., Fueyo, A., Knäuper, V., López, J.M., Álvarez, J., Sánchez, L.M., Quesada, V., Bordallo, J., Murphy, G., López-Otín, C. (2001). Identification and Enzymatic Characterization of Two Diverging Murine Counterparts of Human Interstitial Collagenase (MMP-1) Expressed at Sites of Embryo Implantation. J Biol Chem. **276**: 10253-10262.

Cantemir, V., Cai, D.H., Reedy, M.V., Brauer, P.R. (2004). Tissue inhibitor of metalloproteinase-2 (TIMP-2) expression during cardiac neural crest cell migration and its role in pro-MMP-2 activation. Dev Dynam. **231**: 709-719.

Chandana, E.P.S., Maeda, Y., Ueda, A., Kiyonari, H., Oshima, N., Yamamoto, M., Kondo, S., Oh, J., Takahashi, R., Yoshida, Y., Kawashima, S., Alexander, D.B., Kitayama, H., Takahashi, C., Tabata, Y., Matsuzaki, T., Noda, M. (2010). Involvement of the Reck tumor suppressor protein in maternal and embryonic vascular remodeling in mice. BMC Dev Biol. **10**: 84.

Damjanovski, S. Amano, T., Li, Q., Pei, D., Shi, Y. (2001). Overexpression of matrix metalloproteinases leads to lethality in transgenic *Xenopus laevis*: Implications for tissue-dependent functions of matrix metalloproteinases during late embryonic development. Dev Dynam. **221**: 37-47.

De Robertis, E.M., Kuroda, H. (2008). Dorsal-Ventral Patterning and Neural Induction in Xenopus Embryos. Annu Rev Cell Dev Biol. **20**: 285-308.

Deryugina, E.I., Ratnikov, B.I., Postnova, T.I., Rozanov, D.V., Strongin, A.Y. (2002). Processing of integrin alpha(v) subunit by membrane type 1 matrix metalloproteinase stimulates migration of breast carcinoma cells on vitronectin and enhances tyrosine phosphorylation of focal adhesion kinase. J Biol Chem. **277**: 9749–9756.

Echizenya, M., Kondo, S., Takahashi, R., Oh, J., Kawashima, S., Kitayama, H., Takahashi, C., Noda, M. (2005). The membrane-anchored MMP-regulator RECK is a target of myogenic regulatory factors. Oncogene. **24**: 5850-5857.

Garmon, T., Wittling, M., Nie, S. (2018). MMP14 regulates cranial neural crest epithelial-to-mesenchymal transition and migration. Dev Dynam. **247**: 1083-1092.

Hasebe, T., Hartman, R., Fu, L., Amano, T., Shi, Y. (2007). Evidence for a cooperative role of gelatinase A and membrane type-1 matrix metalloproteinase during *Xenopus laevis* development. Mech Dev. **124**: 11-22.

Holmbeck, K., Bianco, P., Caterina, J., Yamada, S., Kromer, M., Kuznetsov, S.A., Mankani, M., Robey, P.G., Poole, A.R., Pidoux, I., Ward, J.M., Birkedal-Hansen, H. (1999). MT1-MMP deficient mice develop dwarfism, osteopenia, arthritis, and connective tissue disease due to inadequate collagen turnover. Cell. **99**: 81-92.

Itoh, Y., Takamura, A., Ito, N., Maru, Y., Sato, H., Suenaga, N., Aoki, T., Seiki, M. (2001). Homophilic complex formation of MT1-MMP facilitates proMMP-2 activation on the cell surface and promotes tumor cell invasion. EMBO J. **20**: 4782-4793.

Jung, J.C., Leco, K.J., Edwards, D.R., Fini, M.E. (2002). Matrix metalloproteinases mediate the dismantling of mesenchymal structures in the tadpole tail during thyroid hormone-induced tail resorption. Dev Dyn. **223**: 402-413.

Kajita, M., Itoh, Y., Mori, H., Okada, A., Kinoh, H., Seiki, M. (2001). Membrane-type 1 matrix metalloproteinase cleaves CD44 and promotes cell migration. J Cell Biol. **153**: 893-904.

Le Douarin, N., Kalcheim, C. (1999). The Neural Crest. Cambridge University Press, Cambridge, UK.

Lemaître, V., D'Armiento, J. (2006). Matrix metalloproteinases in development and disease. Birth Defects Res C Embryo Today. **78**: 1-10.

Lumsden, A., Sprawson, N., Graham, A. (1991). Segmental origin and migration of neural crest cells in the hindbrain region of the chick embryo. Development. **113**: 1281-1291.

McCawley, L.J., Matrisian, L.M. (2001). Matrix metalloproteinases: they're not just for matrix anymore! Curr Opin Cell. Biol. **13**: 534-540.

Miki, T., Takegami, Y., Okawa, K., Muraguchi, T., Noda, M., Takahashi, C. (2007). The reversion-inducing cysteine-rich protein with Kazal motifs (RECK) interacts with membrane type 1 matrix metalloproteinase and CD13/aminopeptidase N and modulates their endocytic pathways. J Biol Chem. **282**: 12341-12352.

Muraguchi, T., Takegami, Y., Ohtsuka, T., Kitajima, S., Chandana, E.P., Omura, A., Miki, T., Takahashi, R., Matsumoto, N., Ludwig, A., Noda, M., Takahashi, C. (2007). Reck modulates Notch signaling during cortical neurogenesis by regulating ADAM10 activity. Nat Neurosci. **10**: 838-845.

Nieuwesteeg, M.A., Walsh, L.A., Fox, M.A., Damjanovski, S. (2012). Domain specific overexpression of TIMP-2 and TIMP-3 reveals MMP-independent functions of TIMPs during *Xenopus laevis* development. Biochem Cell Biol. **90**: 585-595.

Nieuwkoop, P.D., and Faber, J. (1994). Normal Table of *Xenopus laevis*. Garland Publishing, New York.

Nuttall, R.K., Sampieri, C.L., Pennington, C.J., Gill, S.E., Schultz, G.A., Edwards, D.R. (2004). Expression analysis of the entire MMP and TIMP gene families during mouse tissue development. FEBS Letters. **563**: 129-134.

Oh, J., Takahashi, R., Kondo, S., Mizoguchi, A., Nishimura, S., Imamura, Y., Kitayama, H., Alexander, D.B., Horan, T.P., Arakawa, T., Yoshida, H., Nishikawa, S., Itoh, Y., Seiki, M., Itohara, S., Takahashi, C., Noda, M. (2001). The membrane-anchored MMP inhibitor RECK is a key regulator of extracellular matrix integrity and angiogenesis. Cell. **107**: 789-800.

Patterton, D., Hayes, W.P., Shi, Y.B. (1995). Transcriptional activation of the matrix metalloproteinase gene *stromelysin-3* coincides with thyroid hormone-induced cell death during frog metamorphosis. Dev Biol. **167**: 252-262.

Pagenstecher, A., Stalder, A.K., Campbell, I.L. (1997). RNAse protection assays for the simultaneous and semiquantitative analysis of multiple murine matrix metalloproteinase (MMP) and MMP inhibitor mRNAs. J Immunol Methods. **206**: 1-9.

Prendergast, A., Linbo, T.H., Swarts, T., Ungos, J.M., McGraw, H.F., Krispin, S., Weinstein, B.M., Raible, D.W. (2012). The metalloproteinase inhibitor RECK is essential for zebrafish DRG development. Development. **139**: 1141-1152.

Seiki, M. (2002). The cell surface: the stage for matrix metalloproteinase regulation of migration. Curr Opin Cell Biol. **14**: 624-632.

Sive, H.L., Grainger, R.M., Harland, R.M. (2000). Early Development of *Xenopus laevis*: A Laboratory Manual. Cold Spring Harbor Laboratory Press, New York.

Stetler-Stevenson, W.G. (2008). Tissue inhibitors of metalloproteinases in cell signaling: metalloproteinase-independent biological activities. Sci Signal. **1**: 1-19.

Takagi, S., Simizu, S., and Osada, H. (2009). RECK negatively regulates matrix metalloproteinase-9 transcription. Cancer Res. **69**: 1502-1508.

Takahashi, C., Sheng, Z., Horan, T.P., Kitayama, H., Maki, M., Hitomi, K., Kitaura, Y., Takai, S., Sasahara, R.M., Horimoto, A., Ikawa, Y., Ratzkin, B.J., Arakawa, T., Noda, M. (1998). Regulation of matrix metalloproteinase-9 and inhibition of tumor invasion by the membrane-anchored glycoprotein RECK. Proc Natl Acad Sci USA. **95**: 13221-13226.

Tosney, K.W. (1982). The segregation and early migration of cranial neural crest cells in the avian embryo. Dev Biol. **89**: 13-24.

Visse, R., Nagase, H. (2003). Matrix metalloproteinases and tissue inhibitors of metalloproteinases: structure, function, and biochemistry. Circ Res. **92**: 827-839.

Willson, J.A., Damjanovski, S. (2014). Vertebrate RECK in development and disease. Trends Cell Mol Biol. **9**: 95-105.

Willson, J.A., Nieuwesteeg, M.A., Cepeda, M., Damjanovski, S. (2015). Analysis of *Xenopus laevis* RECK and its relationship to other vertebrate RECK sequences. JSSR. **6**: 504-513.

Wilson, C.L., Heppner, K.J., Rudolph, L.A., Matrisian, L.M. (1995). The metalloproteinase matrilysin is preferentially expressed by epithelial cells in a tissue-restricted pattern in the mouse. Mol Biol Cell. **6**: 851-869.

Zhou, Z., Apte, S.S., Soininen, R., Cao, R., Baaklini, G.Y., Rauser, R.W., Wang, J., Cao, Y., Tryggvason, K. (2000). Impaired endochondral ossification and angiogenesis in mice deficient in membrane-type matrix metalloproteinase 1. Proc Natl Acad Sci USA. **97**: 4052-4057.

Chapter 4

4 Modulation of RECK Levels in Xenopus A6 Cells: Effects on MT1-MMP, MMP-2 and pERK Levels

4.1 Introduction

Remodeling of the ECM primarily occurs through the combined action of MMPs and their endogenous inhibitors, TIMPs, and RECK (Visse and Nagase, 2003). The *RECK* gene encodes a GPI-anchored protein with 3 protease inhibitor-like domains called Kazal motifs. RECK was initially classified as a tumour suppressor protein due to its ability to suppress metastasis when ectopically expressed in transformed cells (Takahashi et al., 1998). *In vitro* studies have shown that RECK can inhibit MMP-2 and MMP-9, secreted gelatinases associated with important developmental events and diseases, as well as MT1-MMP, a multi-functional cell surface MMP (Takagi et al., 2009; Takahashi et al., 1998; Oh et al., 2001). Many studies have investigated the embryonic role of MMPs. Perhaps due to redundant functions between family members, mice knockouts of each *MMP*, apart from *MT1-MMP*, and all *TIMPs* are viable (Amar et al., 2017). This positions MT1-MMP as a uniquely important molecule, and therefore its regulation by other agents, such as RECK, is of interest. Likewise, studies have implicated the importance of RECK during development, as *RECK* knockout in mice is embryonic lethal. In both mice and fish, loss or knockdown of *RECK* causes defects in angiogenesis and neurogenesis, in part due to aberrant regulation of MMPs (Chandana et al., 2010; Muraguchi et al., 2007; Oh et al., 2001; Prendergast et al., 2012). In addition, RECK has been shown to play a role in cell migration signaling pathways independent of its MMP-inhibitory role (Walsh et al., 2015).

Previous studies using epithelial breast cancer cells have revealed a complex pattern of expression between *MT1-MMP* levels and ERK activation into pERK, as well as pro-MMP-2 activation into MMP-2 (Cepeda et al., 2016; 2017; Willson et al., 2017).

MCF-7 cells stably expressing extremely high levels of *MT1-MMP* demonstrated low ERK activation and high pro-MMP-2 activation. Conversely, cells with low levels of *MT1-MMP* demonstrated high ERK activation and low pro-MMP-2 activation (Cepeda et al., 2016). Treatment with the broad spectrum MMP inhibitor Batimastat (BB94) increased *MT1-MMP* expression, but decreased MMP-2 activation and did not alter pERK protein levels (Cepeda et al., 2017). In MDA-MB-231 cells, inhibition of pro-MT1-MMP activation elevated global MT1-MMP and pERK levels, but decreased MMP-2 levels (Willson et al., 2017). These studies demonstrated that when *MT-MMP* levels are altered, pERK and MMP-2 activation levels alter in different ways depending on treatment. This suggests a mechanism that may involve more molecules than just MT1-MMP in the activation of ERK and pro-MMP-2, with RECK possibly playing an important role. I have cloned (Fig. 2.1) and characterized RECK expression during *X. laevis* development (Fig. 2.2), showing that RECK is present at stages where ECM remodeling events are associated with neural function. My recent *in vivo* examination of RECK, MT1-MMP, and TIMP-2 show that these proteins colocalize in the dorsal axis of *X. laevis* tailbud embryos, particularly in the neural tube (Fig. 3.1-3.4). Several other studies have also described interactions between RECK and MT1-MMP proteins *in vivo* and *in vitro* (Dong et al., 2010; Nambiar et al., 2016; Tang et al., 2018), with RECK being shown to complex with MT1-MMP at the cell surface to both attenuate its proteolytic activity and modulate its endocytosis from the cell surface (Miki et al., 2007).

To corroborate past *in vitro* work that link MT1-MMP and pERK levels, as well as build on my *X. laevis in vivo* localization of MT1-MMP and RECK, in this chapter I used an *in vitro* examination of *X. laevis* A6 epithelial cells, one of the few *in vitro* cell

types available for *X. laevis*, to confirm the importance of RECK as it relates to MT1-MMP, pERK, and MMP-2 protein levels. I used a MO approach to knock down *RECK* levels, plasmid transfection to overexpress *RECK*, and PI-PLC treatment to cleave RECK proteins from the surface of A6 cells. *RECK* knockdown did not alter MT1-MMP protein levels, ERK activation, or MMP-2 activity levels. *RECK* overexpression and PI-PLC treatment both resulted in increased MT1-MMP protein levels and MMP-2 activity levels. Only *RECK* overexpression decreased pERK protein levels in A6 cells. From these results, it is suggested that optimal levels of RECK present on the cell surface are important for modulating MT1-MMP protein levels and MMP-2 activation.

4.2   Materials and Methods

4.2.1   Morpholino Design

The design and synthesis of MOs were carried out as described in Section 2.2.1. A translation-blocking *RECK* MO and *β-catenin* MO were engineered as described in Section 2.2.1. Standard scrambled MO (antisense: 3'-CCTCTTACCTCAGTTACAATTT ATA-5') were also purchased from Gene Tools as an additional control.

4.2.2   Cell Culture Conditions, Endo-Porter Treatments, Transfections, and PI-PLC treatments

X. laevis A6 cells (ATCC®CCL-102TM) were maintained at 24°C in Leibovitz's L-15 Medium (Wisent Inc.) containing 10% fetal bovine serum (FBS) and 1% penicillin (100 U/mL)/streptomycin (100 µg/mL) (Fox et al., 2014).

For *RECK* knockdown, cells were seeded on 35 mm dishes at a density of 1×10^6 cells. After 24 hours, spent culture medium was replaced with medium containing

Endo-Porter reagent and MO oligos (Gene Tools) according to manufacturer's instructions. 48 hours following treatment, cell lysates were collected in RIPA buffer. MOs were used in dosages of 1, 10, or 20 μM. Following confirmation of RECK protein decrease, 20 μM MO treatment was used in subsequent experiments.

For *RECK* overexpression, cells were seeded as above. 24 hours later, cells were transfected with hemagglutinin (HA)-tagged *RECK* in pcDNA3.1 using Lipofectamine 2000 (Thermo Fisher) according to manufacturer's instructions. Another 24 hours following transfection, cell lysates were collected using RIPA buffer. The generation of the full-length *RECK* cDNA construct is described in Section 2.2.2, with the HA tag being inserted just following the N-terminal signal sequence such that it would not be removed during secretion, nor would it interfere with GPI anchor formation at the C-terminal end.

PI-PLC is an enzyme from *Bacillus cereus* that cleaves GPI-linked proteins, such as RECK, from the plasma membrane. 24 hours following transfection, *RECK*-transfected and mock-transfected (Lipofectamine only) cells were treated with 100 U/mL of PI-PLC (Thermo Fisher) in serum-free L-15 media according to manufacturer's instructions. 24 hours following PI-PLC treatment, cell lysates were collected using RIPA buffer.

4.2.3   Quantitative Real-Time PCR

To investigate changes in transcript levels, real-time qPCR was performed. Cells were seeded and treated as described in Section 4.2.2. Following treatment, RNA was extracted from cells using an RNeasy Mini Kit (Qiagen) according to manufacturer's instructions. cDNA was synthesized and qPCR was carried out as described in Section

2.2.8. For quantification, the target genes (*MMP-2*, *MMP-9*, *MT1-MMP*, and *TIMP-2*) were normalized to the internal standard of *EF1α* (Krieg et al., 1998). Primer sequences are described in Section 2.2.8. Fold change was calculated according to the ΔΔCT method (Livak and Schmittgen, 2001).

4.2.4   Immunoblot analysis

To investigate changes in RECK, MT1-MMP, and pERK protein levels, immunoblotting was performed. Cells were seeded and treated as described in Section 4.2.2. Following treatment, cells were washed 2X with PBS (pH 7.2) and disrupted using modified RIPA buffer. Collected cell lysates were shaken on ice for 20 minutes and sonicated 3X for 10 seconds each. Protein level was quantified using a bicinchoninic acid (BCA) assay (Thermo Scientific). 10 μg of protein per sample was mixed with 4X loading dye and subjected to a 10% SDS polyacrylamide gel and transferred to a PVDF membrane as described in Section 2.2.7. Membranes were blocked and probed with primary antibody (RECK, 1:200, Cell Signaling Technology, #3433; HA, 1:500, Santa Cruz, #sc-7392; MT1-MMP, 1:200, Millipore, #AB6004; pERK, 1:16000, Cell Signaling Technology, #4370; total ERK1/2, 1:4000, Cell Signaling Technology, #4695; β-actin, 1:1000, Santa Cruz, #sc-47778) followed by secondary antibody as described in Section 2.2.7. Signal was detected and quantified as described in Section 2.2.7. ERK1/2 activation is presented as a ratio between pERK and total ERK1/2 band intensities.

4.2.5   Gelatin Zymography

To measure the activity of secreted MMP-2 and MMP-9 proteins, gelatin zymography was performed. Cells were seeded and treated as described in 4.2.2. 24 hours later, culture media was replaced with serum-free L-15 media. 24 hours

following serum-free treatment, serum-free media was collected and mixed with 2X SDS-loading dye in a 1:1 ratio, with only 5 μL of sample being loaded into the gel (Hawkes and Taniguchi, 2010). To aid in the identification of active versus inactive forms of a MMP, the broad spectrum MMP inhibitor BB94 (10μM) was added to duplicate samples. Media samples were run on an SDS-containing 15% polyacrylamide gel, co-polymerized with 1% gelatin, at 140 V for 6 hours. A Triton X-100 (2.5%) incubation was then used to renature MMP-2 and MMP-9 proteins. Gels were placed in developing buffer (pH 7.5, 50 mM Tris, 200 mM NaCl, 5 mM $CaCl_2$, and 0.02% Brij-35) at 37°C with gentle shaking. After 48 hours, gels were stained with 0.5% Coomassie blue for 1 hour followed by de-staining (50% methanol) for 2 hours. Gels were visualized and band intensities representative of enzyme activity were quantified using Bio-Rad ChemiDoc Imaging system and Bio-Rad Image Lab software. As protein used for zymography was isolated from the media, the use of an internal (loading) standard was not possible. Accordingly, the ratio of active over total (pro, intermediate, and active) forms was determined for MMP-2. These ratios (active MMP-2/total MMP-2) were then used to calculate the percentage change of MMP-2 activation levels between control and treated cells.

4.2.6   Statistical Analysis

Statistical analysis and graphing were performed using Microsoft Excel. Data is presented as mean ± SD, except for qPCR results in Fig. 4.7 which are ± SEM. One-way ANOVA followed by unpaired student's T-tests were used and indicated respectively in each figure legend. The different levels of significance are denoted as follows: ns, $p>0.05$; *, $p \leq 0.05$; **, $p \leq 0.01$; ***, $p \leq 0.001$; ****, $p \leq 0.0001$.

4.3   Results

4.3.1   *RECK* Knockdown in A6 Cells Did Not Alter MT1-MMP or pERK Protein Levels nor MMP-2 Activity Levels

To confirm that the *RECK* MO treatment decreased RECK, protein level in *X. laevis* A6 cells was measured following treatment with different concentrations of *RECK* MO. Immunoblotting demonstrated that RECK protein is endogenously expressed in untreated A6 cells. A dose-dependent decrease in cellular RECK protein level was then seen following treatment of increasing concentrations of *RECK* MO. (Fig. 4.1a). The decrease in RECK was significant when immunological signals were quantified, with the 20 μM treatment reducing RECK protein levels by approximately 60%. (Fig. 4.1b). Having confirmed the efficacy of the *RECK* MO, I examined the levels of MMPs and their activity levels in A6 cells following *RECK* knockdown. *RECK* knockdown did not alter MT1-MMP (Fig. 4.2a) nor pERK protein levels (Fig. 4.2b) as shown by immunoblot analysis. However, this 60% knockdown in *RECK* was large enough to cause a cellular effect, as there was a change in transcription levels (Fig. 4.3).

Zymography was then used to quantify the active and inactive secreted forms of MMP-2 and MMP-9 after *RECK* knockdown. Bands of gelatin degradation representative of MMP activity of specific molecular mass on zymograms were quantified. The addition of the broad spectrum MMP inhibitor BB94 was used to confirm the identity of active MMP-2 versus pro-MMP-2 and intermediate MMP-2 forms (Appendix E). The amount of the active form of MMP-2 was compared to the total amount of MMP-2 (pro-, intermediate, and active forms). The active/total MMP-2 ratio was set to 1 in control cells. The relative level of MMP-2 activity did not change (there was the same ratio

Figure 4.1. Treatment of A6 cells with *RECK* MO resulted in decreased RECK protein levels.

Immunoblot analysis was used to confirm knockdown of *RECK* following treatment of A6 cells with *RECK* MO using Endo-porter delivery reagent. Protein was extracted from cells 48 hours following treatment with increasing concentrations of *RECK* MO. (a) Knockdown of RECK protein occurred in a dose-dependent manner. β-actin was used as a loading control. (b) Quantification of protein levels in (a) were graphed and data are based on 3 biological replicates (mean ± SD) and normalized to control (set to 100%). Data are analyzed via t-test; *, p≤0.05; ***, p≤0.001; ****, p≤0.0001.

(a)
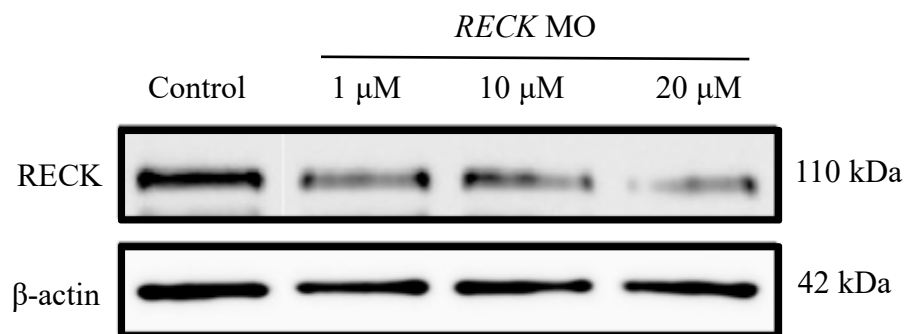
(b)

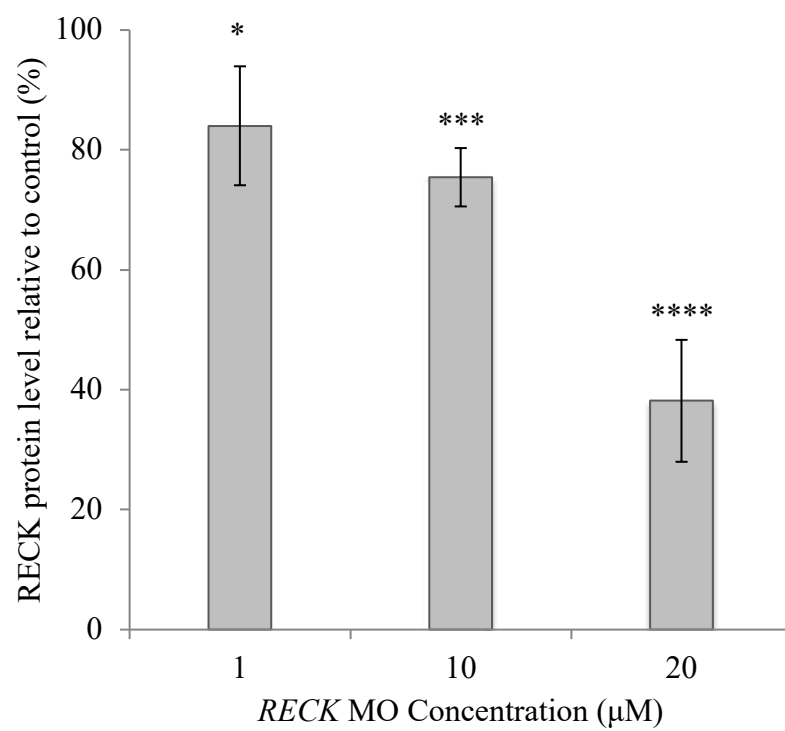**Figure 4.2. *RECK* knockdown did not alter MT1-MMP or pERK protein levels or MMP-2 activity levels.**

(a) Densitometry quantification of MT1-MMP immunoblotted protein normalized to β-actin. MT1-MMP protein levels did not significantly change in *RECK* knockdown cells compared to control (set to 1). β-actin was used as a loading control. b) Densitometry quantification of pERK normalized to total ERK levels. pERK protein levels did not significantly change in *RECK* knockdown cells compared to control (set to 1). (c) Gelatin zymography was used to measure protein activity of secreted pro-, intermediate, and active MMP-2 following *RECK* knockdown in A6 cells. Data are presented as the ratio between active and total (pro-, intermediate, and active) MMP-2 levels between control and *RECK* knockdown cells. Active/total MMP-2 levels did not significantly change in the media of *RECK* knockdown cells compared to control (set to 1). Graphed data are based on 3 biological replicates (mean ± SD). Data are analyzed via t-test; ns, p>0.05.

(a)
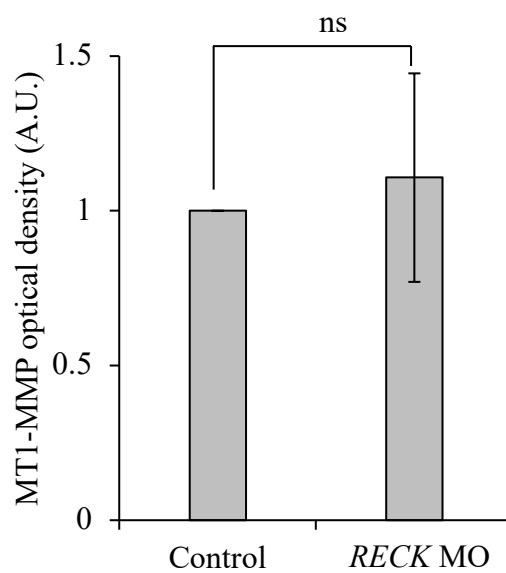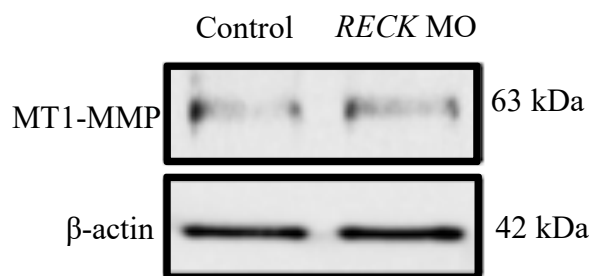
(b)
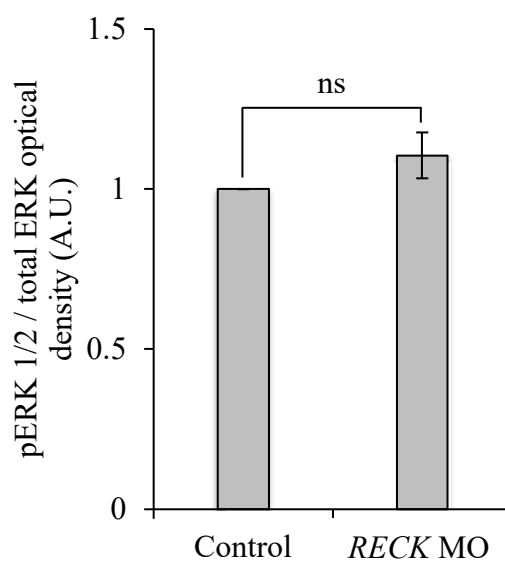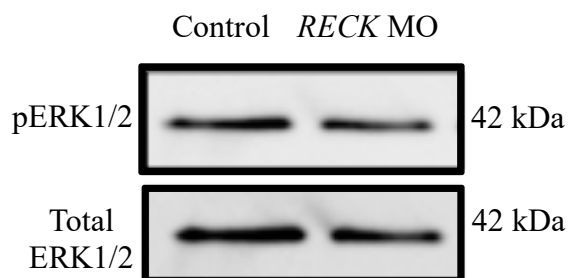
(c)
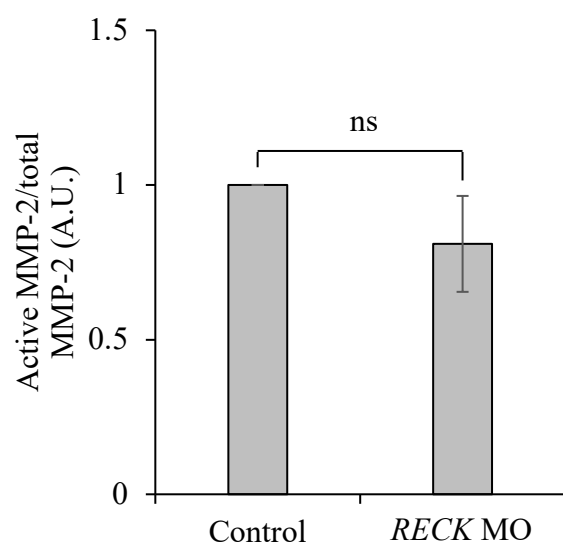
Figure 4.3. Effect of *RECK* knockdown on *MMP-2, -9, MT1-MMP,* and *TIMP-2* mRNA levels.

Following *RECK* knockdown in A6 cells, *MMP-2*, *MMP-9*, and *MT1-MMP* mRNA levels did not change significantly compared to control, however, *TIMP-2* mRNA levels decreased significantly. Changes in gene expression were measured relative to *EF1α* and normalized to control cells (set to 1). Results are based on 3 biological replicates (mean ± SEM; technical replicates, N=9). Data are analyzed via t-test; **, p≤0.01.
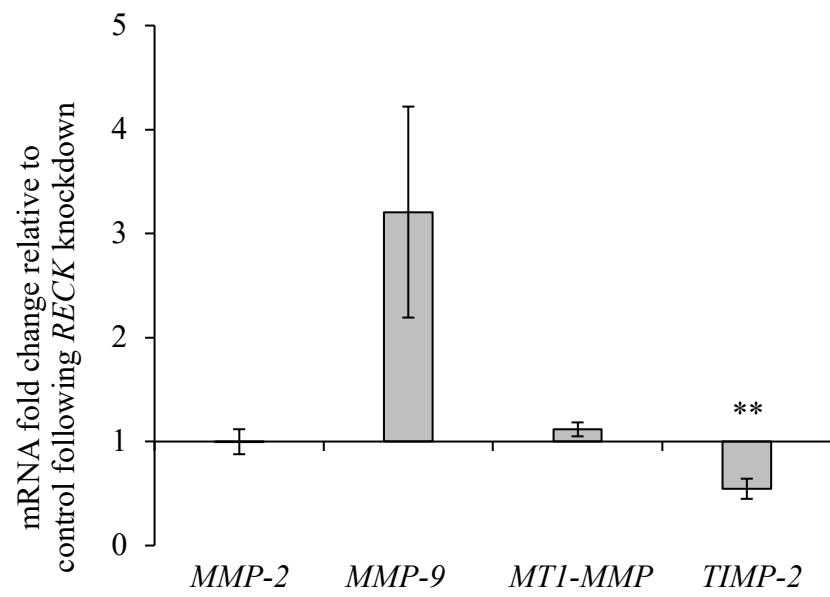
of active to total MMP-2) after *RECK* knockdown (Fig. 4.2c). MMP-9 activity could not be detected in the media (Appendix F) at the previously described molecular masses: 84 kDa (Cepeda et al., 2016; Nieuwesteeg et al., 2014) or 73 kDa (Fujimoto et al., 2006).

4.3.2 RECK Overexpression in A6 Cells Caused an Increase in MT1-MMP Protein Levels and Relative Active MMP-2 Levels, and a Decrease in pERK Protein Levels

After observing no change in MT1-MMP, pERK, and MMP-2 activation following *RECK* knockdown, I proceeded with overexpression of *RECK* in A6 cells. Transfection of an HA-tagged *RECK* construct was confirmed, as the level of RECK protein in transfected cells significantly increased (Fig. 4.4). This increase in protein was detected and quantified using both a RECK and HA antibody (Fig. 4.4).

As was done with the knockdown treatment, cellular proteins of interest were quantified following *RECK* overexpression. Although no change was observed following *RECK* knockdown, *RECK* overexpression resulted in a significant increase in the level of MT1-MMP protein (Fig. 4.5a) as well as a significant decrease in the level of pERK protein (Fig. 4.5b). Following RECK overexpression, zymography of secreted proteins revealed a significant increase in the relative level of active MMP-2 (Fig. 4.5c). Secreted MMP-9 proteins could not be detected via zymography.

4.3.3 Treatment With PI-PLC Reduced Cell-Surface RECK Levels

PI-PLC treatment (which releases GPI-linked proteins) was used to cleave RECK from the cell surface, and also allowed us to confirm the proper trafficking and localization of overexpressed RECK protein to the cell surface in the A6 cells. As expected, PI-PLC treatment significantly reduced the level of membrane localized

Figure 4.4. Transfection of full-length HA-tagged *RECK* constructs in A6 cells resulted in increased RECK levels.

Immunoblot analysis was used to confirm overexpression of RECK protein following transfection with *RECK* cDNA constructs. Mock-transfected and GFP-transfected A6 cells were used as controls. Protein was extracted from cells 24 hours following transfection. β-actin was used as a loading control. Top panel shows increased levels of RECK protein compared to control using a RECK antibody, while bottom panel confirms the presence of HA-tagged proteins only in *RECK*-transfected A6 cells using an HA antibody. Graphed data of top panel are based on 3 biological replicates (mean ± SD) and normalized to control (set to 100%). Data are analyzed via t-test; ***, p≤0.001.
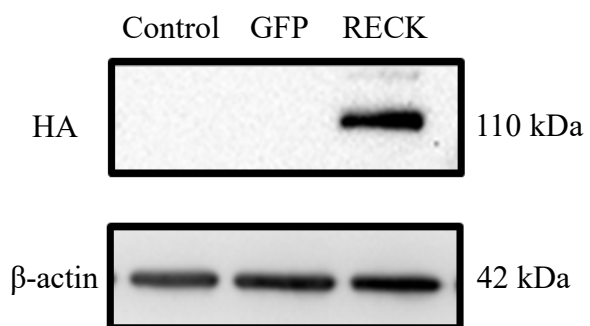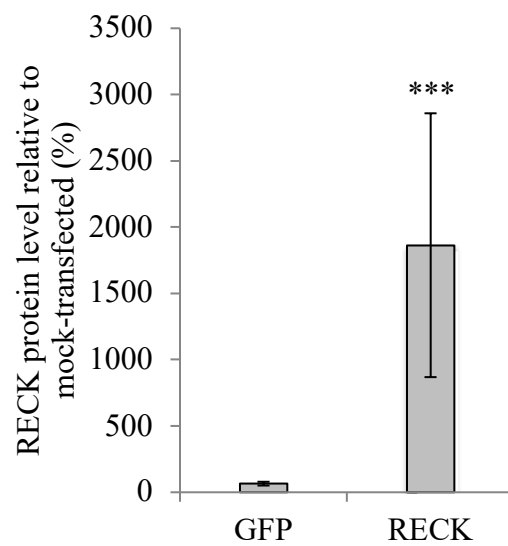
Control GFP RECK

RECK ————————————— 110 kDa

β-actin ————————————— 42 kDa

Control GFP RECK

HA ————————————— 110 kDa
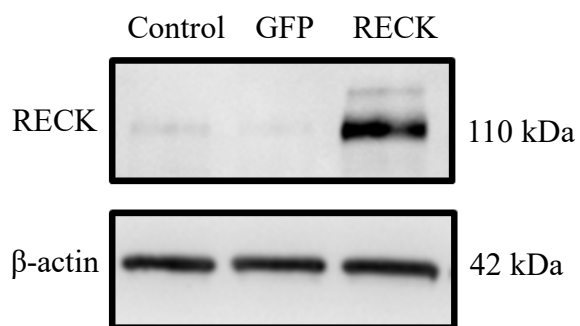
β-actin ————————————— 42 kDa

Figure 4.5. *RECK* **overexpression increased MT1-MMP protein and MMP-2 activity levels and decreased pERK protein levels.**

(a) Densitometry quantification of immunoblots of MT1-MMP protein normalized to β-actin. MT1-MMP protein levels significantly increased in *RECK*-overexpressing cells compared to control (mock-transfected cells) (set to 1). (b) Densitometry quantification of pERK normalized to total ERK levels. pERK protein levels significantly decreased in *RECK*-overexpressing cells compared to control (set to 1). (c) Gelatin zymography was used to measure protein levels of secreted pro-, intermediate, and active MMP-2 following *RECK* overexpression in A6 cells. Data are presented as the ratio between active and total (pro-, intermediate, and active) MMP-2 levels between control and *RECK*-overexpressing cells. Active/total MMP-2 levels significantly increased in the media of *RECK*-overexpressing cells compared to control (set to 1). Graphed data are based on 3 biological replicates (mean ± SD). Data are analyzed via t-test; *, $p \leq 0.05$; **, $p \leq 0.01$.

(a)
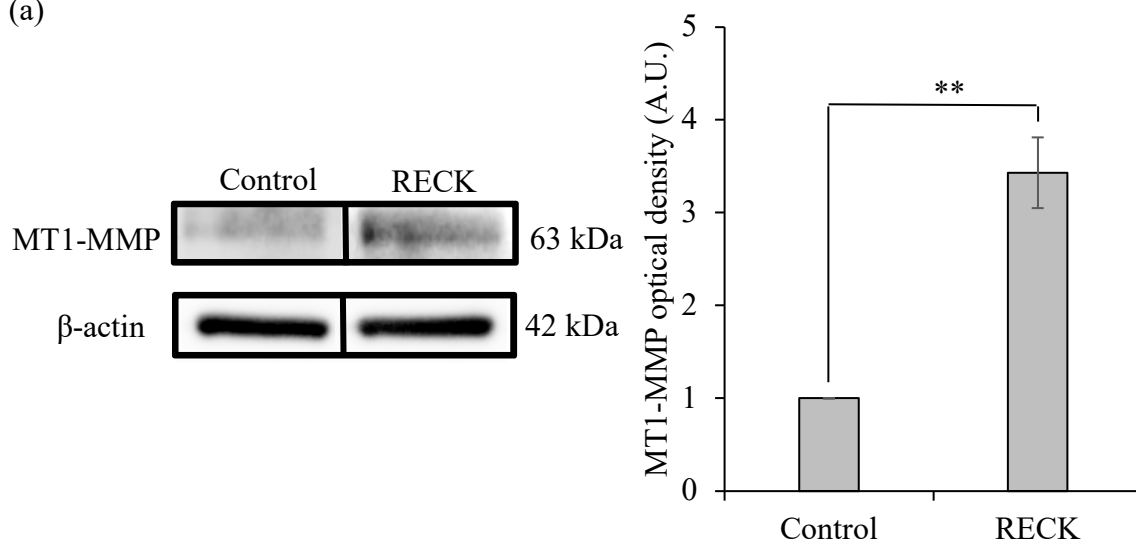
(b)
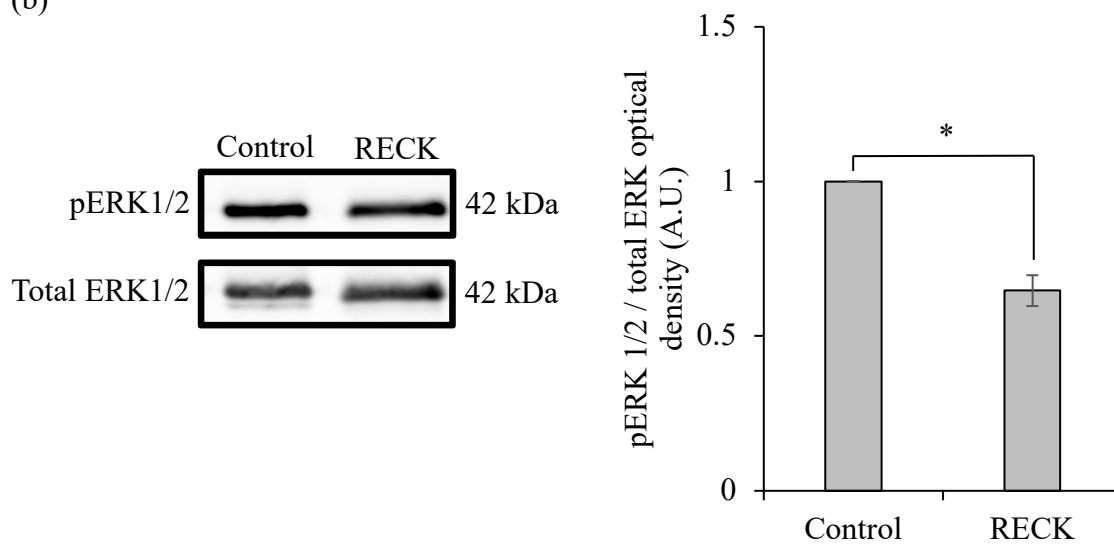
(c)

RECK, both in control and *RECK*-overexpressing cells (Fig. 4.6).
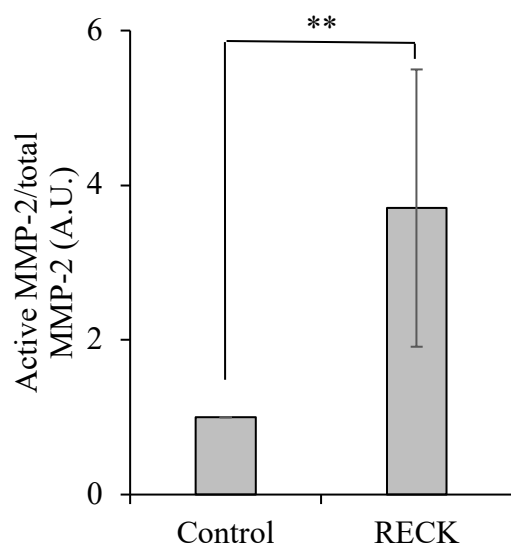
4.3.4 PI-PLC Treatment of A6 Cells Caused an Increase in MT1-MMP and Relative Active MMP-2 Levels

To elucidate the role of RECK at the cell surface in modulating MT1-MMP, pERK, and MMP-2 activation, I shed GPI-anchored proteins, which includes RECK, from the surface using PI-PLC. PI-PLC treatment significantly increased MT1-MMP protein levels (Fig. 4.7a) but did not alter pERK levels (Fig. 4.7b). PI-PLC treatment caused an increase in the relative level of active MMP-2 (Fig. 4.7c). Secreted MMP-9 protein could not be detected. Of note - PI-PLC treatment did not alter the transcription of a variety of genes (Fig. 4.8), nor did it alter the morphology, growth, or survival of these cells.

4.3.5 Alteration in RECK Levels or PI-PLC Treatment had Varying Effects on *MMP-2*, *MMP-9*, *MT1-MMP*, and *TIMP-2* mRNA Levels

Having shown that altered *RECK* levels had varying effects on protein levels of MT1-MMP and pERK, I sought to better understand the mechanism of these changes by examining changes in mRNA levels. Following *RECK* knockdown, qPCR analysis did not reveal a significant change in the level of *MMP-2*, *MMP-9*, nor *MT1-MMP* mRNA. There was, however, a significant decrease in *TIMP-2* mRNA levels (Fig. 4.3).

Following *RECK* overexpression, PCR analysis revealed significant increases in *MT1-MMP* and *MMP-9* transcript levels, but no changes in *MMP-2* nor *TIMP-2* transcript levels (Fig. 4.8a). PI-PLC treatment of A6 cells did not alter the transcript levels of *MMP-2*, *MMP-9*, *MT1-MMP*, nor *TIMP-2* (Fig. 4.8b).

Figure 4.6. Solubilization of RECK proteins following PI-PLC treatment.

24 hours following transfection of *RECK* constructs, control and transfected A6 cells were treated with PI-PLC for 24 hours and cell lysates were collected and analyzed by Western blot. (b) Densitometry quantification confirmed that the level of RECK proteins bound to the cell was significantly reduced following PI-PLC treatment in both mock-transfected and *RECK*-transfected cells. β-actin was used as a loading control. Graphed data are based on 3 biological replicates (mean ± SD). Data are analyzed via t-test; *, $p \leq 0.05$; **, $p \leq 0.01$.

	Control		RECK	
PI-PLC	-	+	-	+

RECK   110 kDa

β-actin   42 kDa

■ - PLC
■ + PLC
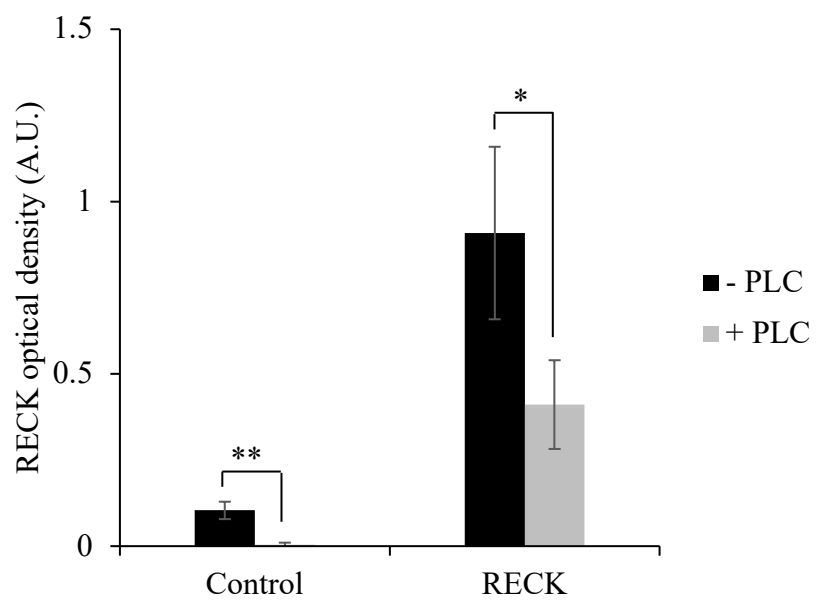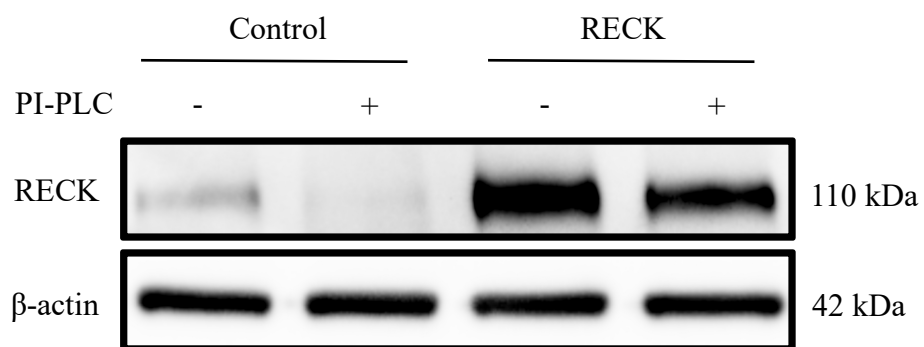
Figure 4.7 PI-PLC treatment caused an increase in MT1-MMP protein and MMP-2 activity levels.

(a) Densitometry quantification of MT1-MMP protein level normalized to β-actin in control A6 cells treated with PI-PLC. MT1-MMP protein levels significantly increased in PI-PLC-treated cells compared to untreated cells (set to 1). (b) Densitometry quantification of pERK normalized to total ERK levels. pERK protein levels did not significantly change following PI-PLC treatment. (c) Gelatin zymography was used to measure protein levels of secreted pro-, intermediate, and active MMP-2 following PI-PLC treatment in A6 cells. Data are presented as the ratio between active and total (pro-, intermediate, and active) MMP-2 levels between untreated cells and PI-PLC-treated cells. Active/total MMP-2 levels significantly increased in the media of PI-PLC-treated cells compared to untreated cells (set to 1). Graphed data are based on 3 biological replicates (mean ± SD). Data are analyzed via t-test; ns, p>0.05; *, p≤0.05; **, p≤0.01.

(a)
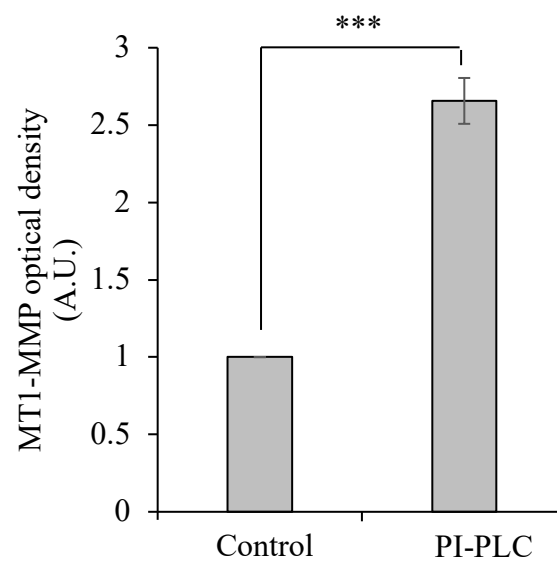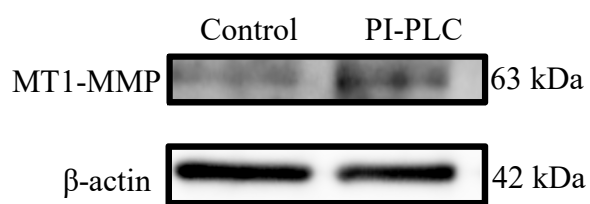
(b)
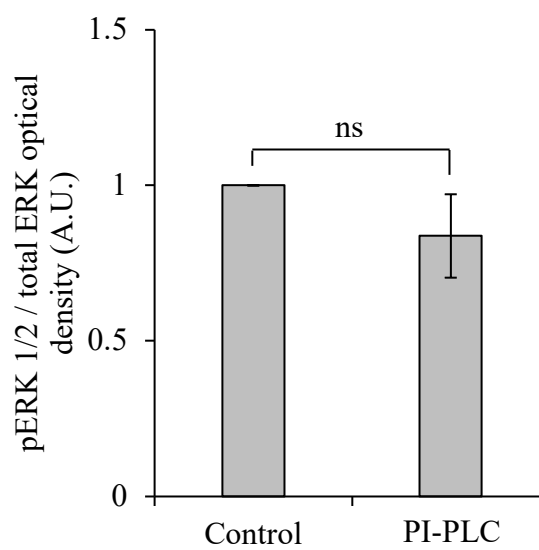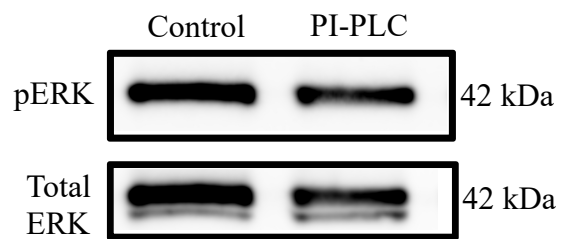
(c)
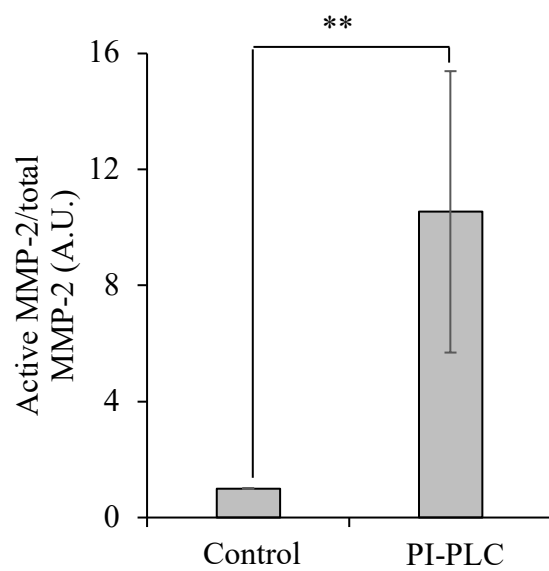
Unlike *MMP-2*, *MMP-9* transcript levels in A6 cells were extremely low (only being detectable after 32 PCR cycles). Although *MMP-9* transcript levels altered under *RECK* manipulation (Fig. 4.8a), they never elevated enough to be detected using zymography even when transcript levels increased.

4.4   Discussion

Adult epithelial cells, unlike their embryonic counterparts, move and invade only under special situations, such as injury or disease. Past *in vitro* examination of MCF-7 epithelial breast cancer cells, which are poorly invasive, has suggested that MT1-MMP orchestrates this transition towards a more migratory phenotype (Cepeda et al., 2016; Walsh and Damjanovski, 2011; Walsh et al., 2015). While the roles of ECM remodeling proteins have gathered much interest due to their broad developmental and disease implications, it has become clear that there isn't a defined relationship between the level of a MMP and the amount of ECM turnover (Cepeda et al., 2016). While not exhibiting overt abilities to remodel the ECM or to become mesenchymal, non-migrating epithelial cells express low levels of the enzymes and signaling molecules needed for these events. Indeed, A6 cells have basal levels of MT1-MMP, MMP-2, RECK and pERK proteins (Fig. 4.1, 4.2). It is this low and appropriately localized levels of MT1-MMP and TIMP-2 which can directly regulate enzymatic activity, including the activation of proMMP-2 (Cepeda et al., 2017; Itoh et al., 2001), as well as ERK cell signaling events (Cepeda et al., 2016; 2017) in human epithelial cells. To address if the maintenance of low levels of MMPs is a common mechanism seen in *X. laevis* epithelial cells, here I investigated the impact of altered *RECK* levels in the context of the ECM remodelers MT1-MMP and MMP-2, as well as pERK in *X. laevis* A6 cells.

Figure 4.8 Effect of *RECK* overexpression and PI-PLC treatment on *MMP-2,*
***MMP-9, MT1-MMP,* and *TIMP-2* mRNA levels.**

The levels of *MMP-2*, *MMP-9*, *MT1-MMP*, and *TIMP-2* mRNA were measured
following *RECK* overexpression and PI-PLC treatment in A6 cells using real-time qPCR.
(a) Following *RECK* overexpression, *MMP-2* and *TIMP-2* mRNA levels did not change
significantly, however, *MMP-9* and *MT1-MMP* mRNA levels increased significantly
compared to control. (b) Treatment of cells with PI-PLC did not change *MMP-2*, *MMP-9*,
MT1-MMP, or *TIMP-2* mRNA levels. Changes in gene expression were measured
relative to *EF1α* and normalized to control cells (set to 1). Results are based on 3
biological replicates (mean ± SEM; technical replicates, N=9). Data are analyzed via
t-test; *, $p \leq 0.05$; **, $p \leq 0.01$.

(a)
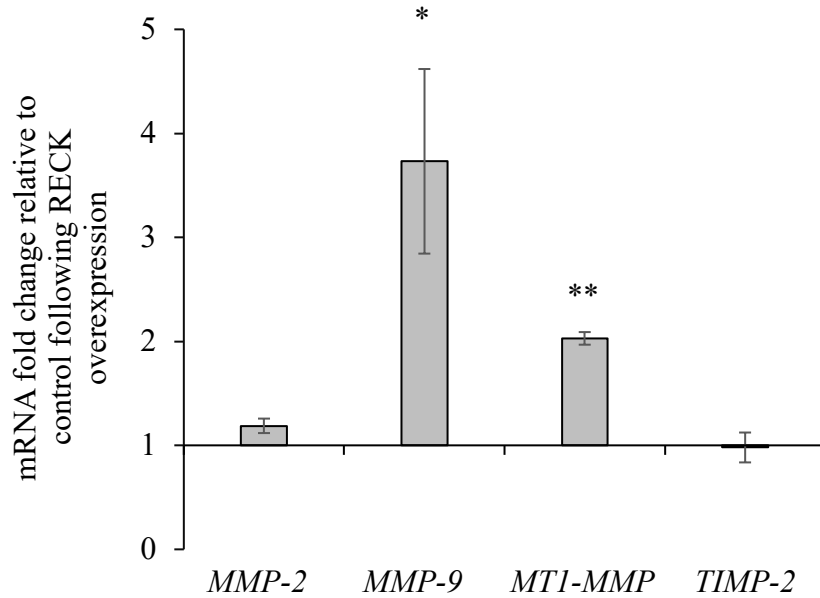
(b)
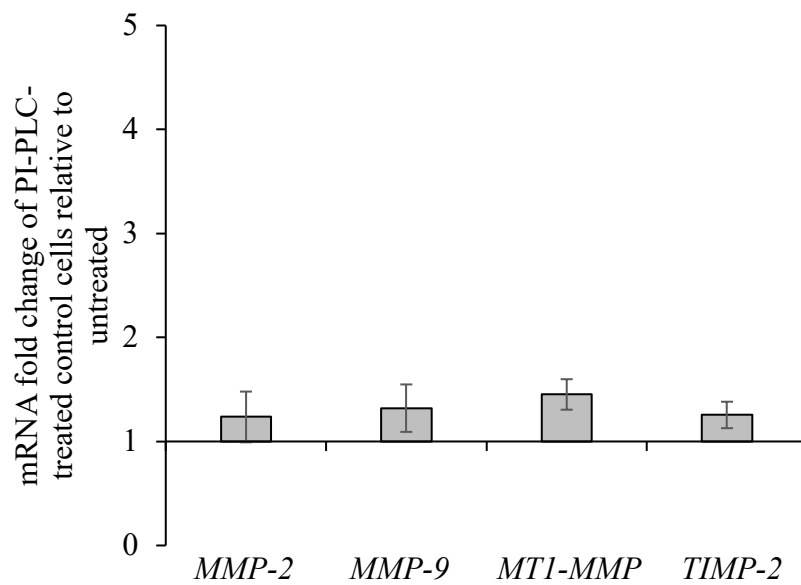
The presence of MT1-MMP and active MMP-2 (measured by zymography) demonstrated that A6 cells have at the least a basal ability to remodel the ECM. When endogenous levels of *RECK* are reduced using MO treatment, no changes were seen in MT1-MMP and pERK protein levels, nor MMP-2 activation (Fig. 4.2). Despite its ability to act as an MMP inhibitor, reduced levels of *RECK* were not substantial enough to alter MT1-MMP or MMP-2 levels, nor the basal level of ECM remodeling that may be associated with them. However, this level of *RECK* knockdown was biologically relevant as it was enough to decrease *TIMP-2* mRNA levels significantly (Fig. 4.3). Thus, it appears that A6 cells maintain low levels of RECK at the cell surface, levels which when further reduced, do not impact the protein levels of MT1-MMP, MMP-2, or pERK.

As *RECK* knockdown did not alter MT1-MMP, pERK, nor MMP-2 activity levels, I next examined the effect of *RECK* overexpression in A6 cells. RECK impedes MT1-MMP activity by binding to its catalytic site and blocking its proteolysis, including its ability to activate pro-MMP-2 (Dong et al., 2010). However, *RECK* overexpression resulted in increased *MT1-MMP* mRNA and protein levels (Fig. 4.8a and 4.5a), and an associated increase in MMP-2 activation (Fig. 4.5c). While A6 cells did not lower their basal ECM remodeling abilities with respect to MT1-MMP and MMP-2 in response to lowered *RECK* levels, increased *RECK* did trigger A6 cells to alter MMP levels. This increase in MT1-MMP and MMP-2 levels could be a compensatory response with the cells increasing these MMP levels to maintain a basal ability to remodel the ECM in response to the increased levels of an inhibitor. Further, RECK is associated with increased MT1-MMP endocytosis (Miki et al., 2007). Accordingly, increased RECK levels may reduce cell-surface MT1-MMP protein levels, triggering the cells to increase

MT1-MMP production. This RECK-mediated increase in MT1-MMP endocytosis rates would also limit the ability of MT1-MMP to activate ERK, thus pERK levels would be reduced under *RECK* overexpression conditions. In the presence of increased levels of an MMP inhibitor, A6 cells attempt to maintain a basal level of ECM remodeling ability by increasing MMP levels.

While A6 cells could tolerate the knockdown of *RECK*, as evident in their maintained MT1-MMP and MMP-2 levels, I next sought to examine the necessity for RECK to be membrane anchored. PI-PLC treatment was used to cleave RECK and other GPI-linked proteins from the cell surface. PI-PLC treatment of A6 cells did not alter transcript levels (Fig. 4.8b), nor did it alter the morphology, growth, or survival of these cells. By these measures, PI-PLC treatment of A6 cells was not detrimental, while immunoblot analysis did reveal a significant decrease in cell surface RECK levels (Fig. 4.6).

Like *RECK* overexpression, PI-PLC treatment of A6 cells elevated both MT1-MMP protein and MMP-2 activation levels (Fig. 4.7a,c). A possible mechanism that may explain this is that while cell surface RECK may play a role in MT1-MMP endocytosis (Miki et al., 2007), solubilized forms of RECK cannot. Following PI-PLC treatment and RECK shedding, less MT1-MMP is internalized and recycled, with more remaining at the cell surface. This increased level of MT1-MMP can then also facilitate higher levels of MMP-2 activity. Indeed, the increase in MT1-MMP protein levels (Fig. 4.7a) despite unaltered *MT1-MMP* mRNA changes (Fig. 4.8b) can be explained by soluble RECK proteins not being able to recycle cell-surface MT1-MMP, independent of transcriptional changes.

Unlike *RECK* overexpression, which decreased pERK levels possibly due to increased MT1-MMP recycling, PI-PLC treatment, which potentially reduced MT1-MMP recycling, did not alter pERK protein levels in A6 cells (Fig. 4.7b). These results suggest that cell surface localization of RECK proteins are important in modulating MT1-MMP function.

4.5 Conclusions

X. laevis A6 cells express RECK, as well as pERK, MT1-MMP and MMP-2 levels that facilitate ECM remodeling activity as seen by zymography. *RECK* knockdown did not alter MT1-MMP, pERK, nor MMP-2 activation and did not lower the ability of the cell to remodel the ECM. Unlike *RECK* knockdown, *RECK* changes (overexpression and cell surface shedding) that reduced the ability of the cell to remodel the ECM are compensated for by increases in MT1-MMP and MMP-2 levels as the cell tries to maintain a basal ability to remodel the ECM. A6 and other epithelial cells may attempt to maintain basal abilities to remodel the ECM even when challenged by changes in MMP inhibitor levels.

4.6   References

Amar, S., Smith, L., Fields, G.B. (2017). Matrix metalloproteinase collagenolysis in health and disease. Biochem Biophys Acta. **1864**: 1940-1951.

Cepeda, M.A., Evered, C.L., Pelling, J.H., Damjanovski, S. (2017). Inhibition of MT1-MMP proteolytic function and ERK1/2 signalling influences cell migration and invasion through changes in MMP-2 and MMP-9 levels. J Cell Commun Signal. **11**: 167-179.

Cepeda, M.A., Pelling, J.J., Evered, C.L., Williams, K.C., Freedman, Z., Stan, I., Willson, J.A., Leong, H.S., Damjanovski, S. (2016). Less is more: low expression of MT1-MMP is optimal to promote migration and tumourigenesis of breast cancer cells. Mol Cancer. **15**: 65.

Chandana, E.P.S., Maeda, Y., Ueda, A., Kiyonari, H., Oshima, N., Yamamoto, M., Kondo, S., Oh, J., Takahashi, R., Yoshida, Y., Kawashima, S., Alexander, D.B., Kitayama, H., Takahashi, C., Tabata, Y., Matsuzaki, T., Noda, M. (2010). Involvement of the Reck tumor suppressor protein in maternal and embryonic vascular remodeling in mice. BMC Dev Biol. **10**: 84.

Dong, Q., Yu, D., Yang, C.M., Jiang, B., Zhang, H. (2010). Expression of the reversion-inducing cysteine-rich protein with Kazal motifs and matrix metalloproteinase-14 in neuroblastoma and the role in tumour metastasis. Int J Exp Pathol. **91**: 368-373.

Fox, M., Nieuwesteeg, M., Willson, J., Cepeda, M., Damjanovski, S. (2014). Knockdown of Pex11β reveals its pivotal role in regulating peroxisomal genes, numbers, and ROS levels in *Xenopus laevis* A6 cells. In Vitro Cell Dev Biol Anim. **50**: 340-349.

Fujimoto, K., Nakajima, K., and Yaoita, Y. (2006). One of the duplicated matrix metalloproteinase-9 genes is expressed in regressing tail during anuran metamorphosis. Develop Growth Differ. **48**: 223-241.

Hawkes, S.P., Li, H., Taniguchi, G.T. (2010). Zymography and reverse zymography for detecting MMPs and TIMPs. Methods Mol Biol. **622**: 257-269.

Itoh, Y., Takamura, A., Ito, N., Maru, Y., Sato, H., Suenaga, N., Aoki, T., Seiki, M. (2001). Homophilic complex formation of MT1-MMP facilitates proMMP-2 activation on the cell surface and promotes tumor cell invasion. EMBO J. **20**: 4782-4793.

Krieg, P.A., Varnum, S.M., Wormington, W.M., Melton, D.A. (1989). The mRNA encoding elongation factor 1-alpha (EF-1 alpha) is a major transcript at the midblastula transition in Xenopus. Dev Biol. **133**: 93-100.

Livak, K., Schmittgen, T. (2001). Analysis of relative gene expression data using real-time quantitative PCR and the $2^{-\Delta\Delta CT}$ method. Method. **25**: 402.

Miki, T., Takegami, Y., Okawa, K., Muraguchi, T., Noda, M., Takahashi, C. (2007). The reversion-inducing cysteine-rich protein with Kazal motifs (RECK) interacts with membrane type 1 matrix metalloproteinase and CD13/aminopeptidase N and modulates their endocytic pathways. J Biol Chem. **282**: 12341-12352.

Muraguchi, T., Takegami, Y., Ohtsuka, T., Kitajima, S., Chandana, E.P., Omura, A., Miki, T., Takahashi, R., Matsumoto, N., Ludwig, A., Noda, M., Takahashi, C. (2007). Reck modulates Notch signaling during cortical neurogenesis by regulating ADAM10 activity. Nat Neurosci. **10**: 838-845.

Nambiar, J., Bose, C., Venugopal, M., Banerji, A., Patel, T.B., Kumar, G.B., Nair, B.G. (2016). Anacardic acid inhibits gelatinases through the regulation of Spry2, MMP-14, EMMPRIN and RECK. Exp Cell Res. **349**: 139-151.

Nieuwesteeg, M.A., Willson, J.A., Cepeda, M., Fox, M.A., Damjanovski, S. (2014). Functional characterization of tissue inhibitor of metalloproteinase-1 (TIMP-1) N- and C-terminal domains during *Xenopus laevis* development. ScientificWorldJournal. **30**: 467907.

Oh, J., Takahashi, R., Kondo, S., Mizoguchi, A., Nishimura, S., Imamura, Y., Kitayama, H., Alexander, D.B., Horan, T.P., Arakawa, T., Yoshida, H., Nishikawa, S., Itoh, Y., Seiki, M., Itohara, S., Takahashi, C., Noda, M. (2001). The membrane-anchored MMP inhibitor RECK is a key regulator of extracellular matrix integrity and angiogenesis. Cell. **107**: 789-800.

Prendergast, A., Linbo, T.H., Swarts, T., Ungos, J.M., McGraw, H.F., Krispin, S., Weinstein, B.M., Raible, D.W. (2012). The metalloproteinase inhibitor RECK is essential for zebrafish DRG development. Development. **139**: 1141-1152.

Takagi, S., Simizu, S., Osada, H. (2009). RECK negatively regulates matrix metalloproteinase-9 transcription. Cancer Res. **69**: 1502-1508.

Takahashi, C., Sheng, Z., Horan, T.P., Kitayama, H., Maki, M., Hitomi, K., Kitaura, Y., Takai, S., Sasahara, R.M., Horimoto, A., Ikawa, Y., Ratzkin, B.J., Arakawa, T., Noda, M. (1998). Regulation of matrix metalloproteinase-9 and inhibition of tumor invasion by the membrane-anchored glycoprotein RECK. Proc Natl Acad Sci USA. **95**: 13221-13226.

Tang, Y., Zhang, Y., Zheng, M., Chen, J., Chen, H., Liu, N. (2018). Effects of treadmill exercise on cerebral angiogenesis and MT1-MMP expression after cerebral ischemia in rats. Brain Behav. **8**: e01079.

Visse, R., and Nagase, H. (2003). Matrix metalloproteinases and tissue inhibitors of metalloproteinases: structure, function, and biochemistry. Circ Res. **92**: 827-839.

Walsh, L.A., Damjanovski, S. (2011). IGF-1 increases invasive potential of MCF 7 breast cancer cells and induces activation of latent TGF-β1 resulting in epithelial to mesenchymal transition. Cell Commun Signal. **9**:10.

Walsh, L.A., Roy, D.M., Reyngold, M., Giri, D., Snyder, A., Turcan, S., Badwe, C.R., Lyman, J., Bromberg, J., King, T.A., Chan, T.A. (2015). RECK controls breast cancer metastasis by modulating a convergent, STAT3-dependent neoangiogenic switch. Oncogene. **34**: 2189-2203.

Willson, J.A., Muir, C.A., Evered, C.L., Cepeda, M.A., Damjanovski, S. (2018). Stable expression of α1-Antitrypsin Portland in MDA-MB-231 cells increased MT1-MMP and MMP-9 levels, but reduced tumour progression. J Cell Commun Signal. **12**: 479-488.

Willson, J.A., Nieuwesteeg, M.A., Cepeda, M., Damjanovski, S. (2015). Analysis of *Xenopus* laevis RECK and its relationship to other vertebrate RECK sequences. JSRR. **6**: 504-513.

Chapter 5

5   General Discussion and Conclusions

5.1 General Overview

5.1.1 Context and Significance of this Research

The ECM not only functions as a structural scaffold for tissues, but it also contributes to the regulation of cell fate and behaviour. For proper ECM remodeling, a delicate balance must exist between MMPs, which cleave components of the ECM, and their inhibitors, TIMPs and RECK. Disruption of this balance leads to aberrant ECM turnover, which is detrimental to the development and maintenance of multicellular organisms. TIMPs were originally thought to be the main inhibitors of MMPs, however, RECK also plays a crucial role in maintaining this delicate balance. RECK is a lipid-anchored protein whose function has been established as an inhibitor of cell migration in both development and disease models (reviewed in Willson et al., 2014).

Not only are MMPs and their inhibitors important for tissue remodeling, but it has become increasingly evident that these proteins also play a critical role in cell fate by modulating cell signaling events (Cepeda et al., 2017; Chirco et al., 2006; Stetler-Stevenson, 2008; Walsh et al., 2015). Indeed, *MMPs*, *TIMPs*, and *RECK* are all expressed during differentiation events in addition to regions where ECM remodeling and large-scale cell movements are occurring (Nuttall et al., 2004). The interplay that exists between MMPs, TIMPs, and RECK is thus made even more complex because of their multifaceted roles. Although past studies have revealed an important role for RECK during embryogenesis (Oh et al., 2001; Prendergast et al., 2012; Yamamoto et al., 2012), the knowledge of the precise functions of RECK during this process is still limited. This research is the first comprehensive examination of RECK during *X. laevis* development.

5.1.2   Research Summary and General Conclusions

The overall goal of this research was to investigate the role of *X. laevis* RECK during development and how it facilitates proper ECM remodeling and tissue patterning. I used a combination of *in vivo* and *in vitro* experiments to accomplish this goal. Data were organized into 3 chapters: Chapter 2: a) I analyzed the *X. laevis* RECK peptide sequence with a variety of vertebrate and invertebrate RECK sequences to determine evolutionary conservation of hallmark domains, and b) I knocked down *RECK* levels in *X. laevis* embryos and assayed for morphological changes in development as well as corresponding changes in developmental marker genes and ECM remodeling genes; Chapter 3: I examined the localization patterns of RECK, MT1-MMP, and TIMP-2 proteins throughout early *X. laevis* development using IHC; Chapter 4: I used *X. laevis* A6 cells to investigate how RECK regulates MT1-MMP, MMP-2, and pERK levels.

In general, I hypothesized that *X. laevis* RECK supports a role in regulating ECM remodeling, as inhibition of MMP activity is a main function of RECK. Indeed, I was able to demonstrate that RECK contributes to *X. laevis* development. Knockdown of *RECK* expression in embryos resulted in neural tube closure failure as well as axial and head defects (Fig. 2.5), suggesting uncontrolled ECM remodeling and impaired cell migration. These phenotypes were attributed to global changes in *MT1-MMP*, *MMP-2*, and *TIMP-2* mRNA levels (Fig. 2.6). Moreover, I showed that *X. laevis* MT1-MMP and TIMP-2 colocalized spatially in the neural tube and different regions of the head where RECK was localized, particularly in the dorsal-ventral differentiation of the neural tube (Fig. 3.1-3.4). Finally, I revealed that RECK modulated MT1-MMP protein levels in *X. laevis* A6 cells, thereby affecting MMP-2 and ERK activation levels (Fig. 4.5, 4.7).

Overall, my findings support the model that RECK is a unique regulator of ECM remodeling and tissue patterning, whose absence leads to developmental defects due to deregulation of MT1-MMP and MMP-2.

5.2 Contributions to the Current Knowledge of ECM Dynamics

5.2.1 Characterization of *X. laevis* RECK

When I began this research, only the mature *X. laevis RECK* sequence, lacking the N- and C-terminal signaling domains, had been previously cloned by me. One of my first tasks was to finish cloning the full-length coding sequence of *X. laevis RECK* (Fig. 2.1) and perform a sequence analysis using a variety of vertebrate and invertebrate RECK sequences to determine evolutionary conservation (Table 2.1). The first part of Chapter 2 revealed that all RECK sequences cloned to date, including *X. laevis* RECK, are highly conserved at the amino acid level and share all the domains characteristic of RECK, which was consistent with my original hypothesis.

RECK proteins are rich in cysteine residues (9%) and contain 5 repeats of a putative cysteine knot motif located near their N-terminus (Table 2.1). The number and placement of these cysteines are highly conserved among both vertebrates and invertebrates. Based on a current NCBI Homologene search of RECK, there are 9 vertebrates: 7 mammalian, as well as chicken and frog, that have been characterized to date. Among these 9 vertebrate RECK peptide sequences, there is 100% conservation of cysteines in each cysteine knot motif. Within the cysteine knot motifs are potential glycosylation sites at 5 asparagine residues that have been identified to contribute to RECK's role as an MMP inhibitor (Simizu et al., 2005).

Of the 3 Kazal motifs, which have been identified as MMP inhibitory domains

(Chang et al., 2008), only the 1st domain completely matches the defined consensus Kazal motif sequence ($X_8CX_6CX_7CX_{10}CX_2CX_{17}C$), whereas the other 2 domains only contain partial Kazal motif identities (Takahashi et al., 1998). The 1st Kazal motif shares 87% identity in mammals and shares 100% conservation of cysteines in vertebrates. Even the 2 partial Kazal motifs are very well conserved and contain conserved cysteine residues as well as the same number of amino acids between the cysteine residues in vertebrates. The high conservation of these 2 partial Kazal motifs suggests that they may also contribute to protease inhibition. Indeed, evidence does show that these Kazal motifs play a role in MMP inhibition (Chang et al., 2008).

The middle portion of RECK proteins also contains 2 partial EGF-like repeats. EGF domains are evolutionary conserved regions found in a variety of membrane-anchored and secreted proteins. Proteins that contain EGF-domains may have the potential to bind to EGF receptors and stimulate cell proliferation, survival, and differentiation (Wouters et al., 2005). The high conservation of these 2 domains among vertebrate RECK sequences suggests that these domains contribute to a cell signaling function that is independent of RECK's MMP inhibitory role, as recent evidence has shown that RECK can trigger such pathways autonomously of MMPs (Walsh et al., 2015).

These characterized domains of RECK, although highly conserved, only make up a small portion of the *RECK* coding sequence. There are other highly conserved, but uncharacterized, regions within RECK that may also represent important functional domains. For example, during sequence analysis of RECK in Chapter 2, following the last cysteine knot motif, I identified a 32 amino acid region, which I termed LAD-RSC

(Fig. 2.1), that is the most conserved region of RECK (91% conserved in mammals and 88% conserved in vertebrates) (Table 2.1). This sequence motif has not previously been reported nor does it have any known homology to other proteins, however, given its extremely high conservation, this suggests that the LAD-RSC domain may have global implications to RECK function.

It is interesting to note that *RECK* sequences are almost 3,000 bp, and throughout evolution, there has never been a duplication or omission of any of the characterized domains, nor of the gene itself. Even in the *X. laevis* genome, which is allotetraploid, meaning that it may contain duplicates for some genes, I only found a single copy of the *RECK* gene. This was also seen in the zebrafish genome, which is also tetraploid. Kumari et al. (2018) only identified a single copy of the *RECK* gene. On the other hand, there are 4 mammalian TIMPs that appear to be a result of gene duplication, since only 1 *TIMP* gene is found in insects, and not all orthologues are present in all vertebrates (Brew and Nagase, 2010). MMPs first appeared as basic proteins with a catalytic domain, but through gene duplication, fusion, and exon shuffling, acquired the additional domains and functional diversity currently exhibited by the various members of the MMP family (Fanjul-Fernández et al., 2010). But the *RECK* gene is the only one of its kind and shares high peptide sequence conservation among vertebrates. This strongly implicates that all vertebrate RECK proteins share a similar biological function.

5.2.2 RECK is a Key Regulator During *X. laevis* Development

It has been well-known for a long time that there needs to be a proper balance between MMPs and their inhibitors in order to facilitate controlled ECM remodeling during development. Numerous studies have already shown that disturbing this balance,

either by disrupting *MMP* or *TIMP* levels, results in a wide array of developmental defects (Lambert et al., 2004; Vu and Werb, 2000). However, unlike MMPs and TIMPs, in which the gene knockout embryos are still viable, most likely due to functional redundancy, there is only one *RECK* gene, and knockout of this gene in mice results in embryonic lethality (Oh et al., 2001). Therefore, RECK must play an essential role during development, although the exact mechanisms remain unclear. The second part of Chapter 2 explored the consequences of knocking down *RECK* expression in *X. laevis* embryos. My data revealed for the first time that RECK contributes to tissue patterning during *X. laevis* development.

RECK knockdown in 1-cell stage embryos led to severe developmental defects in neural tube closure, an event that relies on large-scale cell movements and extensive ECM remodeling. This was consistent with my original hypothesis, which stated that knockdown in *RECK* levels would cause neural tube defects in *X. laevis* embryos. Changes in *chordin* mRNA levels in *RECK* knockdown embryos coincided with this phenotype, as chordin plays an important role in inducing neural structures (Sasai et al., 1994). When comparing data from Chapters 2 and 3, I observed that the sites of prominent defects in *RECK* knockdown embryos (the neural tube and head; Fig. 2.5) coincided with sites of abundant RECK expression in wildtype embryos (Fig. 3.1, 3.2). Also of note was the trending increase that occurred in the mRNA levels of *FoxD3*, a neural crest cell marker, in *RECK* knockdown embryos (Fig. 2.6). Indeed, in Chapters 2 and 3, I revealed that RECK proteins are localized to regions where neural crest cells reside: on the dorsal side of the neural tube prior to migration (the neural crest) and in the branchial arches, a structure in the head region where neural crest cells eventually

migrate (Fig. 2.2, 3.1, 3.2). Given that past studies have already indicated an important role for RECK in the migration of neural crest cells (Prendergast et al., 2012), my results suggest that the axial and head defects that were seen in *RECK* knockdown embryos (Fig. 2.5) may have resulted from aberrant neural crest cell migration. In fact, the reduced head structures that were seen in *RECK* knockdown embryos is similar to the phenotypes observed in zebrafish when neural crest cell migration is disrupted (Tobin et al., 2008).

Because *RECK* knockdown caused global changes in *MT1-MMP* and *TIMP-2* mRNA levels, along with RECK, I also investigated the spatial expression patterns of these 2 proteins during *X. laevis* development. The sites of RECK localization coincided with overlapping expression patterns of MT1-MMP and TIMP-2, especially in the D-V differentiation of the neural tube (as summarized in Fig. 5.1). This was consistent with my hypothesis, which stated that *X. laevis* RECK would colocalize with MT1-MMP in dorsal axial structures, including the neural tube and head region. Given that past *in vitro* studies have shown that RECK interacts with MT1-MMP on the cell surface (Oh et al., 2001; Matsuzaki et al., 2018; Miki et al., 2007), it was not surprising that both proteins displayed highly similar expression patterns throughout early *X. laevis* development. What was intriguing, however, was that TIMP-2 also displayed a very similar expression pattern to RECK, although there is no evidence to suggest they interact with one another on the cell surface. But seeing as how MT1-MMP also shares the same expression pattern as TIMP-2, and there is evidence *in vitro* to show that TIMP-2 complexes with MT1-MMP (Itoh et al., 2001), it is more likely that TIMP-2 and RECK both interact with MT1-MMP and influence its behaviour during development, such as the ability of MT1-MMP to activate MMP-2 (Itoh et al., 2001), or the ability of MT1-MMP to induce

Figure 5.1 Schematic representation of overlapping RECK, MT1-MMP, and TIMP-2 proteins in the D-V differentiation of the neural tube during *X. laevis* development.

Schematic representation of transverse sections of stage 20, 28, and 34 *X. laevis* embryos. Red indicates overlapping expression patterns of RECK, MT1-MMP, and TIMP-2 proteins in the D-V differentiation of the neural tube at stages 20, 28, and 34. Abbreviations: E=endoderm; Ep=epidermis; NT=neural tube; S=somites.
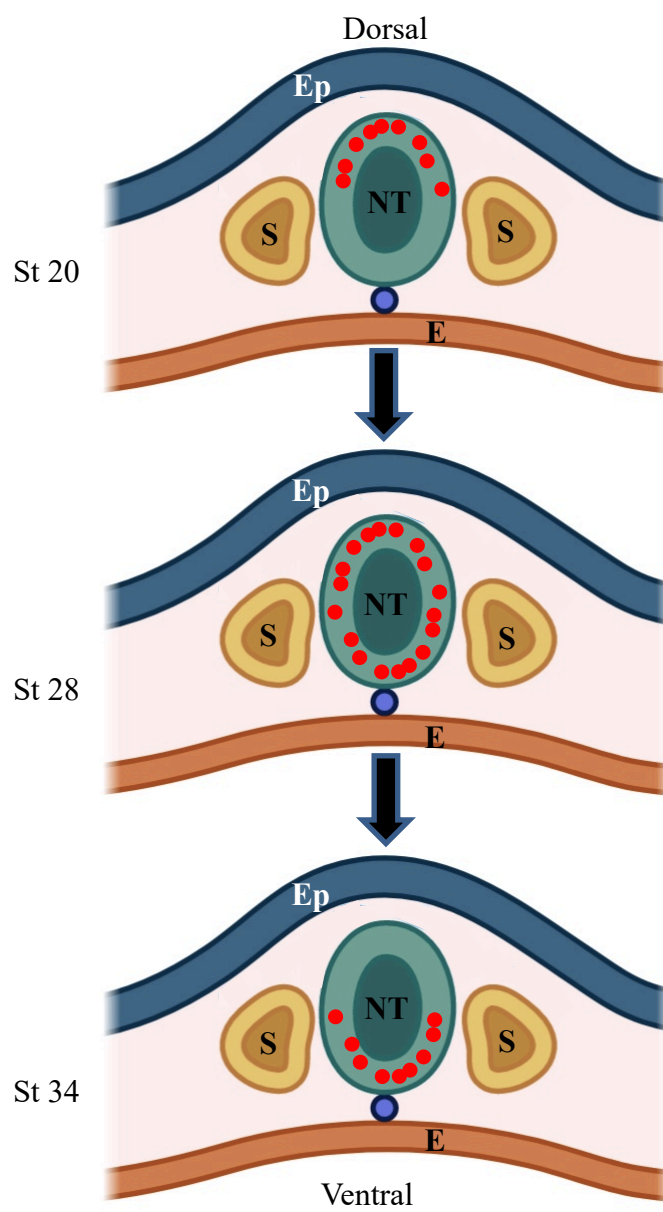
cell signaling cascades (ie. ERK signaling) (Cepeda et al., 2017; Takino et al., 2010).

My global analysis in Chapter 2 showed that *RECK* knockdown altered *MT1-MMP*, *MMP-2*, and *TIMP-2* mRNA levels (Fig. 2.6). Furthermore, in Chapter 3, I showed that RECK and MT1-MMP displayed highly similar expression patterns throughout early *X. laevis* development (Fig. 3.1-3.4), which is suggestive that they interact with one another during development. However, RECK's interaction with molecules and specific cellular pathways are difficult to detect in multicellular embryos. Therefore, in Chapter 4, I analyzed the role of RECK on ECM dynamics in a well-established *X. laevis* cell line, kidney epithelial A6 cells. A6 cells act as typical epithelial cells and express many ECM regulatory genes, including *RECK*, *MT1-MMP*, *MMP-2*, and *TIMP-2*. MT1-MMP's regulation of pro-MMP-2 and ERK activation position it as a key indicator of the cell's ability to remodel the ECM and migrate. Thus, given that MT1-MMP and MMP-2 can be pivotal to ECM remodeling during development, I investigated how modulation of RECK levels would impact both of these MMPs *in vitro*.

Although *RECK* knockdown did not alter MT1-MMP levels nor MMP-2 activity, *RECK* overexpression and PI-PLC treatment both increased ECM remodeling potential through increased MT1-MMP protein and relative MMP-2 activation levels. These results were contrary to my hypothesis, which stated that knockdown/shedding of *RECK* in *X. laevis* A6 cells would result in increased MT1-MMP and MMP-2 levels, whereas overexpression of *RECK* would result in reduced MT1-MMP and MMP-2 levels. Instead, I observed a compensatory feedback response, in which changes in *RECK* levels that reduced the ability of the cell to remodel the ECM (overexpression and cell surface

shedding) were compensated for by cellular increases in MT1-MMP levels and MMP-2 levels as seen by zymography. Taken together, my results are highly suggestive that RECK is a key regulator of MT1-MMP in *X. laevis* (as summarized in Fig. 5.2).

Although RECK is well established as a suppressor of cell migration due to its ability to inhibit MMPs, more recent studies have shed light on MMP-independent functions of RECK, particularly during cell fate and differentiation events. Most recently, Vallon et al. (2018) revealed that RECK is a receptor to the ligand Wnt7 in rat brain blood vessels and mediates canonical Wnt/ß-catenin signaling in endothelial cells by stabilizing active Wnt7 ligands. Interestingly, when I examined the localization pattern of RECK in Chapter 3, I saw that RECK, along with MT1-MMP and TIMP-2, localized in the D-V differentiation of the neural tube (Fig. 5.1). This patterning event relies on coordinated cell signaling events rather than ECM turnover events. Therefore, these results suggest a role for these proteins during patterning events that are independent from their roles as regulators of ECM remodeling. In fact, RECK has already been implicated to be an important player during neurogenesis in mice (Muraguchi et al., 2007; Park et al., 2013).

It is well known that a complex interplay exists between RECK, MMPs, and TIMPs, interactions that need to be examined to truly understand the role of RECK in ECM remodeling during development. Overall, my results support the view that MMP regulation is critical to ensure proper ECM remodeling during development. Furthermore, my results suggest that RECK is a key modulator of MT1-MMP in *X. laevis*.
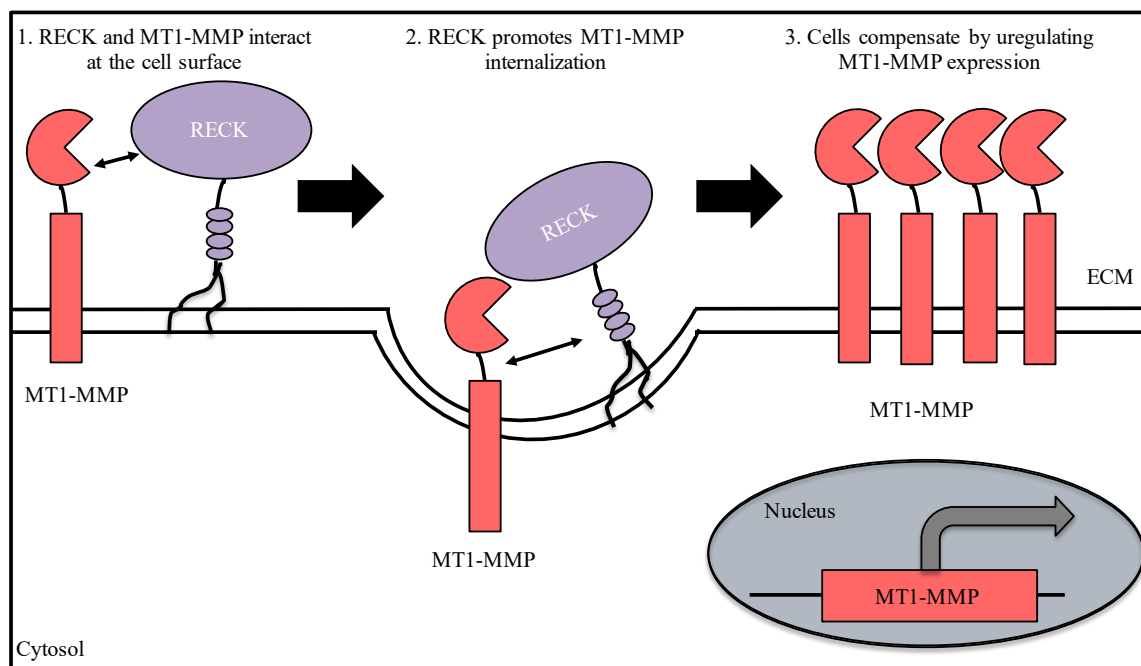
5.3   Limitations of this Research and Future Studies

As my research was the first to characterize RECK function during *X. laevis*

Figure 5.2 Model of RECK modulation of MT1-MMP in *X. laevis*.

(a) Cell surface RECK interacts with MT1-MMP and promotes its internalization in *X. laevis* A6 cells. As a compensatory feedback response, A6 cells upregulate MT1-MMP expression to increase MT1-MMP protein levels on the cell surface. (b) Solubilized RECK (cleaved by PI-PLC) binds to and inhibits MT1-MMP activity but cannot promote MT1-MMP internalization. As a result, MT1-MMP protein levels (but not mRNA levels) increase in A6 cells.

(a)

1. RECK and MT1-MMP interact at the cell surface

2. RECK promotes MT1-MMP internalization

3. Cells compensate by uregulating MT1-MMP expression

RECK

MT1-MMP

ECM

RECK

MT1-MMP

MT1-MMP

Nucleus

MT1-MMP

Cytosol

(b)

1. Solubilized RECK cannot facilitate internalization

2. MT1-MMP proteins accumulate on the cell surface

RECK

RECK

MT1-MMP

ECM

Cytosol

MT1-MMP

MT1-MMP
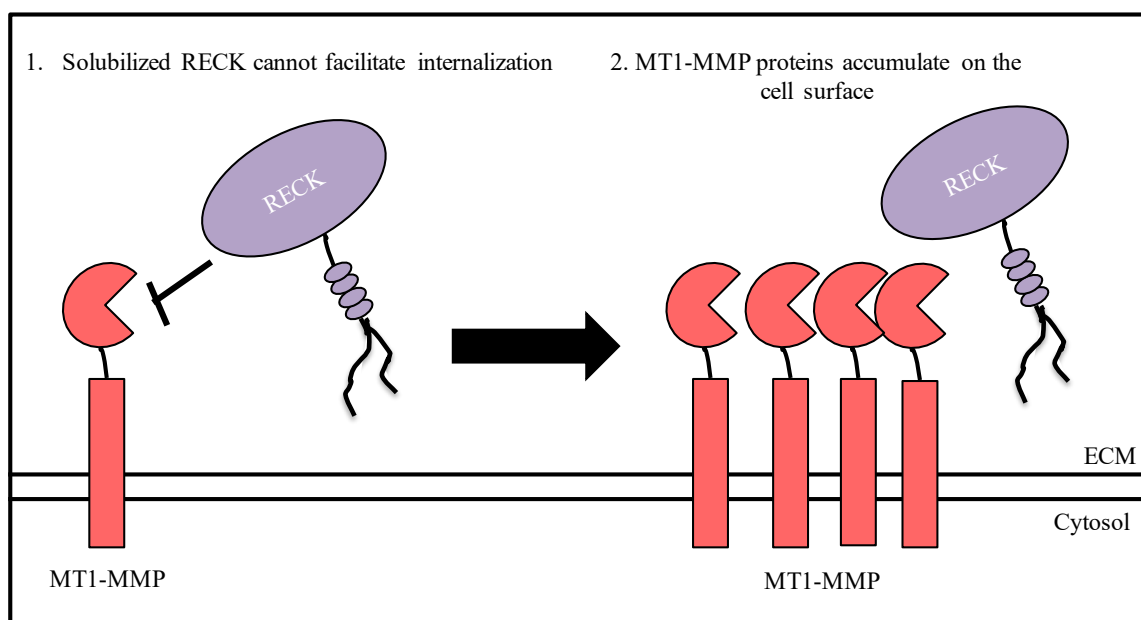
development, I focused on global changes within the whole embryo. Consequently, I was only able to detect large-scale changes in ECM remodeling genes and developmental marker genes (Fig. 2.6) rather than tissue-specific changes. However, since proper ECM remodeling is critical for large-scale cell movements during development, it is quite likely that many tissues besides the neural tube were affected by *RECK* knockdown. Therefore, a more comprehensive analysis of the morphological defects that resulted from reduced *RECK* levels in *X. laevis* embryos is warranted. This should be accomplished through *in situ* analysis of developmental marker genes in *RECK* knockdown embryos versus wildtype. For example, analysis of *crestin*, a marker for migratory neural crest cells (Rubinstein et al., 2000), in *RECK* knockdown embryos would be of great interest given the fact that my results strongly suggest that neural crest cell migration was affected in these embryos.

To attenuate the effects of *RECK* knockdown, future studies should co-inject *MT1-MMP* MOs in *X. laevis* embryos, as they are known to be inhibited by RECK. If the phenotype is rescued, this would imply that RECK is a key regulator of MT1-MMP in *X. laevis*. Finally, examination of changes in additional signaling markers, besides pERK, such as Notch, VEGF, or Wnt7a signaling, using Western blotting, may help link the non-MMP-inhibitory role of RECK.

Although my IHC analysis confirmed that RECK colocalizes with MT1-MMP and TIMP-2 in the neural tube (Fig. 5.1), I did not investigate the specific cell surface binding partners of RECK during *X. laevis* development. However, my last chapter does suggest that RECK modulates MT1-MMP protein levels in *X. laevis*. To build on these results, immunocytochemistry experiments using fluorescently-labeled MT1-MMP

antibodies would be useful to confirm that RECK modulates MT1-MMP internalization in A6 cells. Co-immunoprecipitation experiments could also be useful in determining potential cell surface binding partners for RECK in *X. laevis* A6 cells, such as Wnt7, EGF, and Notch ligands (Muraguchi et al., 2007; Vallon et al., 2018). RECK is a large protein with a number of highly conserved domains, the functions of most of which are currently unknown. Therefore, future work should involve site-specific mutations to disrupt the function of different domains, especially the highly conserved LAD-RSC domain, to determine if they contribute to the overall function of the protein, as was previously done with the glycosylation sites (Simizu et al., 2005). This may help further elucidate the potential non-MMP inhibitory roles of RECK.

5.4 Conclusions

ECM dynamics are very complex, in part due to differing ECM compositions as well as differing expression patterns of MMP and TIMPs/RECK in each tissue. RECK is a recently described player in mediating MMPs. Its large size and high evolutionary conservation suggest it plays an important role in vertebrates. This study is the first to characterize *X. laevis* RECK during early development. My results indicate that inappropriate expression of *RECK* interferes with embryogenesis and causes aberrant expression of MT1-MMP and MMP-2, both of which play a major role in cell migration. The colocalization patterns of RECK and MT1-MMP during neural tube differentiation in *X. laevis* as well as my demonstration *in vitro* that RECK modulates MT1-MMP and MMP-2 protein levels suggest that RECK and MT1-MMP function together during development to ensure proper ECM remodeling and cell signaling. Overall, this study not only supports the role for RECK as a modulator of ECM remodeling during development

but also sheds light on the importance of this protein during patterning and differentiation

events.

5.5   References

Brew, K., Nagase, H. (2010). The tissue inhibitors of metalloproteinases (TIMPs): An ancient family with structural and functional diversity. Biochim Biophys Acta. **1803**: 55-71.

Cepeda, M.A., Evered, C.L., Pelling, J.H., Damjanovski, S. (2017). Inhibition of MT1-MMP proteolytic function and ERK1/2 signalling influences cell migration and invasion through changes in MMP-2 and MMP-9 levels. J Cell Commun Signal. **11**: 167-179.

Chang, C.K., Hung, W.C., Chang, H.C. (2008). The Kazal motifs of RECK protein inhibit MMP- 9 secretion and activity and reduce metastasis of lung cancer cells *in vitro* and *in vivo*. J Cell Mol. Med. **12**: 2781-2789.

Chirco, R., Liu, X.W., Jung, K.K., Kim, H.R. (2006). Novel functions of TIMPs in cell signaling. Cancer Metastasis Rev. **25**: 99-113.

Fanjul-Fernández, M., Folgueras, A.R., Cabrera, S., López-Otín, C. (2010). Matrix metalloproteinases: evolution, gene regulation and functional analysis in mouse models. Biochim Biophys Acta. **1803**: 3-19.

Itoh, Y., Takamura, A., Ito, N., Maru, Y., Sato, H., Suenaga, N., Aoki, T., Seiki, M. (2001). Homophilic complex formation of MT1-MMP facilitates proMMP-2 activation on the cell surface and promotes tumor cell invasion. EMBO J. **20**: 4782-4793.

Kumari, R., Silic, M.R., Jones-Hall, Y.L., Nin-Velez, A., Yang, J.Y., Mittal, S.K., Zhang, G. (2018). Identification of *RECK* as an evolutionarily conserved tumor suppressor gene for zebrafish malignant peripheral nerve sheath tumors. Oncotarget. **9**: 23494-23504.

Lambert, E., Dassé, E., Haye, B., Petitfrére, E. (2004). TIMPs as multifacial proteins. Crit Rev Oncol Hematol. **49**: 187-189.

Matsuzaki, T., Kitayama, H., Omura, A., Nishimoto, E., Alexander, D.B., Noda, M. (2018). The RECK tumor-suppressor protein binds and stabilizes ADAMTS10. Biol Open. **7**: bio033985.

Miki, T., Takegami, Y., Okawa, K., Muraguchi, T., Noda, M., Takahashi, C. (2007). The reversion-inducing cysteine-rich protein with Kazal motifs (RECK) interacts with membrane type 1 matrix metalloproteinase and CD13/aminopeptidase N and modulates their endocytic pathways. J Biol Chem. **282**: 12341-12352.

Muraguchi, T., Takegami, Y., Ohtsuka, T., Kitajima, S., Chandana, E.P., Omura, A., Miki, T., Takahashi, R., Matsumoto, N., Ludwig, A., Noda, M., Takahashi, C. (2007). Reck modulates Notch signaling during cortical neurogenesis by regulating ADAM10 activity. Nat Neurosci. **10**: 838-845.

Nuttall, R.K., Sampieri, C.L., Pennington, C.J., Gill, S.E., Schultz, G.A., Edwards, D.R. (2004). Expression analysis of the entire MMP and TIMP gene families during mouse tissue development. FEBS Letters. **563**: 129-134.

Oh, J., Takahashi, R., Kondo, S., Mizoguchi, A., Nishimura, S., Imamura, Y., Kitayama, H., Alexander, D.B., Horan, T.P., Arakawa, T., Yoshida, H., Nishikawa, S., Itoh, Y., Seiki, M., Itohara, S., Takahashi, C., Noda, M. (2001). The membrane-anchored MMP inhibitor RECK is a key regulator of extracellular matrix integrity and angiogenesis. Cell. **107**: 789-800.

Park, S., Lee, C., Sabharwal, P., Zhang, M., Meyers, C.L., Sockanathan, S. (2013). GDE2 promotes neurogenesis by glycosylphosphatidylinositol-anchor cleavage of RECK. Science. **339**: 324-328.

Prendergast, A., Linbo, T.H., Swarts, T., Ungos, J.M., McGraw, H.F., Krispin, S., Weinstein, B.M., Raible, D.W. (2012). The metalloproteinase inhibitor RECK is essential for zebrafish DRG development. Development. **139**: 1141-1152.

Rubinstein, A.L., Lee, D., Luo, R., Henion, P.D., Halpern, M.E. (2000). Genes dependent on zebrafish cyclops function identified by AFLP differential gene expression screen. Genesis. **26**: 86-97.

Sasai, Y., Lu, B., Steinbeisser, H., Geissert, D., Gont, L.K., De Robertis, E.M. (1994). Xenopus chordin: a novel dorsalizing factor activated by organizer-specific homeobox genes. Cell. **79**: 779:790.

Simizu, S., Takagi, S., Tamura, Y., Osada, H. (2005). RECK-mediated suppression of tumor cell invasion is regulated by glycosylation in human tumor cell lines. Cancer Res. **65**: 7455-7461.

Stetler-Stevenson, W.G. (2008). Tissue inhibitors of metalloproteinases in cell signaling: metalloproteinase-independent biological activities. Sci Signal. **1**: 1-19.

Takahashi, C., Sheng, Z., Horan, T.P., Kitayama, H., Maki, M., Hitomi, K., Kitaura, Y., Takai, S., Sasahara, R.M., Horimoto, A., Ikawa, Y., Ratzkin, B.J., Arakawa, T., Noda, M. (1998). Regulation of matrix metalloproteinase-9 and inhibition of tumor invasion by the membrane-anchored glycoprotein RECK. Proc Natl Acad Sci USA. **95**: 13221-13226.

Takino, T., Tsuge, H., Ozawa, T., Sato, H. (2010). MT1-MMP promotes cell growth and ERK activation through c-Src and paxillin in three-dimensional collagen matrix. Biochem Biophys Res Commun. **396**: 1042-1047.

Tobin, J.L., Di Franco, M., Eichers, E., May-Simera, H., Garcia, M., Yan, J., Quinian, R., Justice, M.J., Hennekam, R.C., Briscoe, J., Tada, M., Mayor, R., Burns, A.J., Lupski, J.R., Hammond, P., Beales, P.L. (2008). Inhibition of neural crest migration underlies craniofacial dysmorphology and Hirschsprung's disease in Bardet-Biedl syndrome. Proc Natl Acad Sci USA. **105**: 6714-6719.

Vallon, M., Yuki, K., Nguyen, T.D., Chang, J., Yuan, J., Siepe, D. (2018). A RECK-WNT7 Receptor-Ligand Interaction Enables Isoform-Specific Regulation of Wnt Bioavailability. Cell Rep. **25**: 339-349.

Vu, T.H., Werb, Z. (2000). Matrix metalloproteinases: effectors of development and normal physiology. Genes Dev. **14**: 2123-2133.

Walsh, L.A., Roy, D.M., Reyngold, M., Giri, D., Snyder, A., Turcan, S., Badwe, C.R., Lyman, J., Bromberg, J., King, T.A., Chan, T.A. (2015). RECK controls breast cancer metastasis by modulating a convergent, STAT3-dependent neoangiogenic switch. Oncogene. **34**: 2189-2203.

Willson, J.A., Damjanovski, S. (2014). Vertebrate RECK in development and disease. Trends Cell Mol Biol. **9**: 95-105.

Wouters, M.A., Rigoutsos, I., Chu, C.K., Feng, L.L., Sparrow, D.B., Dunwoodie, S.L. (2005). Evolution of distinct EGF domains with specific functions. Protein Sci. **14**: 1091-1103.

Yamamoto, M., Matsuzaki, T., Takahashi, R., Adachi, E., Maeda, Y., Yamaguchi, S., Kitayama, H., Echizenya, M., Morioka, Y., Alexander, D.B., Yagi, T., Itohara, S., Nakamura, T., Akiyama, H., Noda, M. (2012). The transformation suppressor gene Reck is required for postaxial patterning in mouse forelimbs. Biol Open. **1**: 458-466.

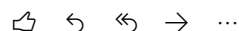# Appendices

Appendix A Copyright Permission

Appendix B *X. laevis RECK* full-length coding sequence

(Accession Number: KM225791.1)

```
   1 atgaagagaa ggagtgggga tgtgatgcat gctgctgtgc gggtcatgtc tgccagtgcc
  61 tcttgtttgg gactgctggg gatctggttc tttcttctga ttttcttgct cctggaggca
 121 gctgatgctt catgctgtaa ccaggcaaag gataatttaa tgtgtcgtga tgtatgtgaa
 181 cagatattat cttcaaaaag tgagtctcgc ataaaacacc tgttgctgag agcaccggat
 241 tactgcccga cttcaatgat tgatgtttgg acgtgtatta attcatcact gccaggtgtt
 301 tccaagaagt cagaaggctg ggtaggcctt ggatgttgtg aactagcaat agctgtggag
 361 tgtcggagag cttgcaagca ggcatcctca caaaatgata tttcaaaatc ctgcaggaaa
 421 caatatgaga ctgcccttat tagctgcatt aacagaaacg aaatgggatc agtgtgctgt
 481 agttgtgcag gacgccacac aaactgccgg gagtactgtc aagccatctt tcggacagat
 541 tcatcaccag gtccatccca aattaaagca gttgaaaatt tttgcgcttc catcagtcct
 601 ccattagttc agtgtgtaaa caactacacc caatcatatc caatgaggaa ccctgtggac
 661 agtttgtact gctgtgatag agctgaggat ccacaatgcc agtcagcttg caaaagaata
 721 cttatgtcta agaaaacaga gcctgagatt gttgatagcc taagtgaagg atgcaccaaa
 781 cctctacccc aggatcccct ttggcagtgc ttcctggaaa gctcaagaac agttcattct
 841 ggagtcaaca ttgttcctcc accttcagca ggtcttgatg gtgctgagct gcattgctgt
 901 tcaaaagcaa actcctcaaa ttgtagggat ttgtgcacta aattatacag tacaagctgg
 961 ggaaatacac aagtttggca agaatttgaa tttgcttgtg aatataaccc tctggaagca
1021 ccaatgttaa catgcttagc tgatgtaaga gaaccatgtc aactgggctg ccgaaatctc
1081 acattctgca caaacttttaa caacagacca acagagttat tccgcagctg caatgttcaa
1141 tcagaccagg gtgctatgaa tgacatgaaa ctatgggaga aaggcagcat taaaatgccc
1201 ttcatgaata ttcctgtact agatattaaa aaatgtcacc cagaaatgtg gaaggcaata
1261 gcttgctcac tgcagattaa accttgtcat agtaaatcta gaggaagcat catctgcaaa
1321 acagattgtg ttgaaatact cacaaagtgc ggtgatcata gtagatttcc tgagagtcac
1381 acggcagaaa gtatttgtga gcttctttct ccttctgatg aaaatgagga ctgtatcccg
1441 cttgacactt atcttagatc aagcccactg gataatgcca tagaggaagt tactcatcca
1501 tgtaatccaa atccttgtcc agcaaatcat ttatgtgagg tgaacaggaa ggggtgcctc
1561 ccaggagaac cctgccttcc atatttctgt agtcaaggat gcaagttagg agagacttct
1621 gattttcttg tgcgccatgg tgtgctaatt caaatgccat cagggtccgt tggctgttac
1681 aaaatttgca cctgtggaca aagtggaact ctggaaaact gtttggacat gcagtgtgtt
1741 gatcttcata aatcatgtct tgttggtgga cagcgaaaaa atcacgggga gtcgtttaaa
1801 gtagattgta acatctgttc atgtgttgct ggcacactga ggtgttcaaa tcatcagtgc
1861 ccccattcag aagaagatcg taggatgttt acaggtctac cctgtaactg tgaagatcag
1921 tttgttcctg tatgtgggca gaatggacgt acatacccaa gtgcatgtat agcacgatgt
1981 gttgggttat tggatcacca gtttgaattt gggctctgtt cttccgtgtg caatccaaac
2041 ccatgttcca gaaatggtat tccaaagcga aaagtttgct taaccagcta tgagaaattt
2101 gggtgtgccc agtatgaatg tatcccaagg catcttaaat gtgaacattc ccgggaccca
2161 atgtgtgaca ctgaaaatgt ggagcacata aacctttgca cattatatca aagaggaaga
2221 ctgctgtcat ataaaggatc atgccaacct ttttgcaaat ctgcagaacc agtttgtggg
2281 cacaatggag agacgtaccc taatgtttgc agtgcatatt ctgatcgtgt tgctgtggat
2341 tattatggac actgccagga cgttggcatc ttctcagacc aaggtcttca taatgaatgc
2401 ttgtctattc agtgccctgc aattcctgtc acagtttgta aacccatcat accacctgga
2461 gcatgttgtc cattgtgtgc tggagtccta agaattttgt ttgacaagga aaaactggat
2521 acttttgcaa cggcaacaaa gaacacacca ataactgtta tggacatcct acagaaaatt
2581 agacaacatg tctctgtacc tcagtgtgat gtatttgggt acttaagtat ggaatctgat
2641 atcattatcc ttattgttcc tgttgatagc cccccaaaat caatacagat tgatgcatgc
2701 aataaggagg ctgagaaaat taattctctt attaattcag acagtccaac actggtatcc
2761 caggtgccac tatcagcact tataacctca gaagttcagg tatcaacaac attaaattct
2821 gattgtaaca gaatatgttt aagtattcat tatatttatt tatatcttgg tatagctttg
2881 ttgtatgtaa cattgaatgc ttaa
```

Appendix C Amino acid sequences of the 3 Kazal motifs among different species

	KM1	KM2	KM3
H. sapiens	CADQFVPVCGQNGRTYPSACIARC	CDTDHMEHNNLCTLYQRGKSLSYKGPCQPFC	CRATEPVCGHNGETYSSVC
M. musculus	CADQFVPVCAQNGRTYPSACIARC	CDTDHMEHSNLCTLYQRGKSLSYRGPCQPFC	CRATEPVCGHNGETYSSVC
G. gallus	CVDQFVPVCGQNGRTYPSACIARC	CDTDSVEYSNVCTLYQKGKNLAYRGPCQPFC	CKSVEPVCGHNGETYSSVC
X. laevis	CEDQFVPVCGQNGRTYPSACIARC	CDTENVEHINLCTLYQRGRLLSYKGSCQPFC	CKSAEPVCGHNGETYPNVC
X. tropicalis	CEDQFVPVCGQNGRTYPSACIARC	CDTENMEHMNLCTLYQRGRLLSYKGSCQPFC	CKSAEPICGHNGETYPNVC
D. rerio	CADHFVPVCAGNGRTYPSACVARC	CDTDNMEHANLCVLNLRGKTLAYSGHCQDAC	CRRPREVCAHNGESYSTVC
D. melanogaster	CPAHYVPVCGSNGNTYPSACVAKC	CDSQGRTYPNACALLKANPQGQVAYWSACQS	NTSPSPVCGINGVTYKSSY

Fig. C.1. Clustal Omega alignment of the 3 Kazal motif domains of select animals.

Amino acid sequences of the 3 Kazal motif domains among different species. Conserved cysteine residues are highlighted in red and conserved tyrosine residues are highlighted in blue.

Appendix D The developmental phenotypes of *X. laevis* embryos

	Number (%) of embryos at specified phenotype 1 day post fertilization			Total number of embryos
	Normal	**Moderate**	**Severe**	
RECK MO	0	83 (59%)	57 (41%)	140
Control	138 (91%)	14 (9%)	0	152

Fig. D.1. The developmental phenotypes of *X. laevis* embryos following RECK Morpholino injection into one-cell stage fertilized embryos.

Appendix E Zymography for BB94 treatment
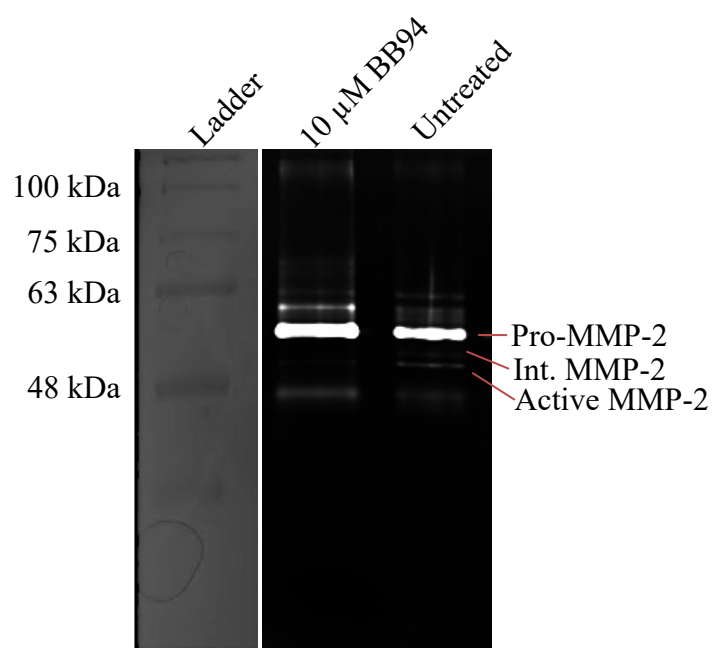
Fig. E.1. Zymography for BB94 treatment.

Gelatin zymography was used to measure protein levels of secreted pro-, intermediate, and active MMP-2 following 10 µM BB94 treatment in A6 cells compared to untreated cells.

Appendix F Zymography for MMP-9 detection
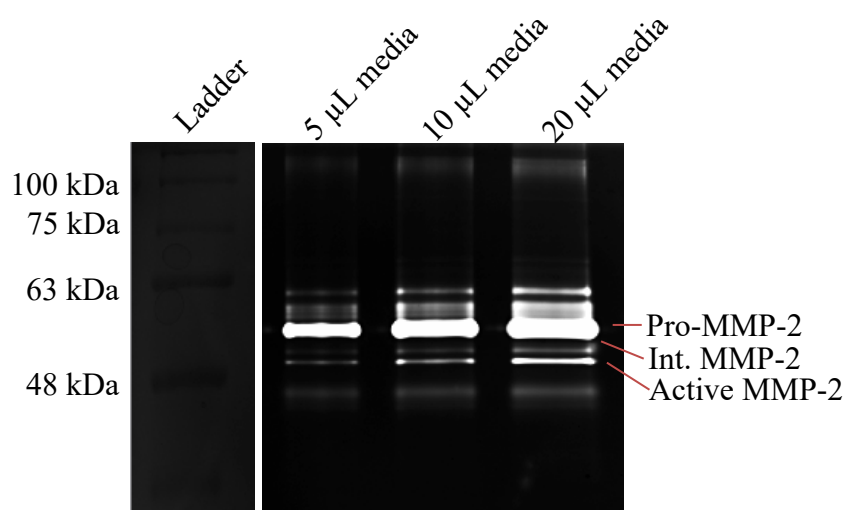
Fig. F.1. Zymography for MMP-9 detection.

Gelatin zymography was used to measure the protein levels of MMP-2 and MMP-9 in A6

cells. MMP-9 protein could not be detected in the media of A6 cells at the expected size

of 84 kDa.

Appendix G UWO Biosafety Certificate

Researcher: Dr. S. Damjanovski

Biosafety Approval Number: BIO-UWO-0141

Expiry Date: June 16, 2014

June 21, 2011

Dear Dr. Damjanovski:

Please note your biosafety approval number listed above. This number is very useful to you as a researcher working with biohazards. It is a requirement for your research grants, purchasing of biohazardous materials and Level 2 inspections.

Research Grants:
- This number is required information for any research grants involving biohazards. Please provide this number to Research Services when requested.

Purchasing Materials:
- This number must be included on purchase orders for Level 1 or Level 2 biohazards. When you order biohazardous material, use the on-line purchase ordering system (www.uwo.ca/finance/people/). In the "Comments to Purchasing" tab, include your name as the Researcher and your biosafety approval number.

Annual Inspections:
- If you have a Level 2 laboratory on campus, you are inspected every year. This is your permit number to allow you to work with Level 2 biohazards.

To maintain your Biosafety Approval, you need to:

- Ensure that you update your Biohazardous Agents Registry Form at least every three years, or when there are changes to the biohazards you are working with.

- Ensure that the people working in your laboratory are trained in Biosafety.

- Ensure that your laboratory follows the University of Western Ontario Biosafety Guidelines and Procedures Manual for Containment Level 1 & 2 Laboratories.

- For more information, please see: www.uwo.ca/humanresources/biosafety.

Please let me know if you have questions or comments.

Regards,

Appendix H Animal Use Protocol

Western

2009-044::3:

AUP Number: 2009-044
AUP Title: MMP Activation During Xenopus Development

Approval Date: 05/29/2009

The YEARLY RENEWAL to Animal Use Protocol (AUP) 2009-044 has been approved.

1. This AUP number must be indicated when ordering animals for this project.
2. Animals for other projects may not be ordered under this AUP number.
3. Purchases of animals other than through this system must be cleared through the ACVS office. Health certificates will be required.

REQUIREMENTS/COMMENTS
Please ensure that individual(s) performing procedures on live animals, as described in this protocol, are familiar with the contents of this document.

The holder of this Animal Use Protocol is responsible to ensure that all associated safety components (biosafety, radiation safety, general laboratory safety) comply with institutional safety standards and have received all necessary approvals. Please consult directly with your institutional safety officers.

Submitted by: Kinchlea, Will D
on behalf of the Animal Use Subcommittee

Curriculum Vitae

Jessica Willson

Education

2013-2019	**PhD**, Department of Biology/Collaborative Graduate Specialization in Developmental Biology, Western University, London ON
2010-2012	**MSc**, Department of Biology, Western University, London, ON
2006-2010	**BSc**, Honours Specialization in Biology, Western University, London ON

Awards and Scholarships

2019	**IDI in Stem Cells and Regenerative Medicine Post-Doctoral Training Award**, Western University, London, ON
2019	**CHRI Post-Doctoral Trainee Award**, Western University, London, ON
2019	**Robert and Ruth Lumsden Graduate Award**, Western University, London, ON
2018	**Dr. Irene Uchida Fellowship in Life Sciences**, Western University, London, ON
2016-2017	**Queen Elizabeth II Graduate Scholarship in Science and Technology**, Western University, London, ON
2014-2015	**Queen Elizabeth II Graduate Scholarship in Science and Technology**, Western University, London ON
2012	**Graduate Thesis Research Award**, Western University, London, ON
2010	**Dean's Honour List**, Western University, London, ON
2009	**Dean's Honour List**, Western University, London, ON
2006	**The Western Scholarship of Distinction**, Western University, London, ON

Contributions to Research

Articles *in press*:

- **Willson, J.A.,** Bork, B., Muir, C.A., & Damjanovski, S. (2019). Modulation of RECK levels in Xenopus A6 cells: effects on MT1-MMP, MMP-2, and pERK levels. Journal of Biological Research. DOI: 10.1186/s40709-19-0108-8.

Peer-Reviewed Publications:

- **Willson, J.A.**, Damjanovski, S. (2019). Spatial analysis of RECK, MT1-MMP, and TIMP-2 proteins during early *Xenopus laevis* development. Gene Expression Patterns. 34: 119066.
- **Willson, J.A.**, Muir, C.A., Evered, C.L., Cepeda, M.A., and Damjanovski, S. (2018). Stable expression of α1-Antitrypsin Portland in MDA-MB-231 cells increased MT1-MMP and MMP-9 levels, but reduced tumour progression. Journal of Cell Communication and Signalling. 12: 479-488.

- Cepeda, M., Pelling, J.J., Evered C.L., Williams, K.C., Freedman, Z., Stan, I., **Willson, J.A.**, Leong, H.S., and Damjanovski, S. (2016). Less is more: low expression of MT1-MMP is optimal to promote migration and tumourigenesis of breast cancer cells. Molecular Cancer. 15: 65.
- **Willson, J.A.**, Nieuwesteeg, M.A., Cepeda, M., and Damjanovski, S. (2015). Analysis of *Xenopus laevis* RECK and its relationship to other vertebrate RECK sequences. Journal of Scientific Research and Reports. 6: 504-513.
- Nieuwesteeg, M.A., **Willson, J.A.**, Cepeda, M., and Damjanovski, S. (2014). Analysis of the effects of Tissue Inhibitor of Metalloproteinases-1, -2, and -3 N- and C-terminal domains on signaling markers during X. laevis development. All Results Journals: Biology. 5: 30-36.
- Nieuwesteeg, M.A., **Willson, J.A.**, Cepeda, M., Fox, M.A., and Damjanovski, S. (2014). Functional characterization of tissue inhibitor of metalloproteinase-1 (TIMP-1) N- and C-terminal domains during *Xenopus laevis* development. The Scientific World Journal. 30: 467907.
- Fox, M.A., Nieuwesteeg, M.A., **Willson J.A.**, Cepeda, M., and Damjanovski, S. (2013). Knockdown of Pex11β reveals its pivotal role in regulating peroxisomal genes, numbers, and ROS levels in *Xenopus laevis* A6 cells. In Vitro Cellular and Developmental Biology – Animal. 50: 340-349.
- Shafer, M.E.R., **Willson, J.A.**, and Damjanovski, S. (2011). Expression analysis of the peroxiredoxin gene family during early development in *Xenopus laevis*. Gene Expression Patterns. 11: 511-6.

Non-Peer-Reviewed Publications – Review:
- **Willson, J.A.**, and Damjanovski, S. (2014). Vertebrate RECK in development and disease. Trends in Cell and Molecular Biology. 9: 95-105.

Oral Presentations:
- **Willson, J.A.** The Role of RECK levels in Development and Disease. (2014). Collaborative Graduate Program in Developmental Biology 6th Annual Research Day. London, ON

Poster Presentations:
- **Willson, J.A.**, Cepeda, M.A., and Damjanovski, S. (2015). Developmental effects of knocking down RECK expression in early *Xenopus laevis* embryos. Collaborative Graduate Program in Developmental Biology 7th Annual Research Day. London, ON
- Cepeda, M.A., **Willson, J.A.**, and Damjanovski, S. (2015). Low Levels of MT1-MMP enhance the migration and proliferation of cells. Collaborative Graduate Program in Developmental Biology 7th Annual Research Day. London, ON
- **Willson, J.A.**, Cepeda, M.A., and Damjanovski, S. (2014). Developmental effects of knocking down RECK expression in early *Xenopus laevis* embryos. Society for Developmental Biology 73rd Annual Meeting, Univ. of Washington, Seattle, WA
- Cepeda, M.A., **Willson, J.A.**, and Damjanovski, S. (2014). MT-1 MMP protein levels affect how this multifunctional protease changes the behavior of breast cancer cells. Society for Developmental Biology 73rd Annual Meeting, Univ. of Washington, Seattle, WA

- **Willson, J.A.**, Nieuwesteeg, M., Cepeda, M.A., and Damjanovski, S. (2013). Analysis of RECK expression during *Xenopus laevis* development and its colocalization with MT1-MMP during neurulation. The International Society of Developmental Biologists, Cancun, Mexico
- Nieuwesteeg, M., **Willson, J.A.**, Cepeda, M.A., and Damjanovski, S. (2013). Analysis of the effects of TIMP-1, -2, and -3 and N- and C-terminal domain overexpression during early *Xenopus laevis* development using immunohistochemistry. The International Society of Developmental Biologists, Cancun, Mexico
- Cepeda, M.A., Nieuwesteeg, M., **Willson, J.A.**, and Damjanovski, S. (2013). TIMP-2 interacts with MT-1 MMP to modulate migration and invasion of MCF-7 cells independent of MMP inhibition. The International Society of Developmental Biologists, Cancun, Mexico
- **Willson, J.A.**, Nieuwesteeg, M., Cepeda, M., and Damjanovski, S. (2013). Analysis of RECK expression in dorsalized and ventralized *Xenopus laevis* embryos. M3: Mostly Mammals Developmental Biology Conference, Montreal, QC
- Cepeda, M., Nieuwesteeg, M., **Willson, J.A.**, and Damjanovski, S. (2013). Tissue inhibitor of metalloproteinase-2 (TIMP-2) with a non-functional N-terminal domain decreases the invasiveness of MCF-7 and MDA-MB231 breast cancer cells. M3: Mostly Mammals Developmental Biology Conference, Montreal, QC
- Nieuwesteeg, M., Cepeda, M., **Willson, J.A.**, and Damjanovski, S. (2013). Functional characterization of tissue inhibitor of metalloproteinase-1 (TIMP-1) N- and C-terminal domains during early *Xenopus laevis* development. M3: Mostly Mammals Developmental Biology Conference, Montreal, QC
- **Willson, J.A.**, Cepeda, M.A., Nieuwesteeg, M.A., and Damjanovski, S. (2012). Analysis of RECK expression in dorsalized and ventralized *Xenopus laevis* embryos. The American Society for Cell Biology Annual Meeting, San Francisco, CA
- **Willson, J.A.** and Damjanovski, S. (2012). Expression analysis of RECK during the early development of *Xenopus laevis*. 25th Annual Western Research Forum, Western University, London ON
- Cepeda, M.A., Nieuwesteeg, M.A., **Willson, J.A.**, and Damjanovski, S. (2012). Tissue inhibitor of metalloproteinase-2 (TIMP-2) with a non-functional N-terminal domain decreases the invasiveness of MCF-7 and MDAMB-231 breast cancer cells. The American Society for Cell Biology Annual Meeting, San Francisco, CA
- Nieuwesteeg, M., Cepeda, M., **Willson, J.A.**, and Damjanovski, S. (2012). Functional characterization of tissue inhibitor of metalloproteinase-1 (TIMP-1) N- and C-terminal domains during early *Xenopus laevis* development. The American Society for Cell Biology Annual Meeting, San Francisco, CA
- Shafer, M.E.R., **Willson, J.A.**, and Damjanovski, S. (2011). Characterization of the temporal and spatial expression patterns of the peroxiredoxin gene family during early development. The Great Lakes Mammalian Development Meeting, Toronto, ON

Research Experience

2010-Current   **Graduate Research**, Department of Biology, Western University, London, ON
- PhD Thesis: The role of *X. laevis* RECK in ECM remodeling and tissue patterning

- MSc Thesis: Cloning and analysis of RECK during early *Xenopus laevis* development

2009-2010 **Undergraduate Research,** Department of Biology, Western University, London, ON

- 4999E Thesis: Characterizing cell surface binding of full-length, N-, and C-terminal domains of TIMP-2 in *Xenopus laevis* A6 cells

Teaching Experience

2010-2019 **Graduate Teaching Assistant**, Department of Biology, Western University, London, ON

2010-2019 **Mentor to 4999E Honour Thesis Students**, Department of Biology, Western University, London, ON

2018 **Lecturer,** Developmental Biology 3338A, Department of Biology, Western University, London, ON,

2013-2015 **Biology 4999E Honour Thesis Advisory Committee Member**, Department of Biology, Western University, London, ON

Academic Appointments

2013-2019 Steering Committee, Collaborative Graduate Specialization in Developmental Biology